

MARIA S. MERIAN-Berichte

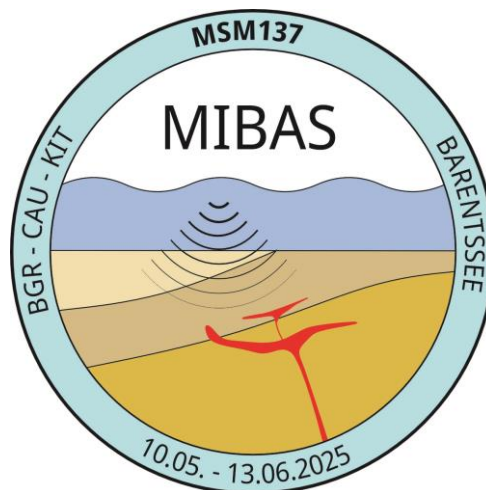
***Magmatic Intrusions in the Barents Sea: Geophysical characterization
of shallow magmatic systems and impact on sedimentary basins***

Cruise No. MSM137

May 10, 2025 – June 13, 2025

Reykjavik (Iceland) – Reykjavik (Iceland)

MIBAS – GPF 20-1_070



Michael Schnabel, Udo Barckhausen, Thomas Behrens, Stephanie Bellenberg, Morgane Belleville, Thomas Bohlen, Ümit Demir, Timo Ebert, Axel Ehrhardt, Martin Engels, Lilianna Kołodziejska, Jan Kuckuck, René Herbst, Ingo Heyde, Michael Schauer, Jens Schneider v. Deimling, Bettina Schramm, Felix Schwer, Peter Steinborn, Chris Straßburger, Viktoria Thamm

Michael Schnabel

Federal Institute for Geosciences and Natural Resources (BGR)

Table of Contents

1	Cruise Summary.....	3
1.1	Summary in English.....	3
1.2	Zusammenfassung.....	3
2	Participants.....	4
2.1	Principal Investigators.....	4
2.2	Scientific Party.....	4
2.3	Participating Institutions.....	4
3	Research Program.....	6
3.1	Description of the Work Area.....	6
3.2	Aims of the Cruise.....	7
4	Narrative of the Cruise.....	11
5	Preliminary Results.....	13
5.1	Multichannel Seismics.....	13
5.2	Bathymetry (incl. SVPs and XSVs).....	14
5.3	Parasound Sediment Echosounder.....	19
5.4	Water Column Imaging.....	23
5.5	Magnetics.....	25
5.6	Gravity.....	28
5.7	Ocean-Bottom Seismics.....	31
6	Station List MSM137.....	34
6.1	Overall Station List.....	34
6.2	Profile Station List.....	35
7	Data and Sample Storage and Availability.....	39
8	Acknowledgements.....	40
9	References.....	40
10	Abbreviations.....	42
11	Appendices.....	43
11.1	Selected Pictures of Shipboard Operations.....	43
11.2	Ocean-Bottom-Seismometer.....	47
11.3	Airguns, Streamer and Data Acquisition.....	48
11.4	ORCA Navigation, Vessel Geometry and Data Protocols.....	52
11.5	Hydroacoustics.....	61
11.6	Magnetics.....	63
11.7	Gravity.....	69
11.8	MMO Report.....	78

1 Cruise Summary

1.1 Summary in English

The cruise MSM137 focused on the investigation of magmatic intrusions within the Norwegian Barents Sea. Therefore, we applied an innovative geophysical approach. Seismic data was acquired in a combination of long offset (6,600 m) streamer cable recordings at the sea surface and wide-angle data at the seafloor. This data set will build the basis for a detailed imaging of the intrusive structures. With these images, we will be able to characterize the interactions between magmatic intrusions and sedimentary successions and further light will be shed onto the formation and internal structure of these bodies. Additionally, we recorded high resolution echo sounder data. With this dataset, we will test the hypothesis if the ancient intrusions are related to reactivated venting structures. Further on, the acquired gravimetric and magnetic data will be used to identify sills and dikes via 3D modeling.

The northern Barents Sea is an ideal region to perform this analysis, as widespread magmatic sills are already reported there. Due to the Cretaceous exhumation and subsequent erosion of the area these sills are situated nowadays significantly shallower than during their time of emplacement – providing unique opportunities for a geophysical investigation of these structures. During cruise MSM137, we acquired 1,968 km of seismic lines, covering three areas at the Vestbakken Volcanic Province, at the Gardarbanken High and at the Edgeøya Platform.

1.2 Zusammenfassung

Ziel der Fahrt MSM137 war die Erkundung magmatischer Intrusionen im Bereich der norwegischen Barentssee. Dafür kam ein innovativer geophysikalischer Ansatz zur Anwendung. Seismische Daten wurden sowohl mit einem 6.600 m langen Messkabel als auch mit Seismometern am Meeresboden aufgezeichnet. Damit ist die Grundlage für eine detaillierte Abbildung dieser Strukturen geschaffen. Diese Abbilder erlauben die Beurteilung der Wechselwirkungen zwischen Intrusionen und umliegenden Sediment sowie die Beschreibung der Entstehung und der inneren Struktur der Intrusionen. Mit parallel aufgezeichneten Hydroakustikdaten wird überprüft, ob durch Intrusionen hervorgerufene Fluidaufstiegskanäle recent reaktiviert werden. Potenzialgeophysikalische Daten (Gravimetrie und Magnetik) werden helfen, die Ausdehnung der entsprechenden Intrusionskörper räumlich zu modellieren.

Die nordwestliche Barentssee ist ein idealer Ort für diese Analysen. Hier sind großräumige Intrusionstrukturen bekannt. Durch starke Hebungsbewegungen und entsprechender Erosion liegen dieser Körper hier aktuell deutlich flacher als zur Zeit ihrer Bildung – dadurch sind sie für unsere geophysikalischen Methoden besonders gut zugänglich. Während der Expedition MSM137 haben wir insgesamt 1.968 km an seismischen Profilen erhoben. Innerhalb von 23 Arbeitstagen wurden drei Arbeitsgebiete (in der *Vestbakken Volcanic Province*, auf dem *Gardarbanken High* und auf der *Edgeøya Platform*) gezielt untersucht.

2 Participants

2.1 Principal Investigators

Name	Institution
Schnabel, Michael, Dr.	BGR
Ehrhardt, Axel, Dr.	BGR
Bohlen, Thomas, Prof.	KIT
Schneider von Deimling, Jens, Dr.	CAU

2.2 Scientific Party

Name	Discipline	Institution
Schnabel, Michael, Dr.	Seismics / Chief Scientist	BGR
Ehrhardt, Axel, Dr.	Seismics / Co-Chief Scientist	BGR
Engels, Martin, Dr.	Seismics	BGR
Schramm, Bettina, Dr.	Seismics	BGR
Schauer, Michael	Seismics	BGR
Steinborn, Peter	Seismics	BGR
Kuckuck, Jan	Seismics	BGR
Demir, Ümit	Seismics	BGR
Behrens, Thomas	Seismics	BGR
Ebert, Timo	Seismics	BGR
Herbst, René	Seismics	BGR
Barckhausen, Udo, Dr.	Magnetics	BGR
Bellenberg, Stephanie	Magnetics	BGR
Heyde, Ingo, Dr.	Gravity	BGR
Straßburger, Chris	Hydroacoustics	CAU
Thamm, Viktoria	Hydroacoustics	CAU
Schwer, Felix	Hydroacoustics	KIT
Belleville, Morgane	Marine Mammal Observer	EPI
Kołodziejska, Lilianna	Marine Mammal Observer	EPI

2.3 Participating Institutions

BGR	Bundesanstalt für Geowissenschaften und Rohstoffe, Hannover
CAU	Christian-Albrechts-Universität zu Kiel
KIT	Karlsruher Institut für Technologie
EPI	EPI Limited, Manchester



Fig. 2.1 Scientific crew of cruise MSM137. From left to right: M. Engels, B. Schramm, C. Straßburger, M. Schauer, V. Thamm, R. Herbst, S. Bellenberg, F. Schwer, L. Kołodziejska, T. Behrens, M. Belleville, U. Barckhausen, T. Ebert, I. Heyde, J. Kuckuck, Ü. Demir, M. Schnabel, P. Steinborn, A. Ehrhardt. Photo by Denny Hermann.

3 Research Program

3.1 Description of the Work Area

The formation of the western passive margin of the Barents Sea is related to the opening of the Norwegian-Greenland Sea. The margin is composed of two large shear segments and a central rifted margin southwest of Bjørnøya – this area is called the Vestbakken Volcanic Province (VVP; Faleide et al., 2008). Prominent sill intrusions in this area have been already reported by Faleide et al. (1988). Drill site 7316/5-1 (black diamond in Fig. 3.1) recovered several layers of igneous material. The igneous rocks within the VVP most probably originated from several magmatic episodes. Omosanya et al. (2016) argued that the main activity was focussed during Late Eocene, Oligocene and Early Pliocene. Most of the resulting sills show a typical saucer-shaped pattern and have a spatial extend of 5 to 10 km (Omosanya et al., 2016).

Within the central western Barents Sea (around 75° N) several wide-angle seismic lines showed shallow velocity anomalies at depths of 2 - 4 km below seafloor. These features are associated with velocities between 6.0 and 6.2 km/s and are generally interpreted as igneous intrusions (Aarseth et al., 2017, Breivik et al., 2003, Breivik et al., 2005, Breivik et al., 2002) and can have a spatial extent of up to 100 km.

The northernmost part of the Barents Sea is characterized by widespread Late Mesozoic magmatism, which is part of the High Arctic Large Igneous Province (HALIP). A comprehensive review can be found at Senger et al. (2014). They have shown that intrusions occur predominantly as sills with a thickness of up to 100 m with local occurrence of dikes. K/Ar dating from the dolerites found on Svalbard yields discrete peaks in magmatic activity between 115 and 78 Ma (Nejbert et al., 2011). Based on an analysis of magnetic data, Grogan et al. (2000) suggested that these dolerite bodies are a widespread phenomenon south and east of Svalbard. These bodies have been exhumed since Cretaceous times. The total amount of Cenozoic net erosion is still a matter of debate. Rasmussen and Fjeldskaar (1996) estimated a maximum uplift of 2000 m. Recent analysis of thermochronology data resulted in an uplift of 4000 m for the central part of Svalbard since the end of Early Eocene (Dörr et al., 2018).

Mafic intrusions east of Svalbard have been imaged by active tomography using wide-angle data (Minakov et al., 2012). At a crustal level between 8 and 32 km depth, they found finger-shaped high-velocity anomalies, reaching up to 12 % of velocity perturbation. These are concomitant with sills already reported by reflection seismic data within the shallow sediments. In a regional study, Minakov et al. (2018) have shown that dikes can be spatially correlated with short wavelength magnetic anomalies. Based on reviewing existing data, Polteau et al. (2016) estimated the volume of the Early Cretaceous Barents Sill Complex to be about 100,000 to 200,000 km³. This massive injection of magmatic material caused rapid organic matter maturation and formation of thermogenic gas and oil in contact aureoles. Polteau et al. (2016) estimate that an oil equivalent of up to 175 trillion barrels were potentially mobilized. However, the work reported only two sites with hydrothermal vent complexes situated in the eastern Barents Sea.

Pockmarks within the Barents Sea have been initially described by Solheim and Elverhøi (1993). The methane budget of these structures has been analyzed within SFB 313 (Lammers et al., 1995). Recently, a large province of blow-out craters within the Bjørnøyrenna has been

analyzed by Andreassen et al. (2017). They concluded that these craters were formed by hydrate-controlled methane expulsion. Studies at the Vøring margin have shown that venting structures above sill tips are active for long time after the deposition of the sills (Svensen et al., 2003, Planke et al., 2005). The possibility of a causal link between recent seafloor craters and buried magmatic features has not been investigated in the Barents Sea up to now.

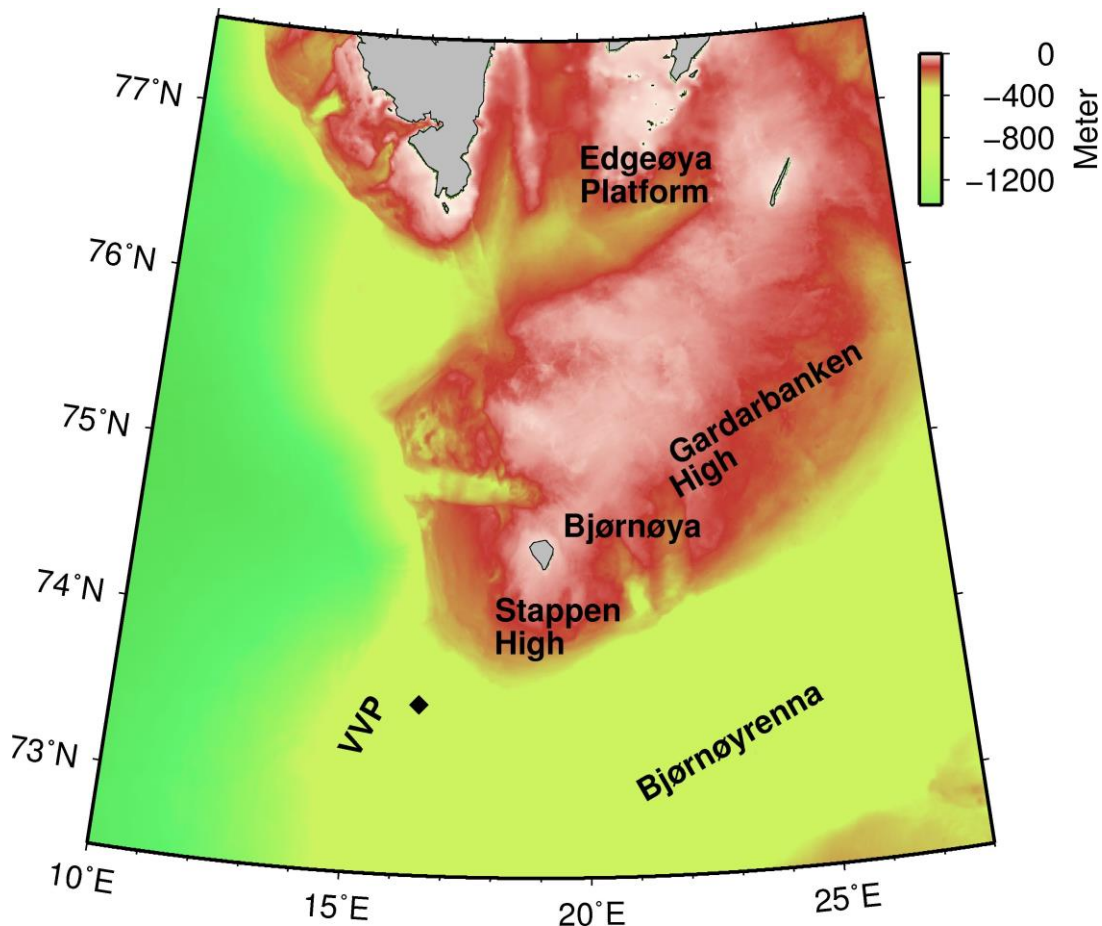


Fig. 3.1 Work area of RV MARIA S. MERIAN cruise MSM137. VVP: Vestbakken Volcanic Province. The black diamond represents drill site 7316/5-1. Bathymetry according to IBCAO 3.0 (Jakobsson et al, 2012).

3.2 Aims of the Cruise

The conventional seismic method is only partly capable to resolve structures in relation to magmatic intrusions. Therefore, a main objective of this cruise is to apply enhanced geophysical methods in order to image and identify sills on a detailed scale. During the cruise, we combined seismic recordings from a towed seismic cable with registrations on the ocean floor via ocean bottom seismometers. The analysis of this data will result in complementary images. The deployed streamer cable had an active length of 6,600 m. This data will be analyzed via full waveform inversion to further enhance the seismic velocity model as input for the resulting imaging, e.g. via reverse time migration (RTM). Additionally, Multibeam and Parasound will constrain the shallow subsurface. Complementary application of magnetics and gravity will resolve deep structures in the area below the intrusions.

The regional focus of cruise MSM137 is the central and northern Norwegian Barents shelf. Here, regional intrusive structures can be found at depth ranges much shallower than during their initial emplacement due to the enormous late Cretaceous uplift and erosion – providing unique opportunities for a geophysical characterization. Further on, results from the Svalbard archipelago offers the opportunity of a direct comparison of offshore geophysical data to already existing onshore observations. This cruise will address the following main points:

(1) How does the emplacement of sills interact with the surrounding sediments?

A central target of this study is the interaction between intrusions and surrounding sediments. Firstly, we will investigate if existing sediment structures favor the development of sills in specific depth intervals. Secondly, we will characterize the area of the resulting contact metamorphism as well as the effects on the physical properties of the sediments. The size and character of the resulting aureoles will form the volumetric basis for an estimate of released thermogenic gas.

(2) Are the sill tips related to venting structures?

We will investigate if the overburden above the sills was affected by fluid flow. Detailed reflection seismic imaging will allow us to identify paleo fluid conduits. We intend to assess if these potential fluid systems have been reactivated later as well as their influence on the present-day bathymetry. Further on, an investigation of selected sites in terms of active gas venting into the water column will be done via hydroacoustic flare imaging.

(3) What is the total amount of intruded material?

To answer this question, sills thinner than the classical resolution of reflection seismics have to be taken into account. Further on, the possibility of stacked sills has to be considered, where the shallow structures are masking the deeper ones. Therefore, highly resolved seismic velocity models are needed. The resulting velocity anomaly will be affected by the total ratio between sedimentary and igneous material. This method will allow us to quantify sills even in the sub-seismic domain.

(4) Are sills related to structures in the lower crust?

The relationship between sills, dikes and deeper melting anomalies is not well understood. Classical seismic profiling is generally not able to produce clear images below the first intrusive layer. Therefore, we will apply a multi-method geophysical approach: the reflection seismic data will be evaluated combined with wide-angle refraction seismic recordings. Vertical dikes will have clear signals in the magnetic field, and large melting anomalies in the middle and lower crust should be detected by gravimetric studies. The integration of these data sets will result in a consistent image of igneous bodies from shallow sills down to the crust mantle boundary.

(5) Do sills show an internal structure?

It is still an open question if sills form within one discrete step or during several sequences over time. The combination of highly resolved seismic velocity analyses with densely spaced data recording and reverse time migration will allow us to produce detailed images of the igneous structures. These images will contain the internal structure of the sills and could be used to characterize the internal heterogeneity.

3.3 Agenda of the Cruise

To reach to aims of the project, it was intended to study three selected sites within the northern Barents Sea with geophysical measurements. Suggested working area A (working area 1 in this report) is at the Vestbakken Volcanic Province. Here, deep seated intrusions has been proven by drilling. Suggested working area B (working area 2 in this report) is at the Gardarbanken High. Sills in this area has been interpreted based on velocities from existing refraction seismic work. The original proposal suggest a third part of this survey (working area C) at the Kong Karls Platform at about 30°E / 78°N. Due to the harsh ice conditions in May / June 2025 we decided to alternatively survey an area further south-west on the Edgeøya Platform, which is called working area 3 in this report. The working areas are shown in Fig. 3.2.

For cruise MSM137, we had a total of 23 working days within the survey area. It was intended to spend roughly one week in each survey area and to perform the following measurements: deployment of ocean bottom seismometers, seismic profiling (including multibeam and sediment echosounder) with towed streamer and towed magnetic sensors, recovery of ocean bottom seismometers, additional hydroacoustic work to fill gaps in the bathymetric coverage and to search for flares within the water column. To comply with the regulations concerning the protection of marine mammals, two external marine mammal observers (MMOs) joined the cruise. In detail, we applied the following methods during the cruise:

Towed Seismic

The seismic signals were recorded with a towed streamer (6,600 m active length) behind the ship. The streamer length allows also the analysis of refracted waves from the subsurface via tomography and full waveform inversion. Densely spaced profiles (separation significantly lower than streamer length) allow lateral characterization via 2.5D imaging. The seismic source was a tuned air gun array comprising 16 G-Guns. Triggering was done at intervals of 50 m distance.

Ocean-bottom Seismic

Additionally, the seismic energy was recorded at the seafloor via up to 16 OBS. By analysis of refracted waves we will obtain 3D velocity fields for the subsurface.

Hydroacoustic Seafloor and Water Column Analyses

A detailed analysis of the seafloor morphology will show if the edges of intrusions can be correlated to active venting structures on the seafloor. Simultaneously, sites will be investigated by high-resolution subbottom / water column data in order to identify possible fluid migration pathways.

Gravimetric Measurements

A sea gravimeter was used for the gravity measurements which were conducted during the entire cruise on all profile and transit lines. Shipboard gravity measurements show a high lateral resolution especially within shallow water depth.

Magnetic Measurements

A towed marine magnetometer was used as long as a minimum water depth of 100 m could be expected. Variations due to strong magnetic disturbances in high latitudes will be corrected after the cruise with magnetic observatory data from the Polish Polar Station Hornsund.

Marine Mammal Observation

Responsible marine research during seismic operations was guaranteed and monitored by two marine mammal observers (MMO), hired by the environmental company EPI Limited. Due to nearly 24 h daylight in the working areas optical monitoring of the mitigation zone was done continuously. During bad weather periods, the mitigation zone was surveyed with an acoustic passive monitoring system (PAM). Seismic profiling always started with a soft start, in compliance with national and international regulations and recommendations for marine seismic surveying. In case of marine mammals within the mitigation zone of 750 m, the seismic sources were stopped immediately. Details are given in the MMO report in the appendix 11.8.

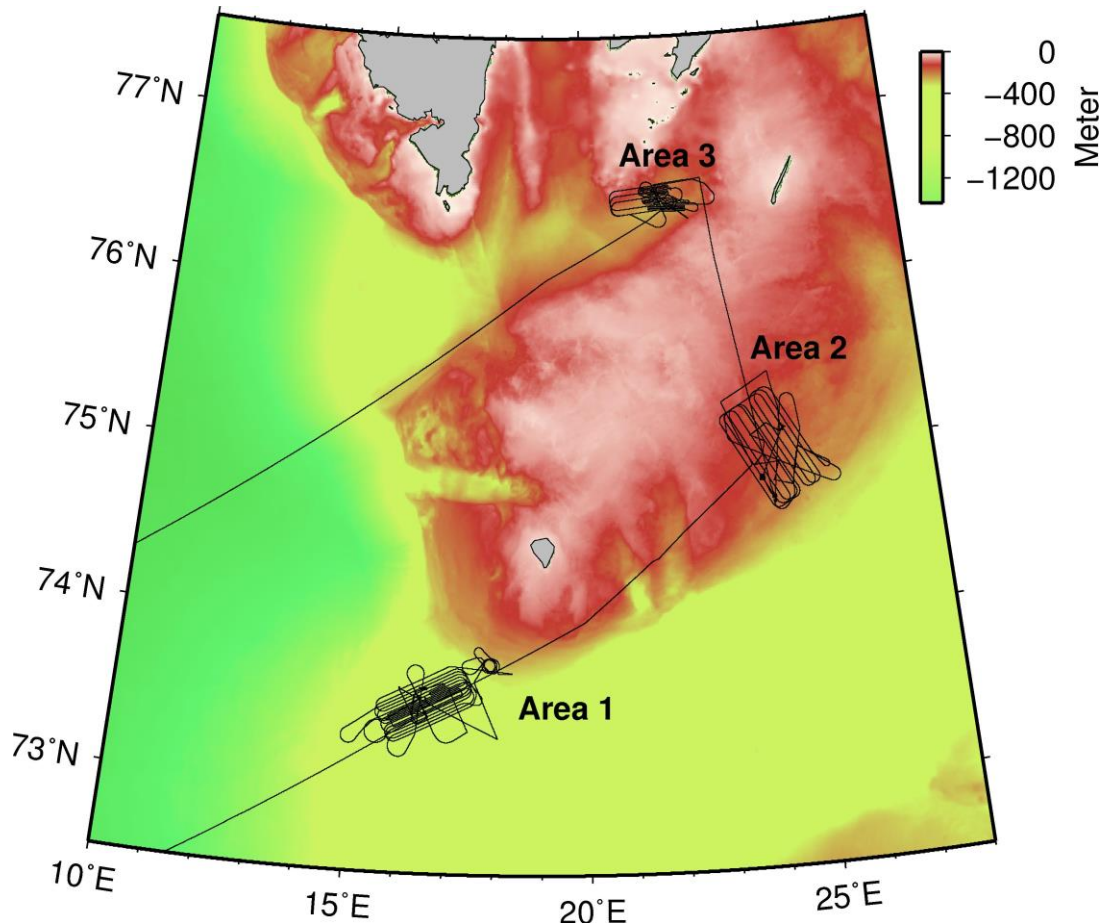


Fig. 3.2 Track chart of RV MARIA S. MERIAN Cruise MSM137. Bathymetry according to IBCAO 3.0 (Jakobsson et al, 2012). Working areas 1 to 3 are shown.

4 Narrative of the Cruise

The mobilization of cruise MSM137 started on May 7 in Reykjavik with the loading of two streamer winches and four containers to RV MARIA S. MERIAN. On May 8, 14 scientists and technicians from the BGR started to unload the equipment and the installation of the scientific instruments was started. The next day, the complete scientific crew of cruise MSM137 boarded the vessel and finalized the set-up of the laboratories.

In the morning of May 10, the vessel left the port of Reykjavik and sailed counter clockwise around Iceland with destination to the Norwegian Barents Sea. The northern Barents Sea at this time was still covered by an unusually large ice cover, with very close ice drifts just north-east of Bjørnøya.

After leaving the Icelandic EEZ in the morning of May 13, we conducted two releaser tests. These tests confirmed that the prepared acoustic releasers for the ocean bottom seismometers (OBS) are working properly. Around noon, the data acquisition was started with the recently installed Deep Sea Multibeam Echosounder EM124. 24 hours later, we switched the data acquisition to the Shallow Water Echosounder EM712, which was used for the rest of the cruise due to the shallow water depths on the Barents Shelf.

As soon as we reached working area 1, we started to deploy 16 OBS at water depths between 400 and 450 m. In addition, we measured a sound velocity profile – this data is needed to process the multibeam echosounder data. In the morning of May 15, we deployed the seismic streamer with a total length of 6,850 m. In the afternoon, we deployed the passive acoustic monitoring (PAM) system, the magnetometer cable as well as both air gun arrays. During final transit to the first line we noticed some technical issues with the tail buoy which was no longer attached to the end of the streamer cable. Therefore, we had to recover the whole cable and we were able to pick-up the freely floating tail buoy in the morning of May 16. After re-deployment of all our gear we started the production of seismic data at 17:53 UTC on May 16. The following days were characterized by a smooth data acquisition; smaller failures of seismic sources were all repaired during line changes, without loss of time. Until 17:17 UTC on May 23, we sailed a total of 19 seismic lines within working area 1. The recovery of OBS in this working area was slightly delayed by rough weather conditions, but around noon of May 25 all equipment was back on deck.

During the previous days, the ice conditions in the northern Barents Sea had greatly improved. Therefore, we decided to sail to the northern edge of working area 2. After we confirmed that this area was totally free from drifting ice, we started the deployment of 12 OBS in working area 2. The seismic cable and sources were also deployed, and at 22:43 UTC on May 26 we started seismic acquisition in working area 2. Here, a significant activity of marine mammals was found. This led to a total of seven shutdowns of seismic work as well as around 5 hours of missing seismic production. Until 13:06 UTC on June 1 we sailed a total of 14 seismic lines within working area 2. Detailed work with the multibeam system was done June 2. This allowed us to identify two active venting systems in this working area.

We conducted the transit to working area 3 in the morning of June 3. Due to the perfect wind conditions of the previous days the ice cover just recently vanished in this area. We deployed the seismic streamer in the afternoon of June 3. During this time, the weather conditions deteriorated. Therefore, we postponed the deployment of seismic sources to the next day. At

14:57 UTC on June 4 we started seismic production in working area 3. In the evening of June 4, the vessel sailed through smaller pieces of ice, but fortunately, the ice had no contact with our towed gear. Consequently, we shortened the following seismic lines. Until 05:29 UTC on June 6 we finished a total of seven lines. On June 7, we completed our bathymetric data set in working area 3. Subsequently, we started our transit back to Reykjavik. There, we arrived as scheduled in the morning of June 13.

5 Preliminary Results

5.1 Multichannel Seismics

(A. Ehrhardt, M. Engels, M. Schnabel)

For the multichannel seismic (MCS) data acquisition we used a 2D seismic setup with a tuned air gun array of 16 G-Guns with a total volume of 3100 in³ (~51 l). The trigger for the G-Guns was provided by the ORCA navigation system. Shot point spacing was 50 m. The seismic streamer cable had an active length of 6.600 m with a total of 588 channels (5,850 m with 12.5 m group distance and 750 m with 6.25 m group distance). A detailed description of the 2D MCS setup is given in Appendix 11.3.

During the cruise, we acquired 40 seismic profiles with a total length of 1,968 km. Details of the lines as well as track charts are provided in chapter 6.2. Aboard RV MARIA S. MERIAN the seismic lines were preliminarily processed in order to quality-control the seismic data and to have a first impression about the geology. The preliminary processing included:

1. Segd-input
2. resampling to 2 ms
3. P190 file import and gridding
4. Bandpass filter, Swell noise filter
5. Deghosting
6. Designature
7. First velocity analysis
8. SRME (surface-related multiple elimination)
9. Second velocity analysis
10. Offset binning
11. Prestack Kirchhoff Time migration
12. Angle stack
13. Fx deconvolution, pred. deconvolution
14. Segy output

Fig. 5.1 shows an exemplary line of working area 1 (line BGR25-108A007, see Fig 6.1 for location). Strong seafloor multiples biased the dataset due to the hard and compacted seafloor in the Barents Sea. However, SRME worked fine for this dataset and a first impression about the subsurface geology is possible. Anyhow, remnants of multiple energy still biases the datasets. Further steps like radon multiple removal are necessary. Intrusive structures are clearly imaged at a two-way traveltimes (TWT) of about 3 seconds in the area 0 to 30 km of the profile. This western part of the profile belongs to the Vestbakken Volcanic Province. The eastern part of the line shows structures at a shallower level. This area may already be part of the Stappen High.

The combination of shallow water, high seismic velocities near the seafloor and a streamer length of more than 6 km produces clear refracted signals in the shot gathers (Fig. 5.2), which are visible as first arrivals in the streamer recording. This data will be used to constrain the shallow subsurface via streamer tomography.

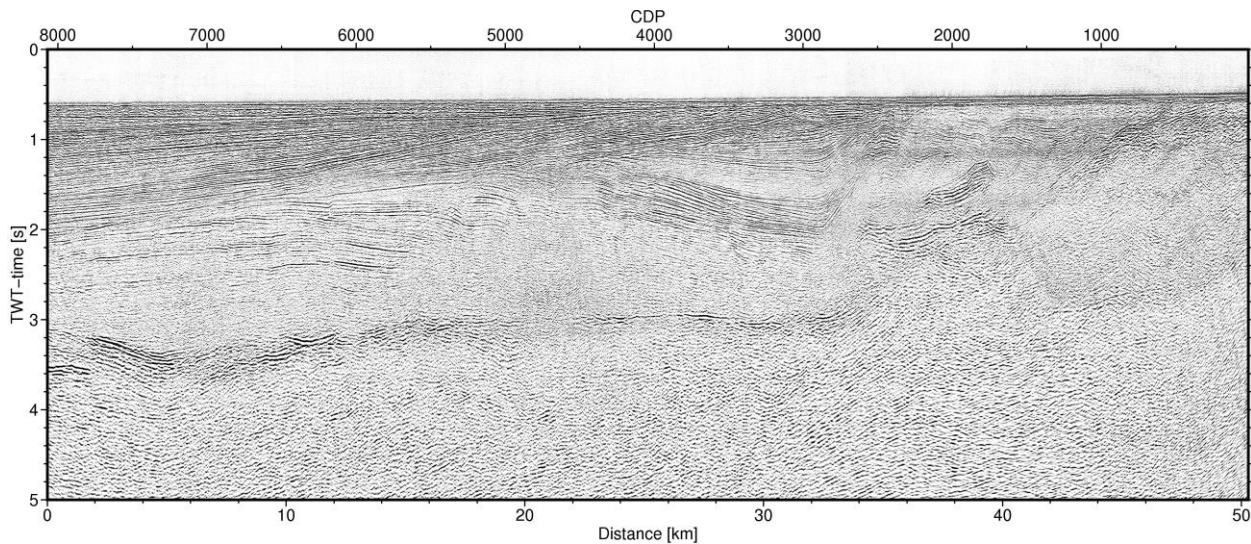


Fig. 5.1 Preliminary processed seismic line BGR25-108A007 (see Fig. 6.1 for location). The line crosses the Stappen High (to the right respectively northeast) and the Bjørnøya Basin (to the left respectively southwest). Below the sediments of the Bjørnøya Basin low frequent – high amplitude reflections are possibly caused by sills. Another set of potential sill reflections are in the transition from Bjørnøya Basin to Stappen High.

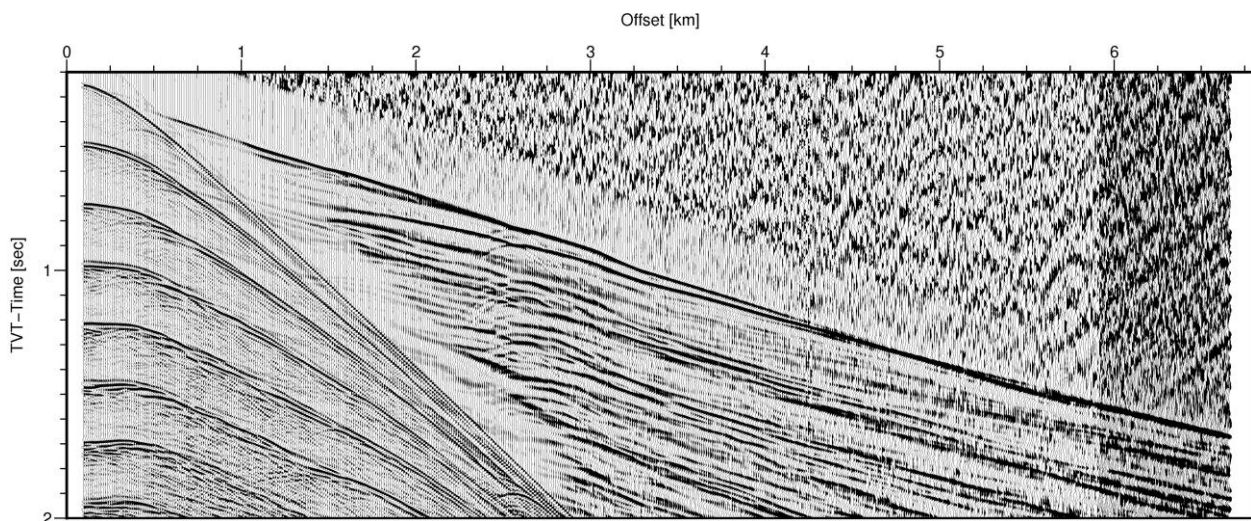


Fig. 5.2 Shot record (raw data) for FFID 34700 on line BGR25-192A048 (working area 3, see Fig. 6.3 for location). Due to the shallow water the near offset shows strong seafloor multiples. As first arrival, a clear refracted phase from the seafloor is visible. The apparent velocity of this event is about 4,500 m/s for the near offset and 5,000 m/s for the far offset.

5.2 Bathymetry (incl. SVPs and XSVs)

(C. Strassburger, V. Thamm, F. Schwer)

Data Acquisition and Processing

We used the new installed EM124 on the transit to the study area from May 13 to 14, mainly for test purposes, and then switched to the EM712 from 1,000 m water depth for the main working area of the cruise. Until May 20, we used the Multibeam in parallel with Parasound. The pulse length was set to “medium” for water depth shallower than 400 m and elsewhere to “deep”. This pulse length limited the water column data resolution, and the data interfered significantly with

Parasound. From May 20 onwards we used the K-Sync trigger box, first we tried 6:1 (6x EM712 to 1x Parasound) but it quickly became clear that the resolution of the Parasound was getting really bad, so we switched to 3:1 and finally to 2:1. The EM 712 acts as an external trigger and the Parasound is set to a fixed time between 800 and 1200 ms depending on the water depth and the time the EM712 needed to ping and receive once. So from May 20 we operated with trigger box and set the pulse length to shallow and left it until the end of the trip. Only on May 24 we set the pulse length to “very shallow” for improved flare imaging. For the EM712 we always used FM chirp, a strong slope filter, 3° pitch tilt, and a strong penetration filter, which resulted in clearly better data. For all slow profile lines (< 5 kn), which corresponds to the seismic profiles, we used the single ping mode. From June 6 onwards, the survey lines were sailed with 6 to 7 knots in “dual fixed” and subsequently “dynamic” mode. All data were acquired using the Kongsberg Simrad SIS (Seafloor Information System) software and the recorded bathymetry and backscatter data were stored as Kongsberg *.all files. Water column data were stored as *.wcd files. The backscatter (amplitude) signal was stored and preprocessed automatically by the Kongsberg software Seafloor Information System (SIS), including altitude processing, time varying gain (TVG) and angle varying gain (AVG) assuming a flat seafloor. The bathymetry data were processed with QPS Qimera (v. 2.7.1) and vertically referenced with the EGM2008-model. The backscatter data were processed with QPS FMGT (v. 7.11.1).

Sound Velocity Profile

The research area is characterized by a dynamic water column and we therefore regularly collected sound velocity profiles (Fig. 5.3). Using an AML Oceanographic AML-3 LGR multiparameter probe capable of acquiring data down to 6000 m water depth. After third use, we had enormous problems connecting the probe to the computer. So we switched to the AML Oceanographic Plus X probe. During the acquisition of sound velocity profiles, the vessel was stationary, the profiles were taken by the winch with rope speed of 0,8 m/s. The Sailfish acquisition software for the AML-3 and the SeaCast software for the AML Plus X directly calculates the sound velocity from the measured values. During the seismic profiling trip. SVP profiles were taken using Lockheed Martin Sippican XSV-02 Expendable Sound Velocimeter Probes. With these probes, the sound velocity is measured directly and recorded via the latching device which is connected to the evaluation software WinMK21. We used 18 SVP profiles during the whole expedition, three of which with the AML-3, three with the AML Plus X and 12 XSV-02 probes (Fig. 5.3).

We used the downcast values from the AML probe as the sound velocity profile. Following acquisition, selected sound velocity profiles were loaded into the multibeam SIS software during surveying. The lines were recalculated during post-processing with QPS Qimera.

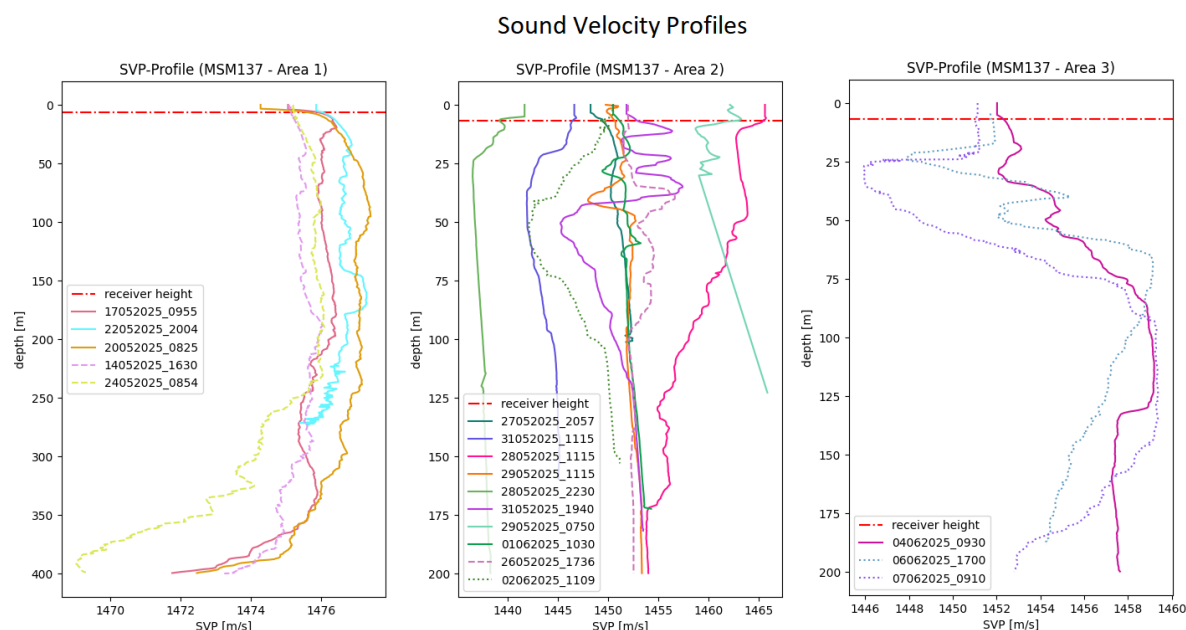


Fig. 5.3 Sound velocity profiles collected during MSM137 for each working area. Plotted are the 18 sound velocity profiles which were used during the cruise. The measured SVPs with the AML-3 is plotted with a dashed graph, with the AML Plus X with a dotted graph and with the XSV-02 SVPs with a line. The names of the profiles correspond to the date and time of sampling. The red dashed and dotted line corresponds to the height of the multibeam array at the hull of the vessel.

Preliminary Results

In total, we collected about 7,980 km² of multibeam data (Table 5.1) with a depth range of 3,712 to 44 m, whereby the main investigation areas in the depth interval of 500 to 44 m. The backscatter data shows a variation between -12 to -36 dB.

Table 5.1 Data coverage of the measured area with multibeam echosounder divided into the System and the three working areas and the transit.

	EM124:	EM712:				
	transit to working area 1:	working area 1:	transit to working area 2:	working area 2:	transit to working area 3:	working area 3:
in km ²	3040,75	2532,8605	202,5752	1347,669	58,7441	795,6992
	total [km ²]: 7978,298					

In the first working area, the lowest point is located in the southwest at about -500 m. The terrain rises with a relatively slight incline in a northeasterly direction and reaches its maximum of -200 m there (Fig. 5.4a). A striking feature of this area is that the seabed has numerous furrows that are up to 3 m deep, in some places even up to 7 m deep. The furrows are between 500 m and over 30 km long and are mostly meandering rather than exactly straight. These are interpreted as iceberg plough marks. However, a clear main direction of the furrows cannot be recognized; they are rather irregularly distributed, with a tendency from northwest to southeast. In addition, parallel, relatively flat and straight furrows are noticeable, which indicate trawler marks.

In the northeastern most part of the area, the furrows are less pronounced and in places merge into small, punctiform depressions. These structures could be the result of repeated icebergs touching down during high and low tide. The shallower water depth in this area favors such dynamics, which shows a clear difference to the deeper southwestern section. The furrows are also visible through the backscatter. However, weaker backscatter is visible in the northeastern area than in the southwestern area (Fig. 5.4b), which indicates that finer sedimentary material is present in the northeast.

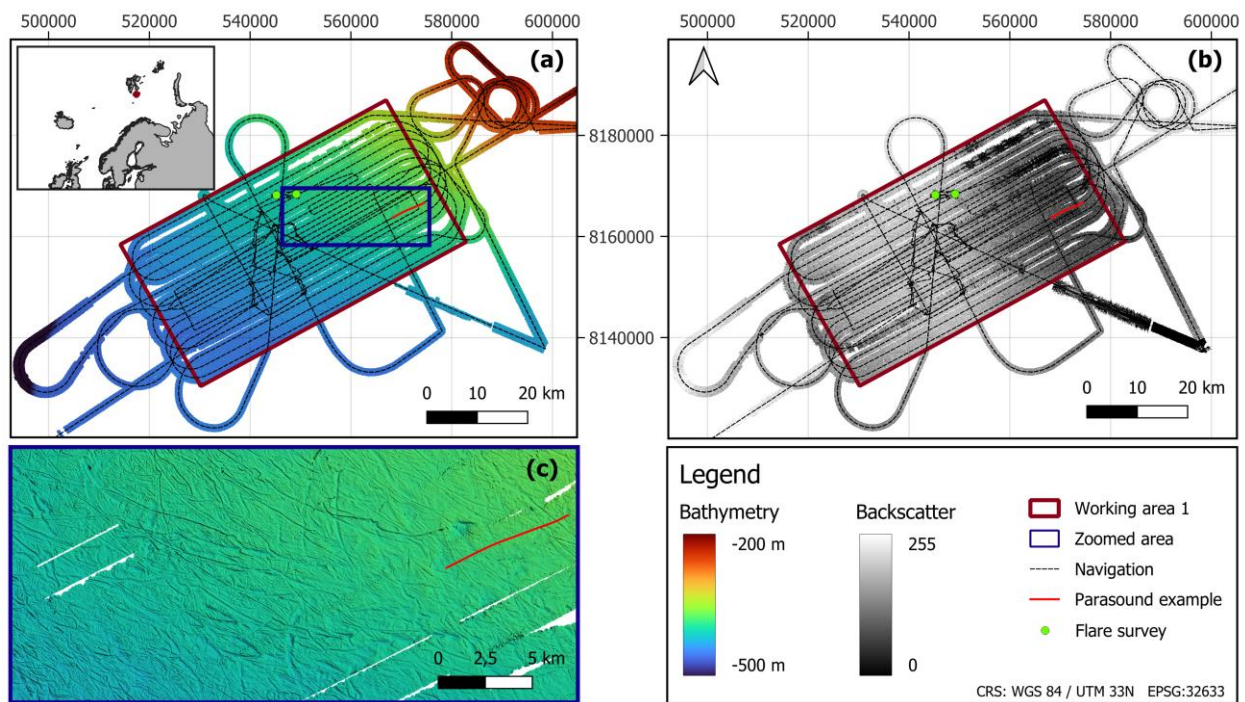


Fig. 5.4 Bathymetric map with EM712 data acquired during MSM137 with insert overview map (a) and the corresponding backscatter (b) of working area 1. High backscatter is bright/white and low backscatter is dark/black. A zoomed section of the bathymetric map is shown in (c) to make the furrows clear visible, which are also visible in the backscatter.

In the second working area, the lowest point (-260 m) is in the southeast. The terrain rises with a slight incline in a northwesterly direction and reaches its highest point there at around 60 m (Fig. 5.5a). Striking features in this area are relatively small but extremely steep elevations with heights of up to 40 m (Fig. 5.5c), which can be seen sporadically from the center of the area to the north.

In addition, numerous pockmark structures with diameters between 20 m and 600 m can be observed and are distributed relatively regularly in the area from west to northeast. These structures have presumably smoothed out the furrows that also occur in this area.

In the backscatter (Fig. 5.5b), a lower intensity is recognizable in the northwest, which indicates finer sedimentary material. This lower intensity extends to the enlarged section in Figure 5.5d. Here it can be seen that the elevations have the same intensity as the surrounding area, which indicates they consist of the same material like the surrounding.

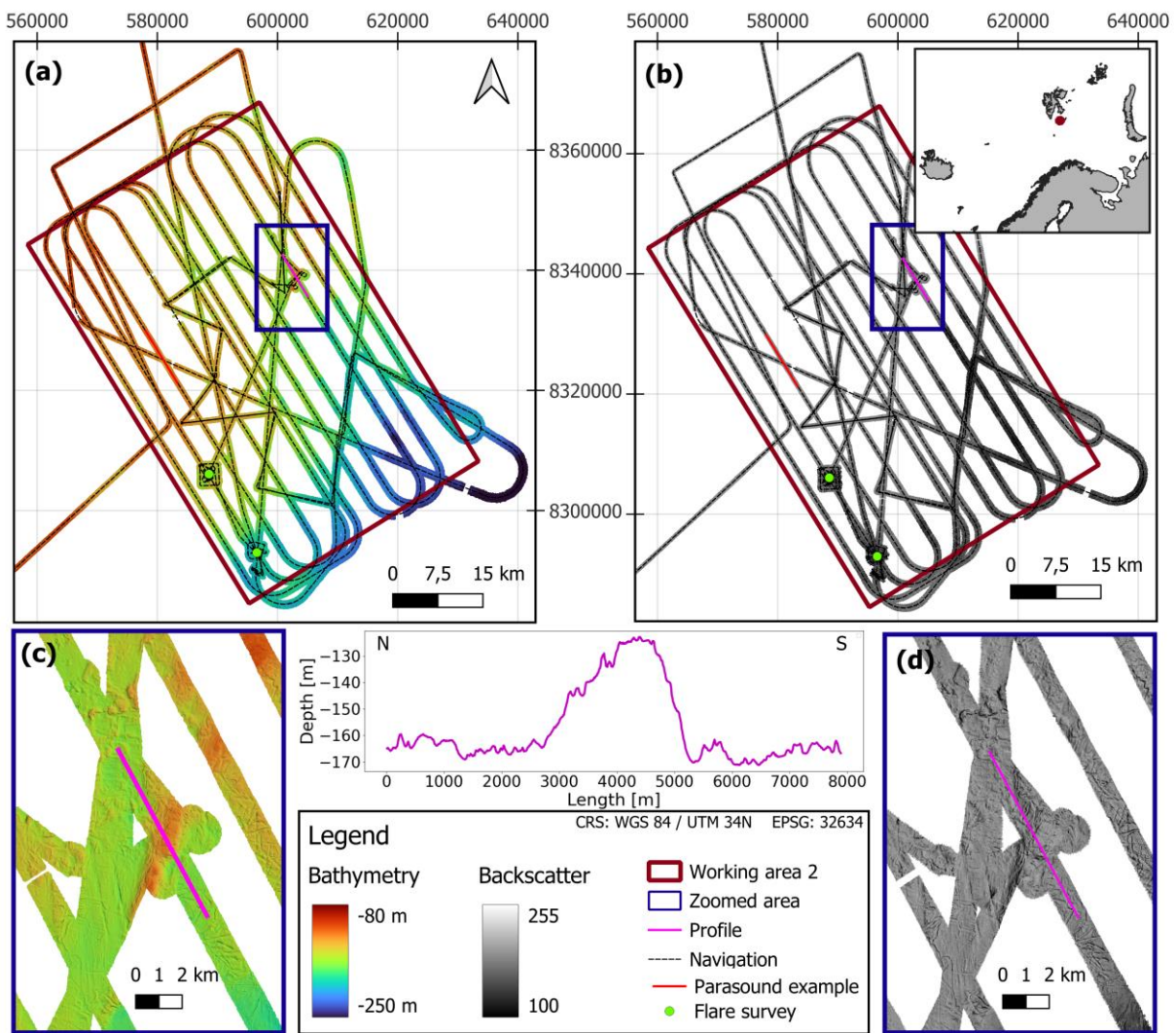


Fig. 5.5 Bathymetric map of working area 2 during MSM137 (a) and the corresponding backscatter with an overview map (b). High backscatter is bright/white and low backscatter is dark/black. A zoomed area over an approx. 30 m elevation is shown for the bathymetry in (c) and the backscatter in (d). The magenta colored profile is shown in the center of the figure.

In the third survey area, the lowest point is in the center (-230 m), while the highest, apart from the basement elevations, is found in the northwest at around -44 m (Fig. 5.6a). In the southern part of the mapped area, numerous small pits with diameters between 3 m and 15 m were also identified and are clearly visible in the magnification area marked in orange.

Distinctive basement highs are visible in the center, which stand out clearly with heights of up to 50 m. An erosion direction from northeast to southwest can be observed (Fig. 5.6c). The basement highs differ clearly in the backscatter and show a higher intensity, which indicates coarser material (Fig. 5.6d).

Erosive structures can be seen around the platforms, which are characterized by high backscatter values in the form of ripple-like patterns. The deeper areas, on the other hand, show a rather weak backscatter intensity and thus indicate finer sedimentary material.

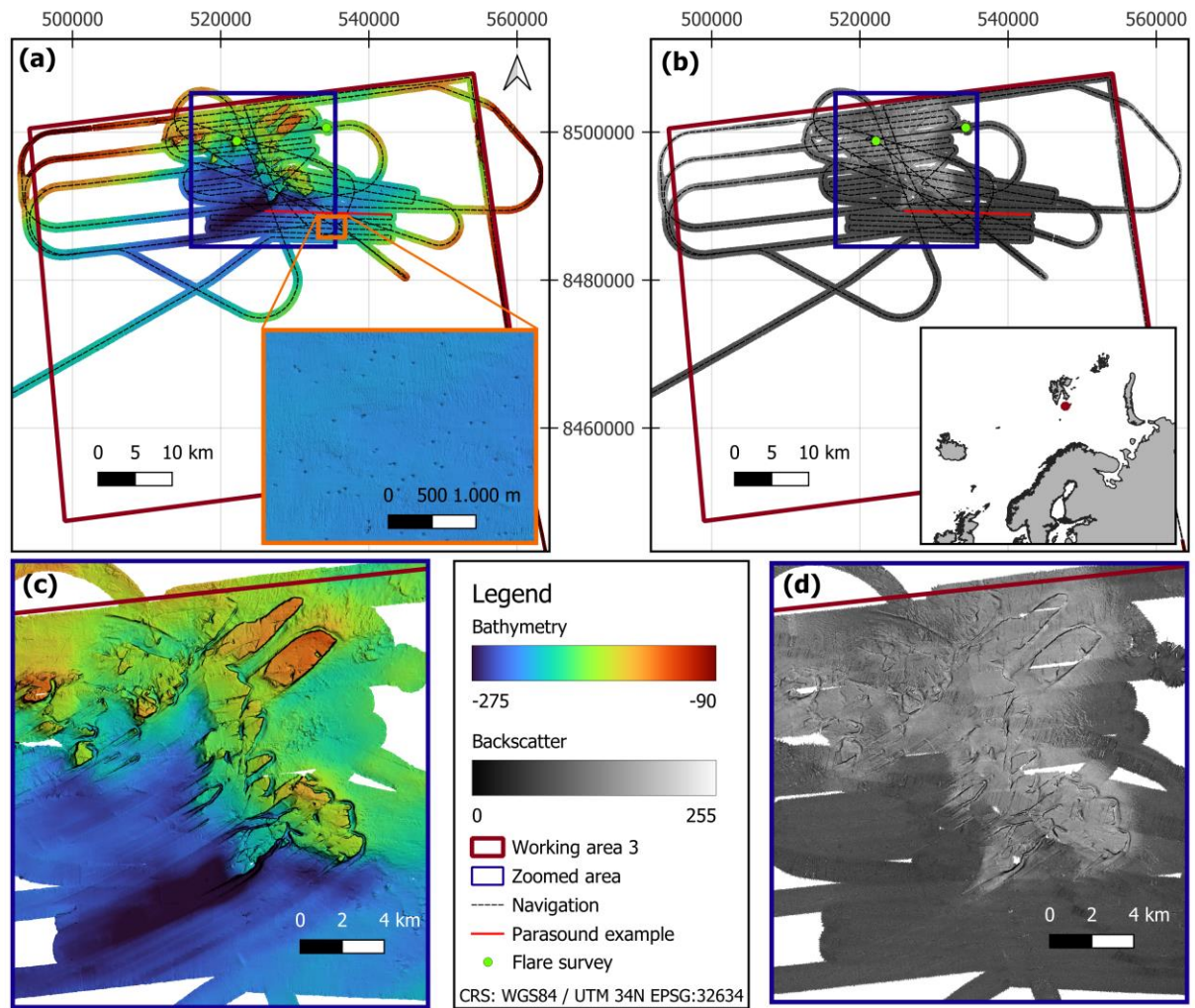


Fig. 5.6 Bathymetry (a) and backscatter (b) map of working area 3. The orange enlarged area shows pit structures. The bathymetry and the backscatter are shown magnified for the basement highs in (c) and (d). High backscatter is bright/white and low backscatter is dark/black.

5.3 Parasound Sediment Echosounder

(V. Thamm, C. Strassburger, F. Schwer)

Data Acquisition and Processing

The Parasound system was first switched on when entering international waters on May 13 at 12:53 UTC, and was finally switched off on June 8 at 01:09 UTC upon departing the working area at the end of the cruise. We did not record data while being on station and recovering OBS on May 14, May 24 and May 25 in working area A. Additionally, the storage was switched off during flare imaging on May 24 and during the patch test calibration survey on June 2. The software failed on the June 13 but was subsequently running continuously. During seismic survey in working area 1 from May 16 until May 23 the seismic source induced a vibration of the ship and caused periodic interferences in the Parasound data. Additionally, we assume more interferences triggered by other vessels operating in the same area. The interferences caused by the seismic source appeared again while surveying from May 26 until June 1 and from June 4 until June 6 in working area 2 and 3, respectively. Between start of pinging on May 13 until

May 20 18:52 UTC the Parasound system was used in single pulse pinging mode. From there on the Kongsberg K-Sync trigger box was used which controlled the pinging of the EM712 and the Parasound until the end of data acquisition. After some testing on May 20 the Parasound was operated with a fixed delay between 850 ms and 1200 ms depending on the water depth in the working areas which varied between 500 m and 50 m approximately. Thereby the roundtrip time was equally to the roundtrip time of the EM712. A ping ratio of 1 (PS70) to 2 (EM712) was chosen in order to ensure a sufficient data quality of the bathymetric and water column data. After enabling the trigger box, the trigger box crashed several times on June 1 and once on June 2 due to the EM712 which resulted in short data gaps. After creating a new survey in the EM712 the system was running continuously again and the Parasound functioned smoothly and reliable during the trip.

Both PHF and SLF were recorded via Parastore and stored as *.asd, *.ps3. The PHF signal was used for detecting rising gas bubble in the water column (flares) and the SLF data (4 kHz) was used to collect sub-bottom information. The depth window of the online displayed PHF and SLF data was controlled manually. The *.ps3 PHF and SLF data were then converted to larger *.sgy-files using the ps32sgy tool (written by Hanno Keil, University of Bremen). The software allows the generation of one SEG-Y file for longer time periods, frequency filtering (low cut 2 kHz, high cut 6 kHz, 1 iteration), subtracting the mean and envelope calculation. We used the described tools and loaded all data into HIS Kingdom ® software (Version 2020) for visualisation.

Preliminary Results

The acquisition of Parasound data shows three different sub-bottom cases of the three working areas. Working area 1 was characterised by low penetration due to hard rock. The seafloor is highly escarped by furrows that we interpret as iceberg plough marks, which have no clear orientation, deepness or length. In working area 2, iceberg plough marks can be found again, but beneath, some sediment layers can be identified down to some 10 ms. This layer is distributed in the south of working area 2 and is interrupted by acoustic blanking. In working area 3, we find the largest penetration into the sub-bottom and can identify three units nearly in the entire area.

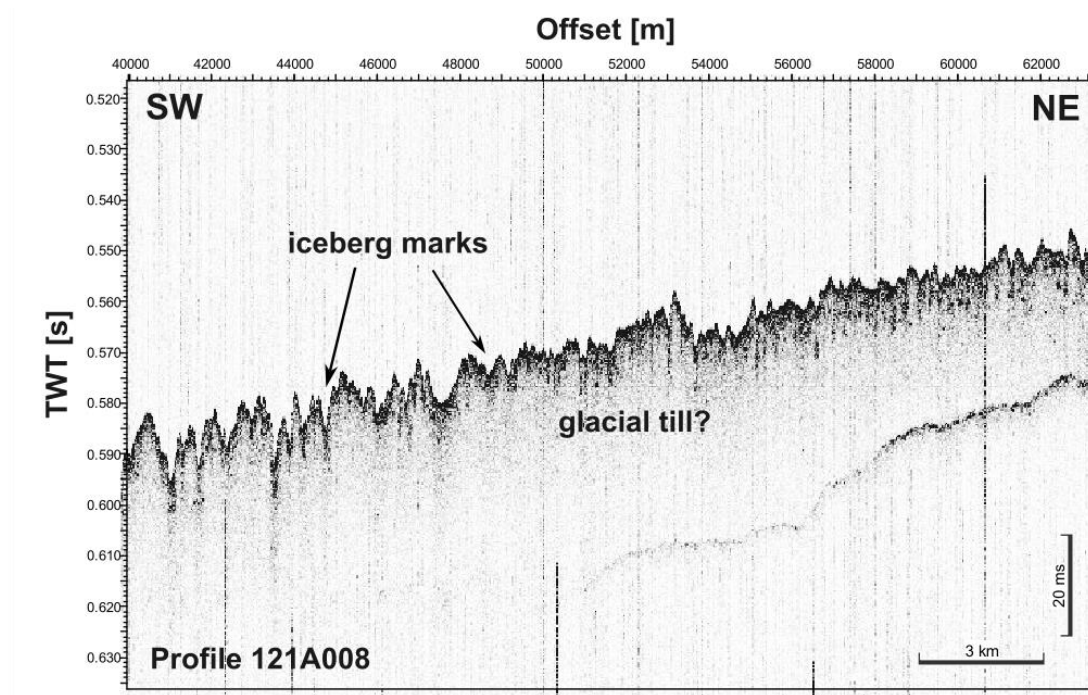


Fig. 5.7 SLF data example profile 121A008 of working area 1 in the northeastern part shows a strong seafloor reflector, which is escarped by many iceberg plough marks. A second reflector dips from northeast to southwest and disappears at the half of the figure.

The SLF profile 121A008 from working area 1 shows a strong and rough seafloor reflector, which is marked by iceberg marks (Fig. 5.7). They occur in a chaotic manner over the entire working area 1. The seafloor dips from northeast to southwest. A second reflector at 0.575 s TWT is visible, which extends towards the south and disappears at 50 km offset. The reflector has a weaker amplitude than the seafloor reflector due to the energy loss during penetration of hard rock. The upper layer can be interpreted as glacial till. The vertical interferences are side effects of seismic shooting and the induced vessel's vibrations. The second reflector is only visible in the northeastern part of the working area and runs out after approximately 10 km from the start of the profiles. Apart from this reflector, no other layers are visible.

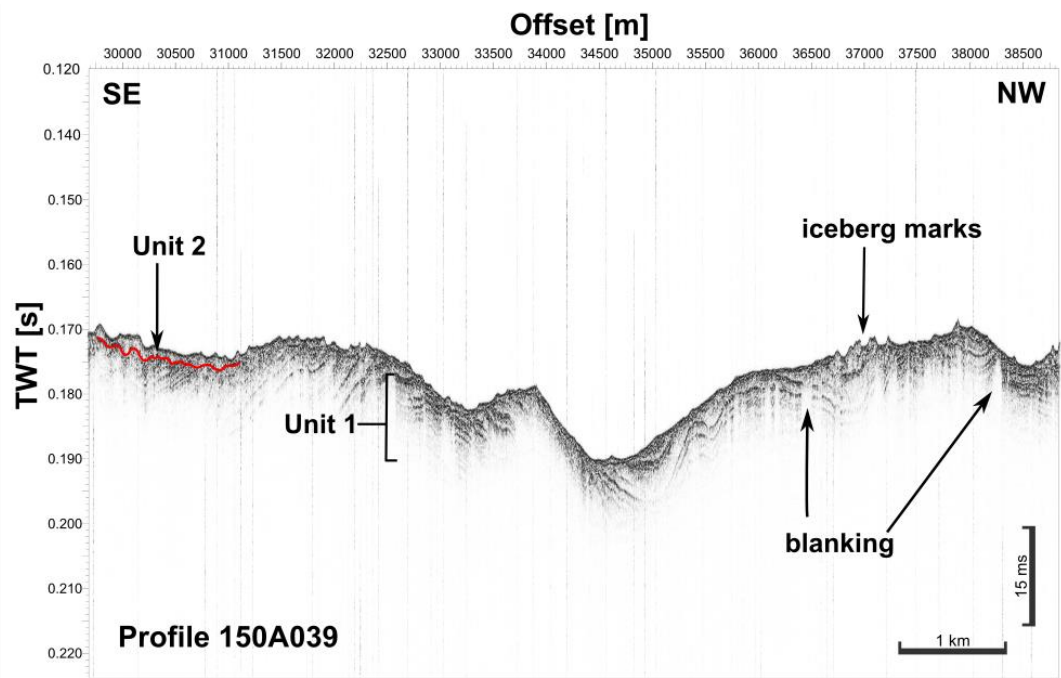


Fig. 5.8 The profile 150A039 shows again an iceberg marked seafloor reflector in working area 2. Beneath the upper thin Unit 2 indicated by the red line on the left, a stratified layer of older sediments is visible, which shows several discontinuities and undulations. The blanked parts in this Unit 1 can be interpreted as gas.

The figure 5.8 shows a SLF profile 150A039 extending from northeast to southeast in the southern part of working area 2 again showing some iceberg plough marks, without any preferred orientation. We divided the profile into two units. The older and lower Unit 1 shows some stratified layers with discontinuities and undulations. Additionally, acoustic blanking occurs at some parts within Unit 1, which we attribute to shallow gas. This unit is not always visible in the profile. Between an offset of 34 to 34.5 km, Unit 1 is not seen. On top of Unit 1, a thin transparent layer is defined as Unit 2, which reaches up to the seafloor surface. The lower boundary is indicated by the red line on the left side. The layer varies in thickness due to the iceberg plough marks.

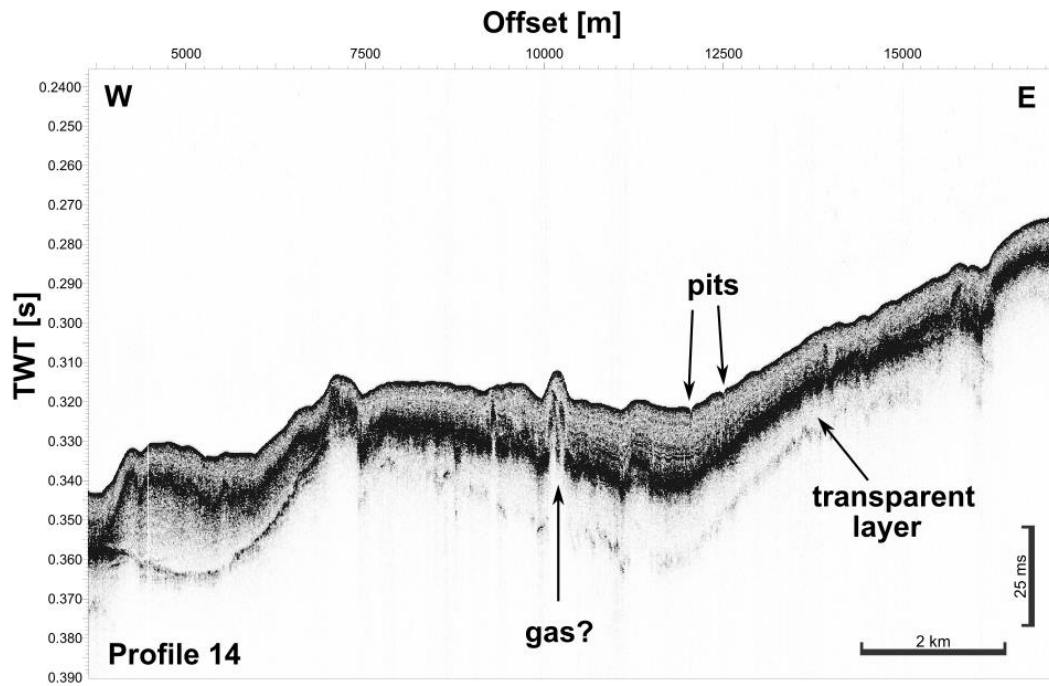


Fig. 5.9 The SLF profile 14 of the working area 3 shows pits in the seafloor reflector. At 10 km offset a path of upward migrating gas which elevated the seafloor could be interpreted.

The SLF profile 14 (Fig. 5.9) acquired during the bathymetry survey in working area 3 did not suffer in any of the former interferences. We can divide the profile into 3 units, with Unit 1 as the oldest, terminating on the western end of the profile at 0.36 s TWT. The upper boundary reflector has a higher amplitude in the west than in the east, where it is nearly invisible due to the thick and high amplitude reflector above. Unit 2 is characterised by a strong reflector confining the upper boundary. The Unit is mostly transparent and interrupted at an offset of 7 km. The uppermost unit 3 is less transparent but shows no clear stratification. The seafloor reflector shows small depressions (pits), which can be also seen in the bathymetry. At an offset of 10 km the seafloor is elevated, and the strong reflector of Unit 2 is interrupted and blanked out. This can be interpreted as upward migrating gas.

5.4 Water Column Imaging

(C. Strassburger, V. Thamm, F. Schwer)

The Kongsberg EM712 multibeam echo sounder works with high-frequency acoustic pulses (70 – 100 kHz) that are emitted into the water column in a fan shape. Time-of-flight measurement and angle-dependent signal processing (beamforming) enable reflected signals from different depths and directions to be detected precisely. In addition to the bathymetric measurement, the recording of water column data enables the analysis of acoustic scattering within the water column, for example due to schools of fish, gas leaks or other heterogeneous structures. The data is saved as .wcd files using the SIS software. To handle the large data volumes we downsampled the water column data in processing using FMMidwater (QPS) by a factor of two. After reviewing the water column data, suspicious targets were identified, which were subsequently resurveyed by a dedicated, slow sailing speed flare imaging survey. Two locations in each survey area were examined more closely. The dedicated flare imaging surveys were sailed in figures of

eights with minimum speed (<2 kn) to resolve individual gas bubbles and to determine ascent speeds. Except for the first survey area, all the flare surveys were successfully completed with identification of signals meeting the criteria for gas bubble detection over fish as a possible candidate for confusion.

The filtered fan recordings from working area 2 are shown in Fig. 5.10, which show clear bubble rises in the form of increased amplitudes in the center. The red line at the bottom represents the seabed. The example on the left is located in the northern part and the one on the right in the southern part of the zoomed area yellow outlined shown in Fig 5.11. Gas rises of up to approx. 75 m can be detected in the northern part and up to approx. 85 m in the southern part. In both areas, an extremely large number of strong gas seeps are observed.

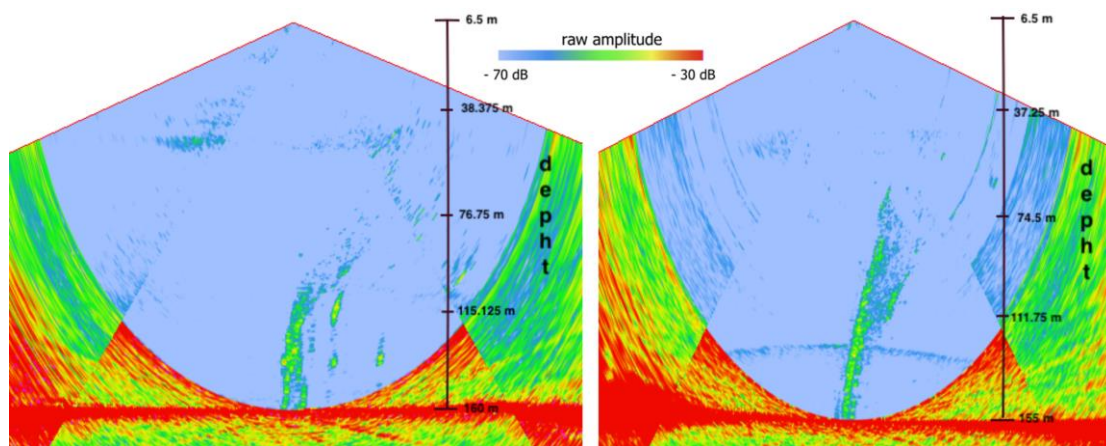


Fig. 5.10 Filtered multibeam echo sounder fan images from working area 2 show clearly pronounced gas seeps in the central area of the image. These seeps can be recognized by increased acoustic amplitudes in the water column, which indicate rising gas bubbles.

After analyzing the data, QPS Fledermaus was used to create a model to link gas flares with underlying bathymetry (Fig. 5.11). It can be seen that in the northern survey (blue outline) the gas flares do not originate directly from the pockmarks but rather from the margins. The southern flag survey (outlined in yellow) shows that gas seeps are predominant in the iceberg furrows.

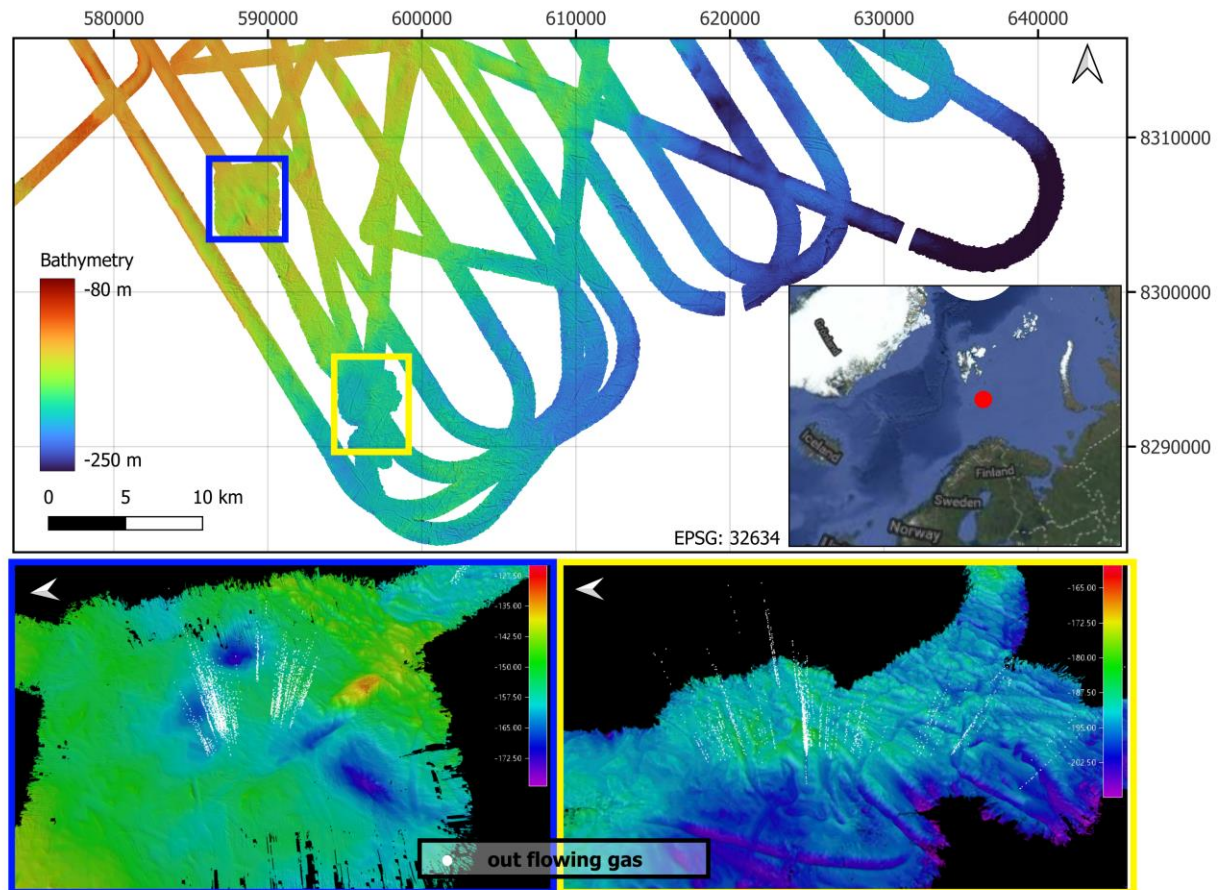


Fig. 5.11 Overview map of the bathymetry from working area 2 with model-generated images of the seabed and its out flowing gas which are white color-coded.

5.5 Magnetics

(U. Barckhausen)

The magnetic data collected on more than 30 profiles totaling 2,776 km in the three survey areas during cruise MSM137 provide the basis for an analysis of small-scale magnetization contrasts in the selected areas of the Barents shelf. The general expectation was that a generally weakly magnetized continental basement in the background may be locally overprinted by magmatic intrusions into the massive overlying sedimentary layers. Whether such intrusions cause a detectable magnetic signal at the sea surface depends on their depth and on how massive they are. The best chance to get a clear magnetic signal from such an intrusion is when at a clearly defined intrusion edge a strong magnetization contrast to the surrounding sediments exists.

The preliminary magnetic anomaly map compiled from the data collected in area 1 show the expected low amplitude anomalies with short wavelengths with only a few higher amplitude anomalies. Most striking is a small-scale but high amplitude negative anomaly almost in the center of the survey area, which is clearly documented on three of the survey lines (Fig. 5.12). It remains to be seen in the post cruise data evaluation and modeling whether this negative anomaly can be attributed to intrusive structures.

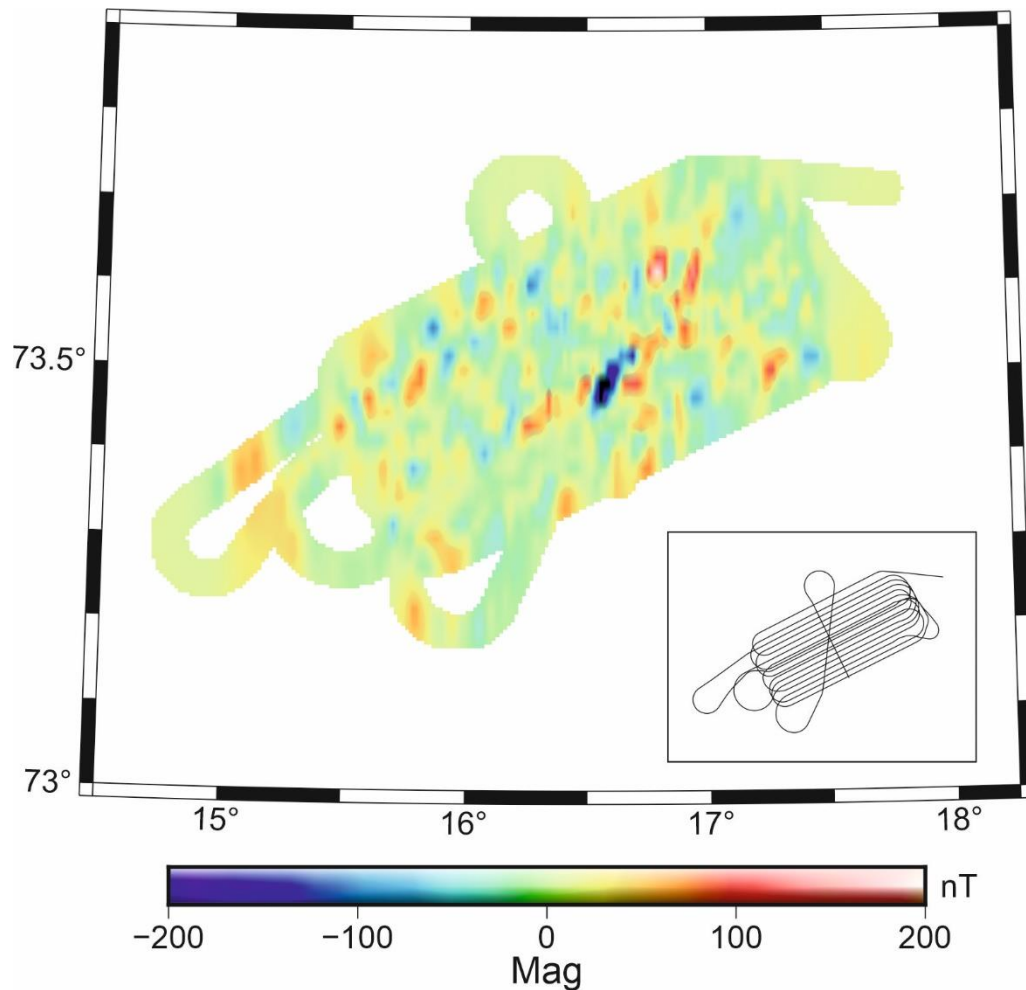


Fig. 5.12 Preliminary magnetic anomaly map of survey area 1. The inset shows a sketch of the survey lines. Data of the grid are shown up to 2.5 km distance from the ship track.

The magnetic anomaly map of survey area 2 (Fig. 5.13) shows similar characteristics to Area 1. Even though the coverage with survey lines is less dense than in the case of Area 1, the same type of low amplitude anomalies with short wavelengths with only a few higher amplitude anomalies is present. A prominent small-scale but high amplitude negative anomaly almost in the center of the survey area is accompanied by some higher amplitude positive magnetic anomalies in the western part of the survey area. How these anomalies relate to intrusive structures needs to be tested in a comparison with the other geophysical data and modeling efforts based on a concept of the structural elements present in the survey area 2.

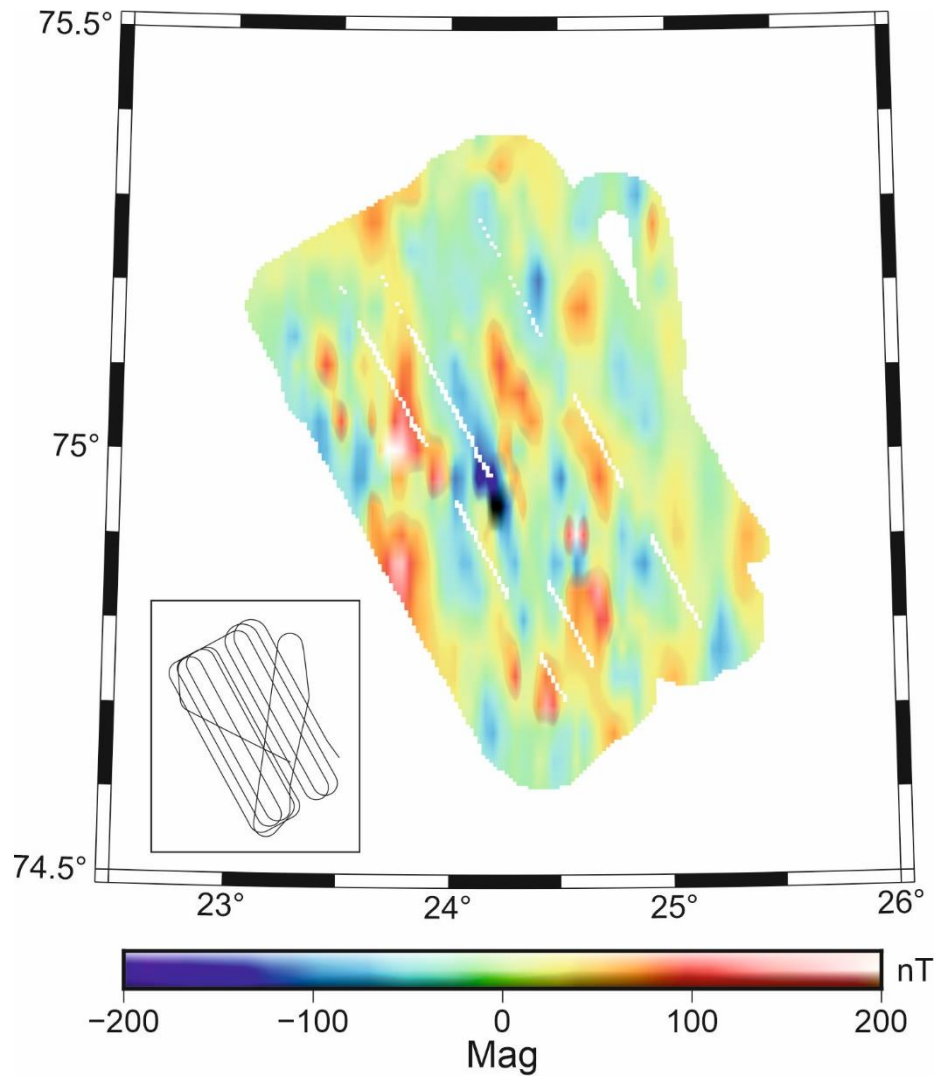


Fig. 5.13 Preliminary magnetic anomaly map of survey area 2. The inset shows a sketch of the survey lines. Data of the grid are shown up to 2.5 km distance from the ship track.

Due to limited time, shallow water depths, and weather conditions, only four survey lines could be completed with magnetics in survey area 3. This coverage is not sufficient for compiling a magnetic anomaly map. Therefore, Fig. 5.14 shows the measured and processed data as wiggles along the survey track lines. The general trend is the same as in the areas 1 and 2 with relatively low amplitude magnetic anomalies of short wavelength pointing at small magnetization contrasts in the shallow sub-surface of the sea bottom. In the case of area 3, no prominent single anomaly was detected. However, the limited data coverage may have hindered the detection of such anomalies between the survey lines.

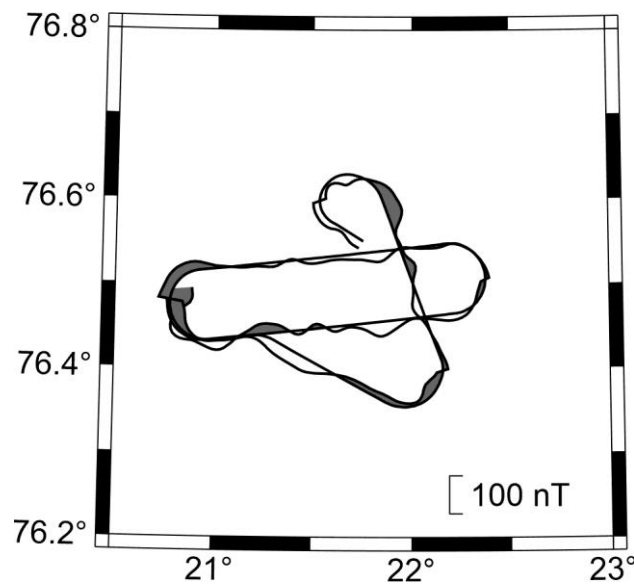


Fig. 5.14 Magnetic data of four survey lines in area 3 shown as wiggles along the track lines of the ship. Positive anomalies are filled in grey color.

5.6 Gravity

(I. Heyde, U. Barckhausen, S. Bellenberg)

System Overview and Data Processing

During cruise MSM137 MIBAS a sea gravimeter system KSS32-M was installed in the Gravimeter Lab one level below the main deck. The KSS32-M (S/N 21) is owned by BGR and was installed on May 8 when RV MARIA S. MERIAN moored in Port Reykjavik harbor.

The gravimeter system KSS32-M is a high performance instrument for marine gravity measurements, manufactured by BGGs (Bodenseewerk Gravimeter Geosystem GmbH). The straight-line gravity sensor is installed on a gyro-stabilized platform. It is thus a relative scalar instrument measuring differences in vertical gravity acceleration. The system is controlled by a notebook which transmits also the data to the BGR data acquisition and processing system in the Data Processing Lab on the main deck. The data were recorded with a data rate of 1 Hz. Online ship navigation data from the BGR system are sent to the KSS32-M to support the stabilizing platform.

The relative gravity measurements have to be connected to the International Gravity Standardization Net IGSN71. Furthermore, the instrumental drift of the KSS32-M can be derived by the tie measurements at the beginning and the end of the cruise. For the connection measurements a LaCoste&Romberg gravity meter, model G, no. 666 was used. The measured instrumental drift was only -2.63 mGal in about 34.15 days reflecting the excellent quality of the gravity sensor.

The processing of the gravity data was performed onboard and resulted in free-air gravity anomalies. The data had to be slightly low pass filtered. Infrequent outliers were removed manually in advance. Additionally, data recorded during sharp turns and rapid speed changes of the vessel show disturbed values and were removed manually.

Gravity anomaly maps

Gravity measurements were carried out continuously during the complete cruise. However, the data acquisition started only after leaving the EEZ of Norway (13.05.2025, 12:50 UTC), respectively was stopped leaving the working area (08.06.2025, 01:52 UTC). Additionally, data on the transit back were acquired in international waters on the 09.06.2025 (02:27 – 13:40 UTC). Therefore, gravity data along all survey profiles and transit profiles to and between the three survey areas with a total length of about 4,650 km were measured.

Fig. 5.15 shows the map of the free-air gravity anomalies in survey area 1. The anomalies range from about 0 mGal in the SE to +55 mGal in the NE of area 1. It is remarkable that the anomalies are independent from the bathymetry which is generally decreasing from SW to NE. The most prominent features are two connected gravity maxima whereby the eastern one is more pronounced. They probably result from basement highs. Towards east the decreasing gravity indicates an increase in the sediment thickness.

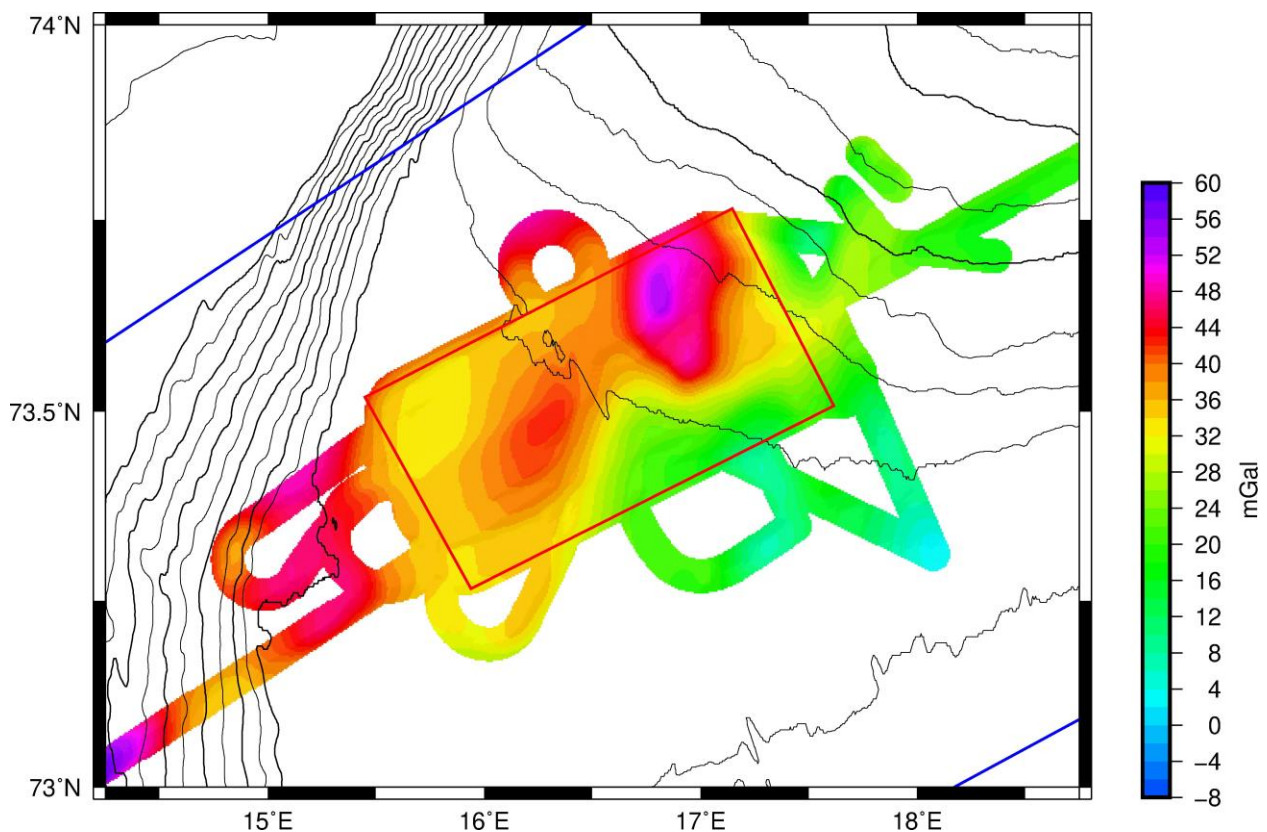


Fig. 5.15 Map of the free-air gravity anomalies acquired during cruise MSM137 in survey area 1. The map is drawn up to a distance of 2.5 kilometers from all tracks with considered data. The map is based on a 0.25 x 0.25 km grid and is underlain by the GEBCO_2024 bathymetry.

Fig. 5.16 shows the map of the free-air gravity anomalies in survey area 2. The anomalies range from about -8 mGal in the SE to +26 mGal in the SW of area 2. The general decrease of gravity towards SE reflects the increasing water depth. The two gravity maxima in the SE and NE again give indication to localized basement highs.

Fig. 5.17 shows the map of the free-air gravity anomalies in survey area 3. The anomalies range from about -6 mGal in the north central part to +12 mGal in the NE. Low gravity values reflect the bathymetry with water depths of more than 200 m. With decreasing water depth the

gravity values increase towards N and E. Small gravity maxima give hints to local basement highs.

The data will be combined with the bathymetric data from the cruise and gravity and bathymetric from global data sets. Afterwards Bouguer and isostatic gravity anomalies will be determined. Additionally forward density modeling will be performed along selected MCS lines taking into account the structural interpretation and the results of the velocity distribution.

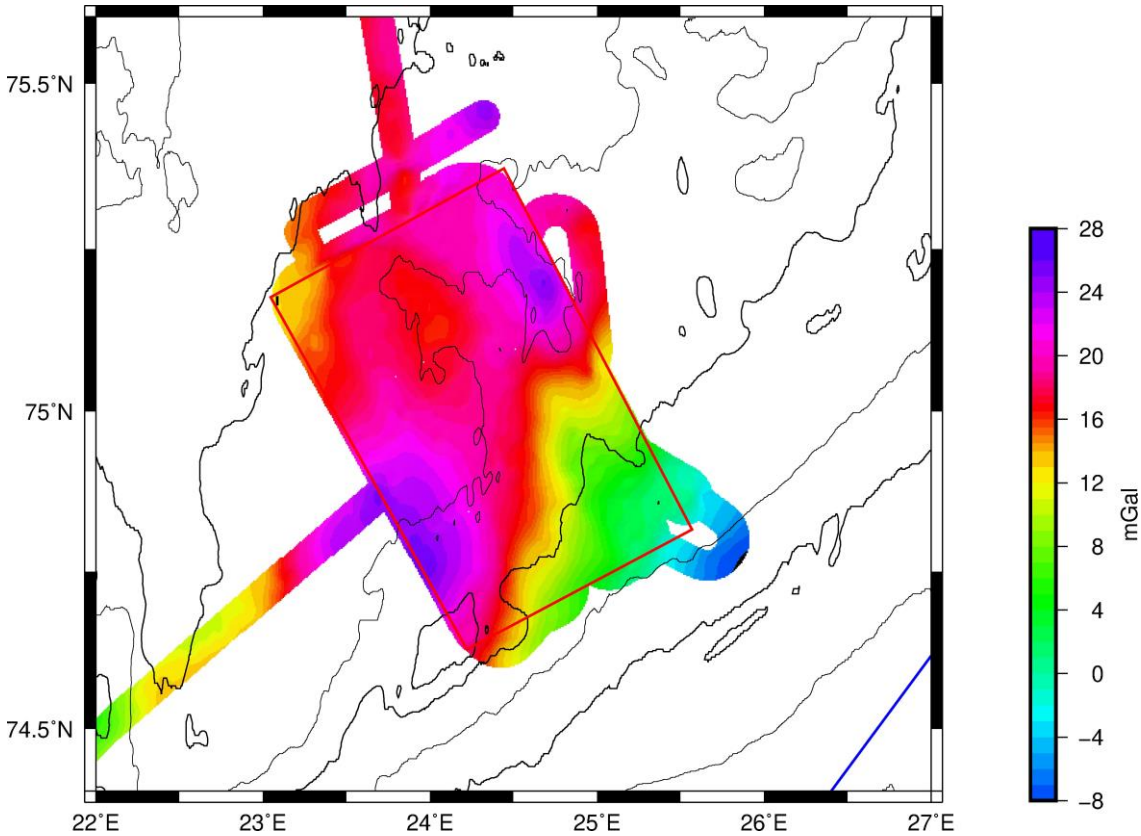


Fig. 5.16 Map of the free-air gravity anomalies acquired during cruise MSM137 in survey area 2. The map is drawn up to a distance of 2.5 kilometers from all tracks with considered data. The map is based on a 0.25 x 0.25 km grid and is underlain by the GEBCO_2024 bathymetry.

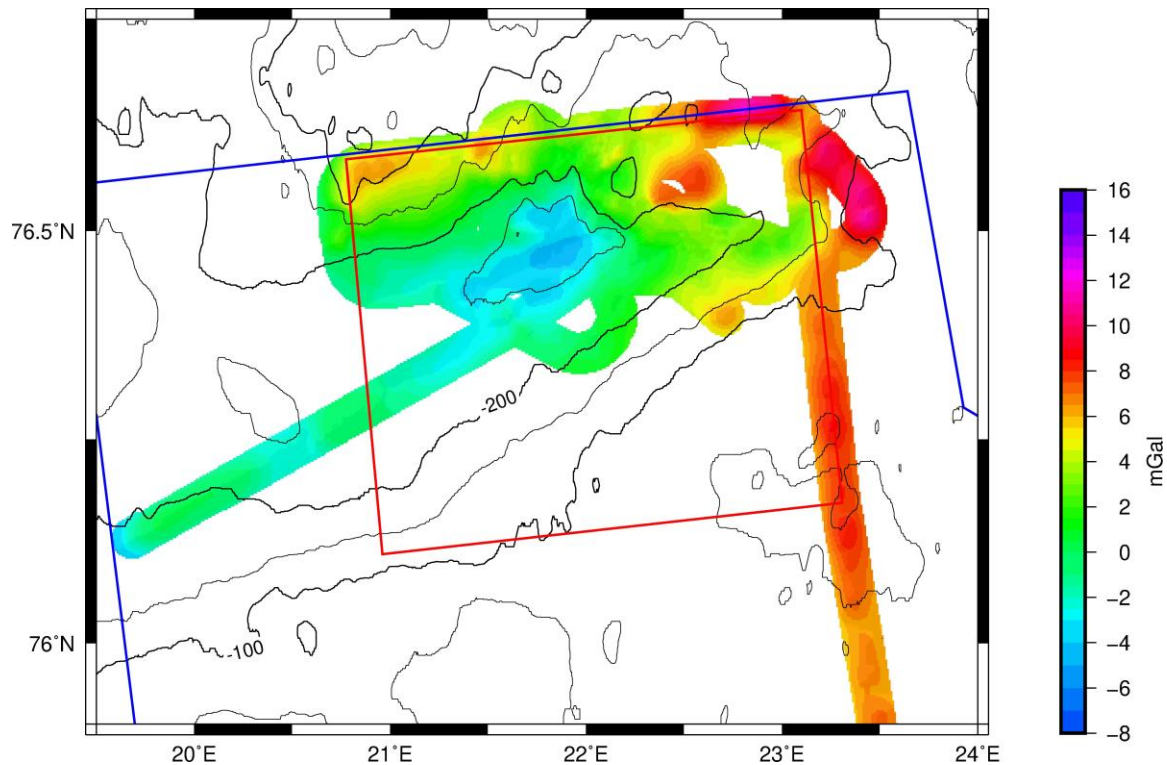


Fig. 5.17 Map of the free-air gravity anomalies acquired during cruise MSM137 in survey area 3. The map is drawn up to a distance of 2.5 kilometers from all tracks with considered data. The map is based on a 0.25 x 0.25 km grid and is underlain by the GEBCO_2024 bathymetry.

5.7 Ocean-Bottom Seismics

(B. Schramm, M. Schauer, M. Schnabel)

For deployment during cruise MSMS137 we used short-period Ocean Bottom Seismometer (OBS) instruments provided by the BGR pool. Two types of OBS designed by KUM were used: Nammu and Lobster. Both types are equipped with a hydrophone (HTI-04) and a data recorder (6D6 and 6D7) in a high-pressure tube. Additionally, the Nammu OBS is equipped with a seismometer, Lobster OBS with a geophone. The system itself floats at the sea surface. In order to deploy the device on the ocean bottom a weight is mounted to the frame and attached to a so-called releaser. This releaser has an acoustic communication unit, which can be addressed from the ship in order to disconnect the weight after the experiment. The OBS will then ascend to the surface and can be recovered. A flashlight, radio transmitter and a flag are attached to the frame to increase the visibility of the OBS and to facilitate an easy and quick recovery.

The experiment consists of 28 deployments of OBS: one 3D array with 16 instruments in working area 1 (Fig. 5.18) and another 3D array with 12 OBS in working area 2 (Fig. 5.19). The sampling rate was 500 Hz for the recorders. The shot interval was every 50 m (approximately every 21 sec). The volume of the air gun array is 3,100 inch³. The station list with additional information is given in Appendix 11.2.

A first quality control shows promising data. Refracted energy is generally visible for the full offset range up to 25 km (Fig 5.20). For offsets beyond 8-9 km, the refractions show velocities clearly exceeding the expected sediment velocity of about 3,800 m/s (see Fig. 5.20 and 5.21).

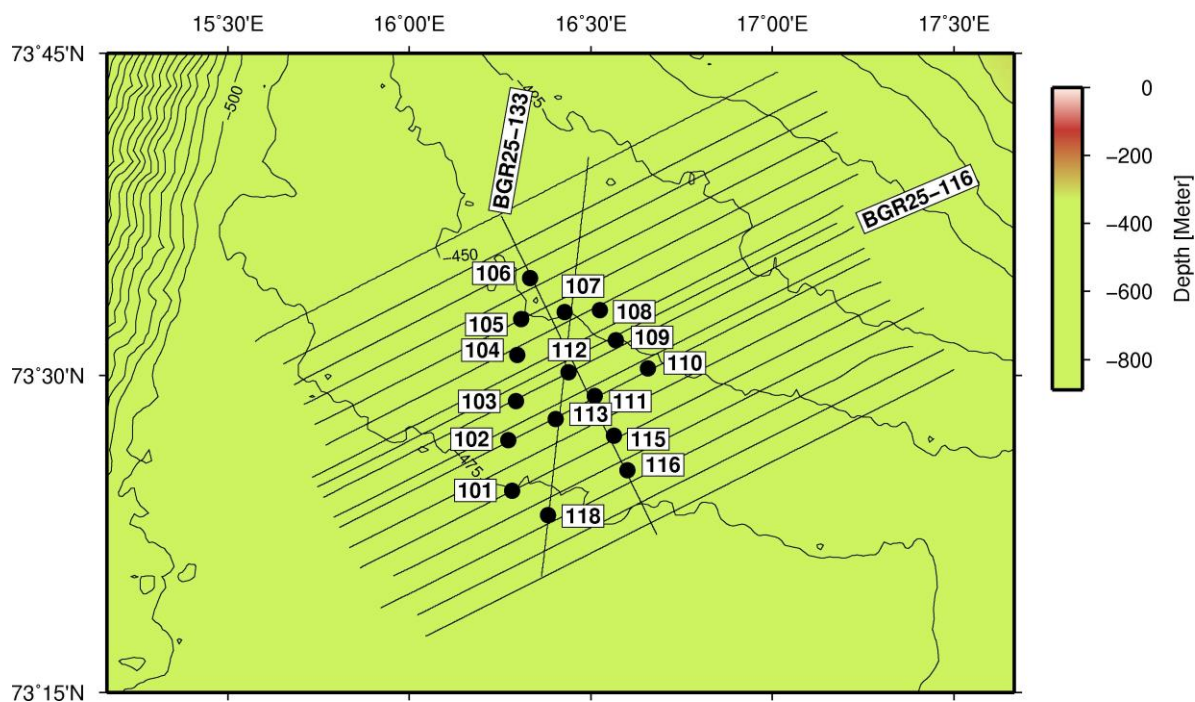


Fig. 5.18 Station map of OBS in working area 1. Line BGR25-116 (see Fig. 5.20) and line BGR25-133 (see Fig. 5.21) are annotated by line name.

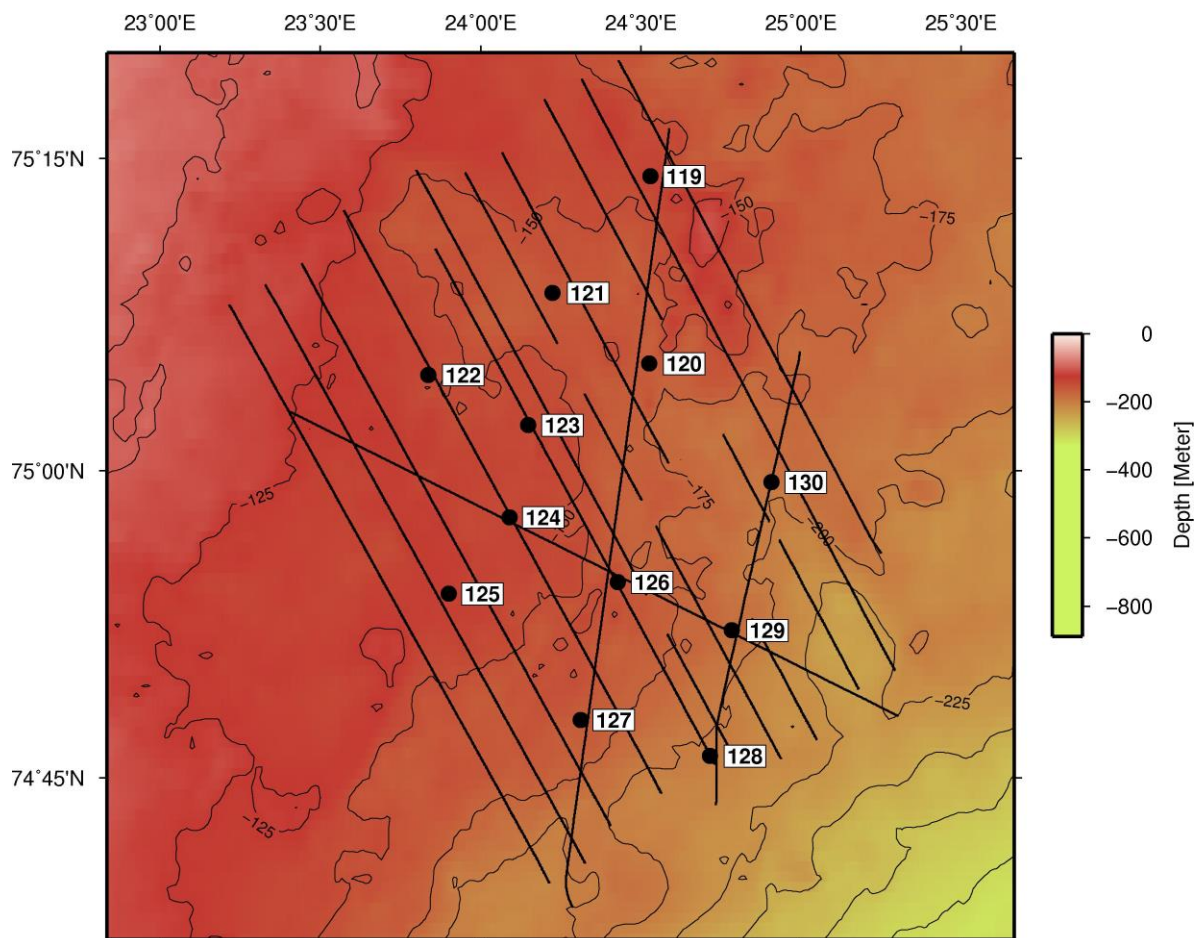


Fig. 5.19 Station map of OBS in working area 2.

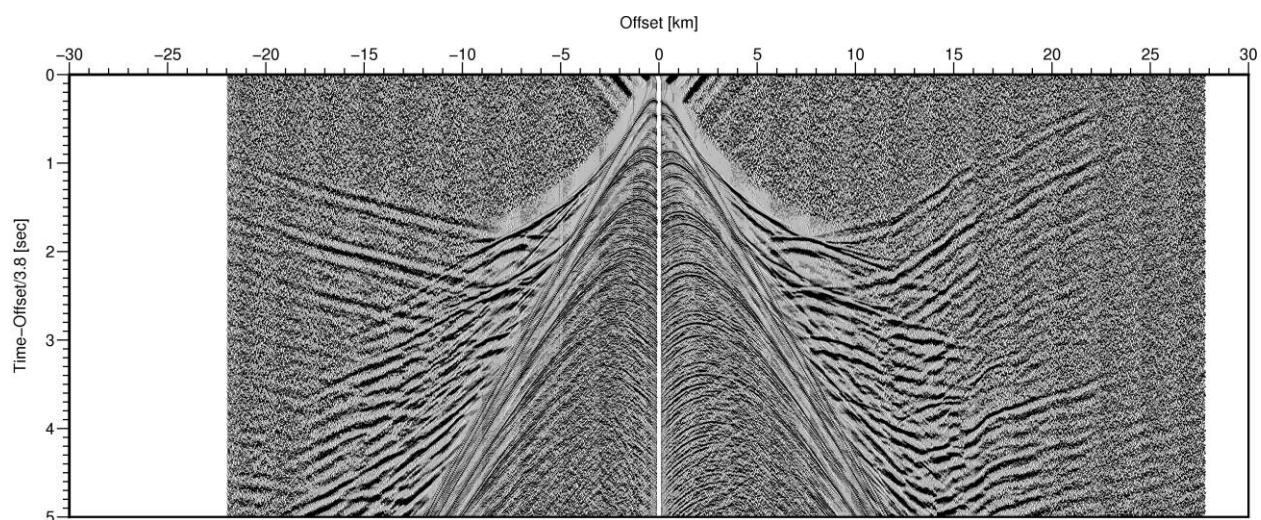


Fig. 5.20 Data example for OBS112 on line BGR25-116A (southwest to northeast). Reduction velocity is set to 3,800 m/s.

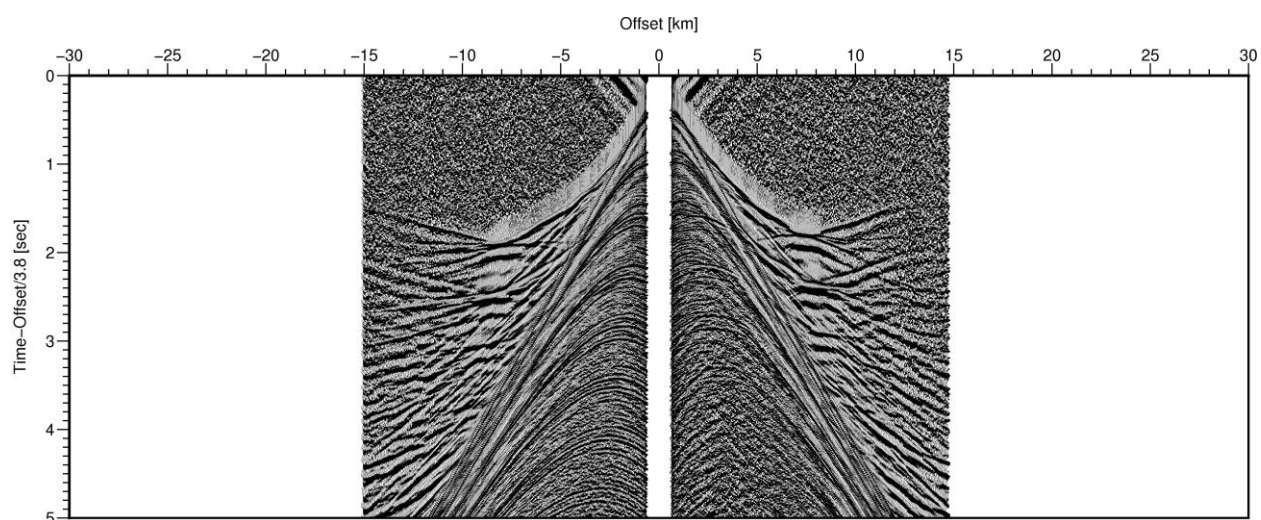


Fig. 5.21 Data example for OBS112 on line BGR25-133A (northwest to southeast). Reduction velocity is set to 3,800 m/s.

6 Station List MSM137

6.1 Overall Station List

Station No.		Date	Gear	Time	Latitude	Longitude	Remarks/Recovery
MERIAN	BGR25-	2025		[UTC]	[°N]	[°E]	
MSM137_1-1		14.5.	EM712 / P70	14:06	73° 12,827'	015° 13,944'	Until 23.05.2025 22:02
MSM137_2-1		14.5.	SVP	16:13	73° 24,549'	016° 17,093'	448 m depth
MSM137_3-1	OBS101	14.5.	OBS	16:45	73° 24,551'	016° 17,036'	
MSM137_4-1	OBS102	14.5.	OBS	17:26	73° 26,934'	016° 16,372'	
MSM137_5-1	OBS103	14.5.	OBS	17:46	73° 28,789'	016° 17,661'	
MSM137_6-1	OBS104	14.5.	OBS	18:08	73° 30,985'	016° 17,973'	
MSM137_7-1	OBS105	14.5.	OBS	18:26	73° 32,671'	016° 18,593'	
MSM137_8-1	OBS106	14.5.	OBS	18:47	73° 34,584'	016° 20,138'	
MSM137_9-1	OBS107	14.5.	OBS	19:11	73° 32,973'	016° 25,730'	
MSM137_10-1	OBS108	14.5.	OBS	19:28	73° 33,059'	016° 31,420'	
MSM137_11-1	OBS109	14.5.	OBS	19:47	73° 31,680'	016° 34,099'	
MSM137_12-1	OBS110	14.5.	OBS	20:10	73° 30,359'	016° 39,408'	
MSM137_13-1	OBS111	14.5.	OBS	20:51	73° 29,055'	016° 30,663'	
MSM137_14-1	OBS112	14.5.	OBS	21:12	73° 30,202'	016° 26,337'	
MSM137_15-1	OBS113	14.5.	OBS	21:35	73° 27,961'	016° 24,372'	
MSM137_16-1	OBS115	14.5.	OBS	22:03	73° 27,178'	016° 33,916'	
MSM137_17-1	OBS116	14.5.	OBS	22:23	73° 25,542'	016° 36,106'	
MSM137_18-1	OBS118	14.5.	OBS	23:00	73° 23,413'	016° 22,861'	
MSM137_19-1		15.5.	SEISSTR	08:10	73° 18,850'	018° 04,435'	Until 23.05.2025 22:01
MSM137_20-1		17.5.	XSV	09:55	73° 33,084'	016° 59,405'	
MSM137_21-1		20.5.	XSV	08:25	73° 26,435'	015° 56,643'	
MSM137_22-1		22.5.	XSV	20:04	73° 29,576'	017° 08,671'	
MSM137_23-1		23.5.	EM712 / P70	23:50	73° 36,911'	017° 00,751'	Until 24.05.2025 07:47
MSM137_24-1		24.5.	SVP	08:42	73° 34,180'	016° 19,753'	430 m depth
MSM137_25-1		24.5.	EM712 / P70	20:41	73° 24,291'	015° 50,064'	Until 25.05.2025 09:17
MSM137_26-1	OBS119	26.5.	OBS	09:37	75° 14,152'	024° 31,742'	
MSM137_27-1	OBS120	26.5.	OBS	10:31	75° 05,162'	024° 31,458'	
MSM137_28-1	OBS121	26.5.	OBS	11:10	75° 08,565'	024° 13,605'	
MSM137_29-1	OBS122	26.5.	OBS	11:55	75° 04,630'	023° 50,174'	
MSM137_30-1	OBS123	26.5.	OBS	12:30	75° 02,216'	024° 08,754'	
MSM137_31-1	OBS124	26.5.	OBS	13:02	74° 57,682'	024° 05,391'	
MSM137_32-1	OBS125	26.5.	OBS	13:33	74° 54,019'	023° 53,954'	
MSM137_33-1	OBS126	26.5.	OBS	14:25	74° 54,559'	024° 25,617'	
MSM137_34-1	OBS127	26.5.	OBS	15:07	74° 47,856'	024° 18,596'	
MSM137_35-1	OBS128	26.5.	OBS	15:50	74° 46,059'	024° 42,943'	
MSM137_36-1	OBS129	26.5.	OBS	16:31	74° 52,194'	024° 46,975'	
MSM137_37-1	OBS130	26.5.	OBS	17:22	74° 59,397'	024° 54,376'	
MSM137_38-1		26.5.	SVP	17:30	74° 59,423'	024° 54,412'	170 m depth
MSM137_39-1		26.5.	SEISTR	18:00	74° 59,304'	024° 55,209'	Until 01.06.2025 17:08
MSM137_39-4		26.5.	EM712 / P70	18:00	74° 59,304'	024° 55,207'	Until 01.06.2025 17:08
MSM137_40-1		27.5.	XSV	20:57	75° 09,662'	024° 37,740'	
MSM137_41-1		28.5.	XSV	11:19	74° 50,157'	025° 09,124'	
MSM137_42-1		28.5.	XSV	22:33	75° 07,791'	023° 13,360'	
MSM137_43-1		29.5.	XSV	07:49	74° 39,709'	024° 34,963'	
MSM137_44-1		29.5.	XSV	11:18	74° 51,352'	024° 36,400'	
MSM137_45-1		31.5.	XSV	11:22	75° 05,221'	023° 27,771'	
MSM137_46-1		31.5.	XSV	20:00	74° 46,563'	024° 29,095'	
MSM137_47-1		1.6.	XSV	10:45	74° 52,773'	024° 41,915'	
MSM137_48-1		2.6.	EM712 / P70	05:15	75° 08,707'	024° 32,311'	Until 02.06.2025 08:55
MSM137_49-1		2.6.	SVP	10:58	74° 48,997'	024° 01,293'	155 m depth
MSM137_50-1		2.6.	EM712 / P70	11:15	74° 49,010'	024° 01,333'	Until 02.06.2025 23:27
MSM137_51-1		3.6.	SEISTR	12:59	76° 36,305'	021° 54,234'	Until 06.06.2025 11:46
MSM137_52-1		4.6.	XSV	09:47	76° 28,978'	022° 41,119'	
MSM137_53-1		6.6.	SVP	16:58	76° 34,953'	022° 15,029'	190 m depth
MSM137_54-1		6.6.	EM712 / P70	17:34	76° 36,316'	022° 13,570'	Until 07.06.2025 22:00
MSM137_55-1		7.6.	SVP	08:59	76° 30,457'	021° 35,907'	235 m depth

6.2 Profile Station List

Station MSM137_19-1 SEISTR

Profile	Start End	Date	Time	Latitude	Longitude	Course	SP	FFID	Profile length
BGR		2025	UTC	[°N]	[°E]				[km]
BGR25-101A002	Start	16.05.	17:53:26	73°44.135'	17°00.877'	247.4°	2000	341	
	End	16.05.	23:46:26	73°31.588'	15°34.510'		1647	694	50.73
BGR25-110A003	Start	17.05.	01:18:24	73°27.692'	15°44.356'	67.4°	1000	715	
	End	17.05.	06:47:59	73°40.146'	17°10.668'		2020	1735	50.96
BGR25-119A004	Start	17.05.	08:45:39	73°35.470'	17°16.128'	247.4°	2000	1755	
	End	17.05.	14:45:48	73°22.829'	15°48.433'		960	2793	52.01
BGR25-129A005	Start	17.05.	16:48:32	73°18.685'	16°01.314'	67.4°	1005	2816	
	End	17.05.	22:40:50	73°31.214'	17°28.324'		2040	3851	51.76
BGR25-118A006	Start	18.05.	00:54:19	73°35.961'	17°15.219'	247.4°	2000	3872	
	End	18.05.	06:48:48	73°23.320'	15°47.481'		960	4912	52.01
BGR25-108A007	Start	18.05.	08:44:22	73°28.678'	15°42.647'	67.4°	1000	4930	
	End	18.05.	14:57:45	73°41.350'	17°10.735'		2040	5970	52.01
BGR25-121A008	Start	18.05.	17:28:47	73°34.373'	17°17.985'	247.4°	2000	5991	
	End	18.05.	23:12:54	72°21.877'	15°50.120'		960	7031	52.03
BGR25-131A009	Start	19.05.	01:11:02	73°17.674'	16°02.666'	67.4°	1000	7052	
	End	19.05.	07:00:05	73°30.270'	17°29.999'		2040	8092	52.02
BGR25-114A010	Start	19.05.	10:22:17	73°37.950'	17°11.741'	247.4°	2000	8113	
	End	19.05.	16:13:49	73°25.208'	15°44.018'		960	9153	52.03
BGR25-125A011	Start	19.05.	18:38:29	73°20.553'	15°57.461'	67.4°	1000	9174	
	End	20.05.	00:57:30	73°33.157'	17°25.027'		2040	10178	52.04
BGR25-115A012	Start	20.05.	03:22:06	73°37.117'	17°10.645'	247.4°	1976	10223	
	End	20.05.	09:14:51	73°24.756'	15°44.445'		960	11238	50.82
BGR25-104A013	Start	20.05.	11:38:28	73°30.531'	15°39.849'	67.4°	1000	11259	
	End	20.05.	17:44:50	73°43.255'	17°07.375'		2040	12299	52.03
BGR25-116A014	Start	20.05.	20:09:32	73°36.953'	17°13.485'	247.4°	2000	12320	
	End	21.05.	02:13:02	73°24.255'	15°45.769'		960	13360	52.02
BGR25-106A015	Start	21.05.	11:42:20	73°29.560'	15°40.958'	67.4°	1000	13381	
	End	21.05.	17:47:13	73°42.304'	17°09.055'		2040	14421	52.02
BGR25-123A016	Start	21.05.	20:51:37	73°33.525'	17°19.459'	247.4°	2000	14442	
	End	22.05.	03:02:29	73°20.913'	15°51.877'		960	15482	52.01
BGR25-112A017	Start	22.05.	08:15:53	73°26.718'	15°46.202'	67.4°	1000	15503	
	End	22.05.	14:18:59	73°39.402'	17°14.158'		2040	16542	52.01
BGR25-127A018	Start	22.05.	19:02:11	73°31.220'	17°23.220'	247.4°	2000	16563	
	End	23.05.	01:43:12	73°19.025'	15°55.308'		960	17603	52.15
BGR25-134A019	Start	23.05.	06:16:24	73°20.522'	16°21.842'	10.8°	1000	17622	
	End	23.05.	10:34:57	73°40.214'	16°29.577'		1737	18359	36.86
BGR25-133A020	Start	23.05.	13:46:19	73°37.456'	16°15.200'	158.4°	1599	18380	
	End	23.05.	17:17:16	73°22.500'	16°40.879'		980	18999	30.96
									$\Sigma = 948.48$

Station MSM137_39-1 SEISTR

Profile	Start End	Date	Time	Latitude	Longitude	Course	SP	FFID	Profile length
BGR		2025	UTC	[°N]	[°E]				[km]
BGR25-186A026	Start	26.05.	22:43:01	74°55.970'	25°15.059'	328.3°	1200	19001	
	End	27.05.	04:45:28	75°19.663'	24°25.786'		2199	20000	49.98
BGR25-172A027	Start	27.05.	07:10:27	75°15.262'	24°04.026'	148.3°	2160	20021	
	End	27.05.	10:55:21	75°00.338'	24°35.221'		1530	20651	31.51
BGR25-172B028	Start	27.05.	12:53:02	74°52.783'	24°50.829'	148.3°	1211	20652	
	End	27.05.	14:22:26	74°46.838'	25°03.030'		960	20903	12.56
BGR25-182A029	Start	27.05.	16:12:30	74°50.256'	25°17.626'	328.3°	1000	20924	
	End	27.05.	23:10:39	75°18.752'	24°18.927'		2200	22124	60.02
BGR25-168A030	Start	28.05.	01:52:42	75°14.294'	23°57.099'	148.3°	2160	22145	
	End	28.05.	03:49:23	75°06.114'	24°14.391'		1814	22491	17.31

BGR25-168B031	Start	28.05.	04:24:47	75°03.700'	24°19.448'	148.3°	1712	22492	
	End	28.05.	05:41:21	74°58.540'	24°30.194'		1494	22710	10.90
BGR25-168C032	Start	28.05.	06:01:25	74°57.290'	24°32.827'	148.3°	1441	22711	
	End	28.05.	08:58:36	74°45.905'	24°56.298'		960	23192	24.06
BGR25-178A033	Start	28.05.	11:07:11	74°49.327'	25°10.833'	328.3°	1000	23206	
	End	28.05.	12:54:36	74°56.612'	24°55.966'		1307	23513	15.36
BGR25-178B034	Start	28.05.	13:07:24	74°57.516'	24°54.129'	328.3°	1345	23514	
	End	28.05.	14:07:23	75°01.735'	24°45.416'		1523	23692	8.90
BGR25-178C035	Start	28.05.	15:29:47	75°07.264'	24°33.986'	328.3°	1756	23693	
	End	28.05.	18:03:53	75°17.791'	24°11.952'		2200	24137	22.21
BGR25-142A036	Start	28.05.	22:30:07	75°07.984'	23°12.900'	148.3°	2160	24158	
	End	29.05.	06:07:43	74°39.769'	24°12.933'		960	25358	60.02
BGR25-164A037	Start	29.05.	09:57:21	74°46.076'	24°47.343'	328.3°	1000	25379	
	End	29.05.	11:28:12	74°52.028'	24°34.995'		1252	25631	12.61
BGR25-164B038	Start	29.05.	11:57:32	74°53.927'	24°31.125'	328.3°	1332	25632	
	End	29.05.	17:12:25	75°14.436'	23°47.914'		2200	26500	43.42
BGR25-150A039	Start	29.05.	19:36:36	75°02.951'	23°26.500'	148.3°	2160	26521	
	End	30.05.	02:37:30	74°42.630'	24°24.360'		1000	27681	58.02
BGR25-187A040	Start	30.05.	04:23:52	74°43.623'	24°44.118'	9.0°	1000	27699	
	End	30.05.	09:28:11	75°05.731'	24°59.752'		1557	28256	41.96
BGR25-188A041	Start	30.05.	13:20:48	75°16.412'	24°35.367'	184.6°	1905	28281	
	End	30.05.	21:47:57	74°38.589'	24°17.279'		960	29226	71.12
BGR25-162A042	Start	31.05.	00:42:50	74°45.607'	24°43.993'	328.3°	1000	128277	
	End	31.05.	07:38:28	75°12.989'	23°46.593'		2061	129338	53.07
BGR25-146A043	Start	31.05.	10:23:10	75°08.959'	23°19.616'	148.3°	2160	29378	
	End	31.05.	17:26:15	74°40.734'	24°19.649'		960	30578	60.03
BGR25-156A044	Start	31.05.	19:24:13	74°44.190'	24°33.930'	328.3°	1000	30599	
	End	01.06.	02:21:08	75°12.511'	23°34.348'		2200	31799	60.03
BGR25-189A045	Start	01.06.	05:43:23	75°02.831'	23°24.308'	113.3°	1822	31818	
	End	01.06.	13:06:34	74°48.018'	25°18.282'		1000	32640	61.68
									$\Sigma = 774.77$

Station MSM137_51-1 SEISTR

Profile	Start End	Date	Time	Latitude	Longitude	Course	SP	FFID	Profile length
BGR		2025	UTC	[°N]	[°E]				[km]
BGR25-190A046	Start	04.06.	14:57:20	76°37.789'	22°53.270'	262.9°	2000	32645	
	End	04.06.	21:00:05	76°34.835'	20°53.291'		960	33685	52.04
BGR25-191A047	Start	04.06.	23:27:04	76°28.057'	21°02.338'	82.9°	1000	33706	
	End	05.06.	03:58:23	76°30.519'	22°31.556'		1781	34487	39.13
BGR25-192A048	Start	05.06.	05:16:19	76°35.092'	22 24.198'	262.9°	1741	34498	
	End	05.06.	09:41:02	76°32.851'	20°54.369'		960	35279	39.07
BGR25-193A049	Start	05.06.	12:09:59	76°26.064'	21°03.387'	82.9°	1000	35300	
	End	05.06.	15:55:13	76°28.228'	22°17.392'		1650	35950	32.58
BGR25-194A050	Start	05.06.	17:16:55	76°32.857'	22°11.110'	262.9°	1620	35951	
	End	05.06.	20:59:34	76°30.881'	20°55.428'		960	36611	33.02
BGR25-196A051	Start	05.06.	22:38:48	76°25.949'	20°57.684'	118.3°	1001	36617	
	End	06.06.	01:36:48	76°21.643'	21°51.684'		1984	37600	25.83
BGR25-197A052	Start	06.06.	02:54:53	76°24.426'	22°09.311'	338.9°	1924	37601	
	End	06.06.	05:29:14	76°36.161'	21°50.684'		993	38532	23.29
									$\Sigma = 244.96$

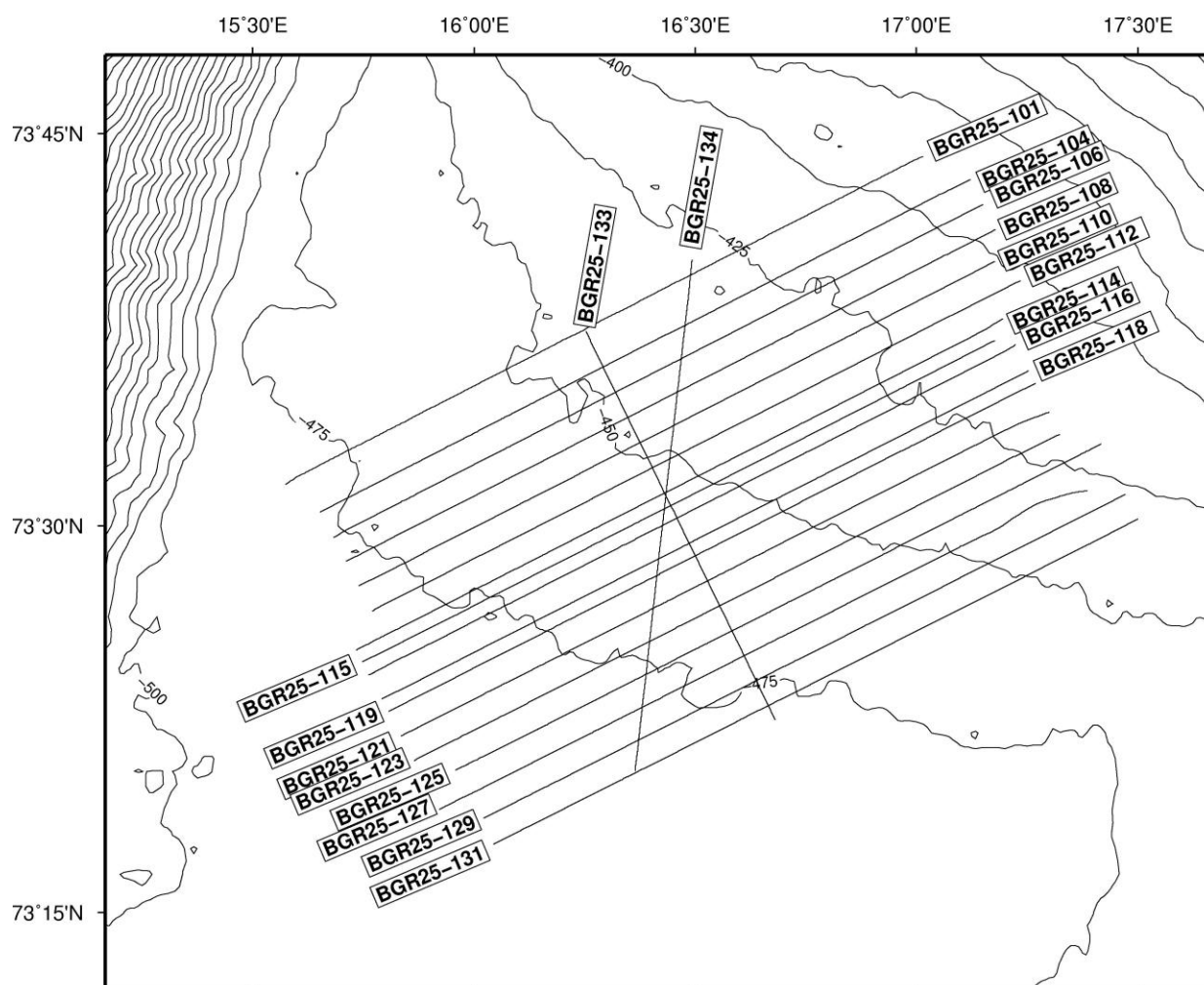


Fig. 6.1 Profile plot of working area 1.

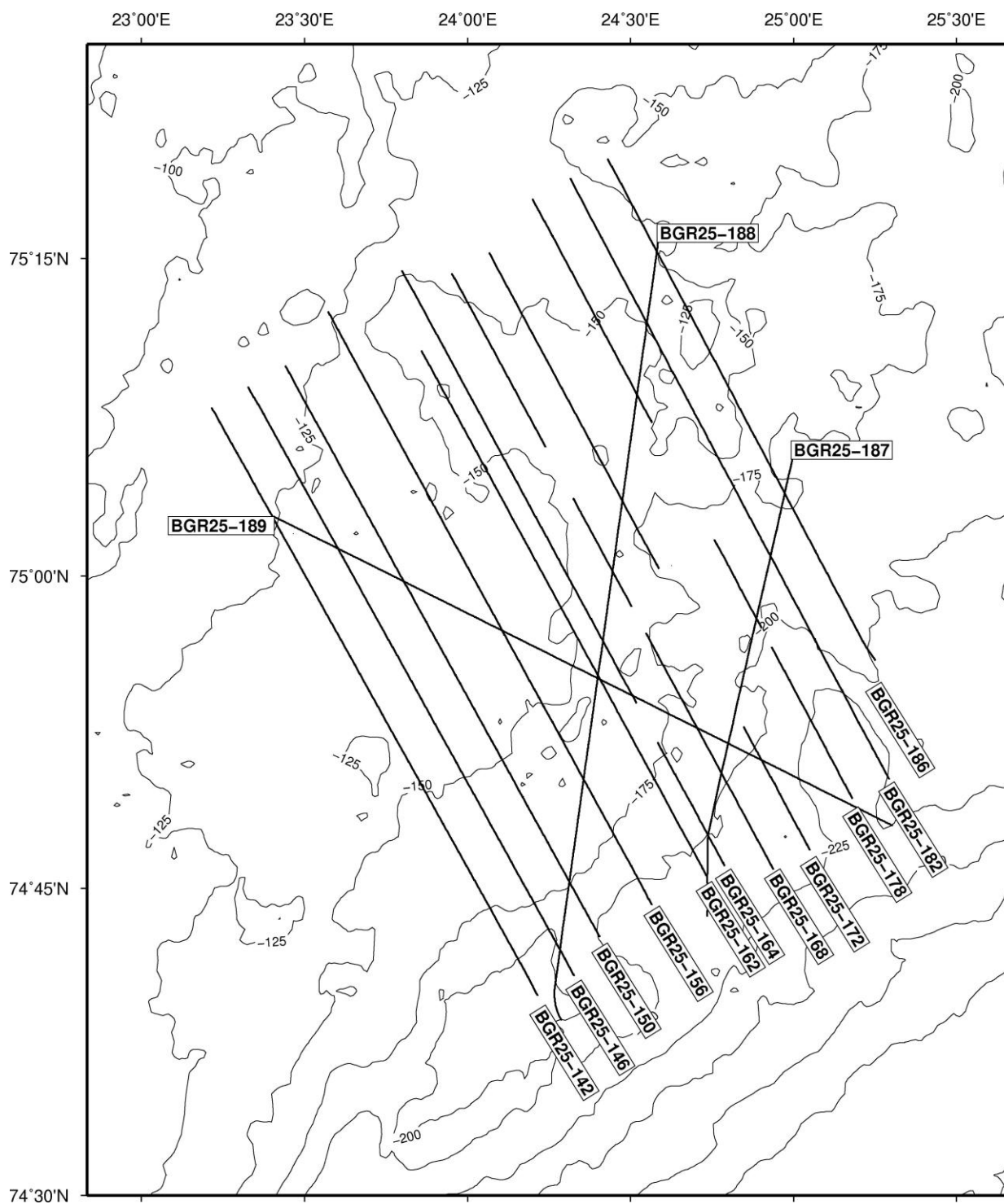


Fig. 6.2 Profile plot of working area 2.

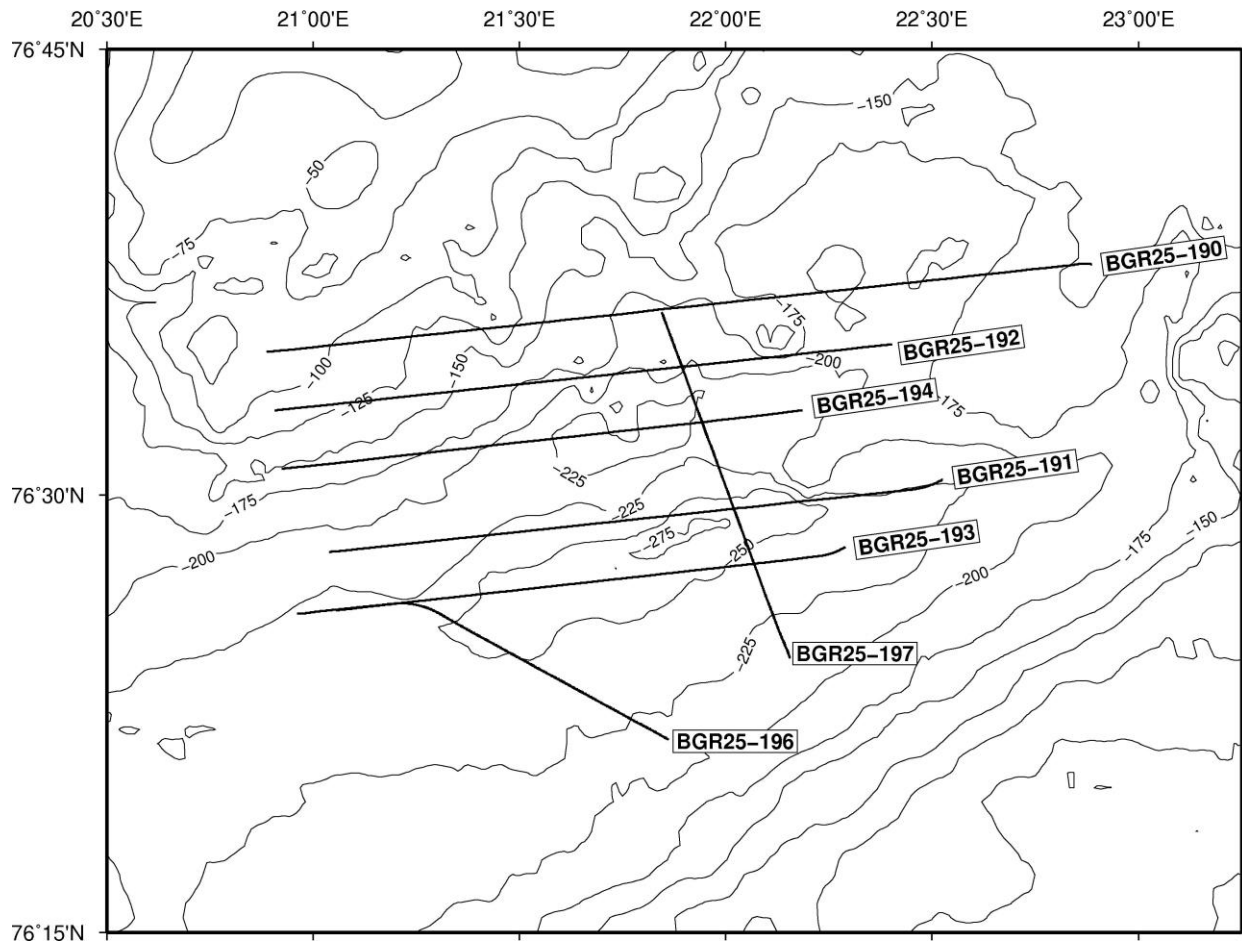


Fig. 6.3 Profile plot of working area 3.

7 Data and Sample Storage and Availability

Within the DAM project underway data, the following data types have been sent directly from the vessel to the land-based data centers: seismic raw data (SEISTR), PARASOUND, Bathymetry (EM712 and EM124) and general data from DSHIP. These data sets will be prepared for publication within PANGAEA. All other data (gravity, magnetics, OBS-recordings) will be initially processed and archived within BGR and will be published via the BGR repository Geoportal (geoportal.bgr.de). The cruise track of MSM137 (<https://doi.org/10.1594/PANGAEA.984443>) as well as the station list (<https://www.pangaea.de/expeditions/events/MSM137>) are available directly after the cruise.

Table 7.1 Overview of data availability

Type	Database	Available	Free Access	Contact
MCS raw data	DAM / PANGAEA	Jun. 2026	Jun. 2029	michael.schnabel@bgr.de
OBS data	BGR / PANGAEA	Jun. 2026	Jun. 2028	michael.schnabel@bgr.de
magnetic/gravity	BGR	Jun. 2026	Jun. 2028	michael.schnabel@bgr.de
multibeam	BSH / PANGAEA	Jun. 2026	Jun. 2028	michael.schnabel@bgr.de
Parasound	BGR / PANGAEA	Jun. 2026	Jun. 2028	michael.schnabel@bgr.de

8 Acknowledgements

We like to thank captain Björn Maaß and his crew for their immense support during this cruise. We thank the German Research Fleet Coordination Center, Briese Research (Klaus Bergmann) and the Geschäftsstelle des Begutachtungspanels Forschungsschiffe (GPF) for their support during preparation of the cruise. The DWD (Thies Schlünzen, Customer Service Division Maritime Shipping) delivered dedicated weather forecasts for the survey area several times per day. We acknowledge the financial support from the German Research Foundation (DFG) under grant number GPF 20-1/070.

9 References

- Aarseth, I., Mjelde, R., Breivik, A.J., Minakov, A., Faleide, J.I., Flueh, E. and Huisman, R.S., 2017. Crustal structure and evolution of the Arctic Caledonides: Results from controlled-source seismology. *Tectonophysics* 718, 9-24, doi:10.1016/j.tecto.2017.04.022.
- Andreassen, K., Hubbard, A., Winsborrow, M., Patton, H., Vadakkepuliambatta, S., Plaza-Faverola, A., Gudlaugsson, E., Serov, P., Deryabin, A., Mattingsdal, R., Mienert, J. and Büinz, S., 2017. Massive blow-out craters formed by hydrate-controlled methane expulsion from the Arctic seafloor. *Science* 356, 948-953, doi:10.1126/science.aal4500.
- Breivik, A.J., Mjelde, R., Grogan, P., Shimamura, H., Murai, Y. and Nishimura, Y., 2003. Crustal structure and transform margin development south of Svalbard based on ocean bottom seismometer data. *Tectonophysics* 369, 37-70, doi:10.1016/S0040-1951(03)00131-8.
- Breivik, A.J., Mjelde, R., Grogan, P., Shimamura, H., Murai, Y. and Nishimura, Y., 2005. Caledonide development offshore–onshore Svalbard based on ocean bottom seismometer, conventional seismic, and potential field data. *Tectonophysics* 401, 79-117, doi:10.1016/j.tecto.2005.03.009.
- Breivik, A.J., Mjelde, R., Grogan, P., Shimamura, H., Murai, Y., Nishimura, Y. and Kuwano, A., 2002. A possible Caledonide arm through the Barents Sea imaged by OBS data. *Tectonophysics* 355, 67-97, doi:10.1016/S0040-1951(02)00135-X.
- Dörr, N., Lisker, F., Jochmann, M., Rainer, T., Schlegel, A., Schubert, K., and Spiegel, C., 2018. Subsidence, rapid inversion and slow erosion of the Central Tertiary Basin of Svalbard: Evidence from the thermal evolution and basin modeling, in Piepjohn, K., Strauss, J.V., Reinhardt, L., and McClelland, W.C., eds., *Circum-Arctic Structural Events: Tectonic Evolution of the Arctic Margins and Trans-Arctic Links with Adjacent Orogens: Geological Society of America Special Paper 541*, p. 1–20, doi:10.1130/2018.2541(09).
- Faleide, J.I., Myhre, A.M. and Eldholm, O., 1988. Early Tertiary volcanism at the western Barents Sea margin. *Geological Society, London, Special Publications* 39, 135-146, doi:10.1144/gsl.sp.1988.039.01.13.
- Faleide, J.I., Tsikalas, F., Breivik, A.J., Mjelde, R., Ritzmann, O., Engen, O., Wilson, J. and Eldholm, O., 2008. Structure and Evolution of the Continental Margin off Norway and the Barents Sea. *Episodes* 31, 82-91.
- Grogan, P., Nyberg, K., Fotland, B., Myklebust, R., Dahlgren, S. and Riis, F., 2000. Cretaceous magmatism south and east of Svalbard: evidence from seismic reflection and magnetic data. *Polarforschung* 68, 25-34, doi:10.2312/polarforschung.68.25.
- Jakobsson, M., Mayer, L., Coakley, B., Dowdeswell, J.A., Forbes, S., Fridman, B., Hodnesdal, H., Noormets, R., Pedersen, R., Rebesco, M., Schenke, H.W., Zarayskaya, Y., Accettella, D.,

- Armstrong, A., Anderson, R.M., Bienhoff, P., Camerlenghi, A., Church, I., Edwards, M., Gardner, J.V., Hall, J.K., Hell, B., Hestvik, O., Kristoffersen, Y., Marcussen, C., Mohammad, R., Mosher, D., Nghiem, S.V., Pedrosa, M.T., Travaglini, P.G. and Weatherall, P., 2012. The International Bathymetric Chart of the Arctic Ocean (IBCAO) Version 3.0. *Geophysical Research Letters* 39, L12609, doi:10.1029/2012GL052219.
- Lammers, S., Suess, E. and Hovland, M., 1995. A large methane plume east of Bear Island (Barents Sea): implications for the marine methane cycle. *Geologische Rundschau* 84, 59-66, doi:10.1007/bf00192242.
- Minakov, A., Mjelde, R., Faleide, J.I., Flueh, E.R., Dannowski, A. and Keers, H., 2012. Mafic intrusions east of Svalbard imaged by active-source seismic tomography. *Tectonophysics* 518-521, 106-118, doi:10.1016/j.tecto.2011.11.015.
- Minakov, A., Yarushina, V., Faleide, J.I., Krupnova, N., Sakoulina, T., Dergunov, N. and Glebovsky, V., 2018. Dyke emplacement and crustal structure within a continental large igneous province, northern Barents Sea. Geological Society, London, Special Publications 460, 371-395, doi:10.1144/sp460.4.
- Nejbert, K., Krajewski, K.P., Dubinska, E. and Pécskay, Z., 2011. Dolerites of Svalbard, north-west Barents Sea Shelf: age, tectonic setting and significance for geotectonic interpretation of the High-Arctic Large Igneous Province. *Polar Research* 30, 7306, doi:10.3402/polar.v30i0.7306.
- Omosanya, K.O., Johansen, S.E. and Abrahamson, P., 2016. Magmatic activity during the breakup of Greenland-Eurasia and fluid-flow in Stappen High, SW Barents Sea. *Marine and Petroleum Geology* 76, 397-411, doi:10.1016/j.marpetgeo.2016.05.017.
- Planke, S., Rasmussen, T., Rey, S.S. and Myklebust, R., 2005. Seismic characteristics and distribution of volcanic intrusions and hydrothermal vent complexes in the Vøring and Møre basins. Geological Society, London, Petroleum Geology Conference series 6, 833-844, doi:10.1144/0060833.
- Polteau, S., Hendriks, B.W.H., Planke, S., Ganerød, M., Corfu, F., Faleide, J.I., Midtkandal, I., Svensen, H.S. and Myklebust, R., 2016. The Early Cretaceous Barents Sea Sill Complex: Distribution, $^{40}\text{Ar}/^{39}\text{Ar}$ geochronology, and implications for carbon gas formation. *Palaeogeography, Palaeoclimatology, Palaeoecology* 441, 83-95, doi:10.1016/j.palaeo.2015.07.007.
- Rasmussen, E. and Fjeldskaar, W., 1996. Quantification of the Pliocene-Pleistocene erosion of the Barents Sea from present-day bathymetry. *Global and Planetary Change* 12, 119-133, doi:10.1016/0921-8181(95)00015-1.
- Senger, K., Tveranger, J., Ogata, K., Braathen, A. and Planke, S., 2014. Late Mesozoic magmatism in Svalbard: A review. *Earth-Science Reviews* 139, 123-144, doi:10.1016/j.earscirev.2014.09.002.
- Solheim, A. and Elverhøi, A., 1993. Gas-related sea floor craters in the Barents Sea. *Geo-Marine Letters* 13, 235-243, doi:10.1007/bf01207753.
- Svensen, H., Planke, S., Jamtveit, B. and Pedersen, T., 2003. Seep carbonate formation controlled by hydrothermal vent complexes: a case study from the Vøring Basin, the Norwegian Sea. *Geo-Marine Letters* 23, 351-358, doi:10.1007/s00367-003-0141-2.

10 Abbreviations

DWD	Deutscher Wetterdienst
EOL	end of line
GEBCO	General Bathymetric Chart of the Oceans
IBCAO	International Bathymetric Chart of the Arctic Ocean
MCS	multichannel seismic
OBS	ocean bottom seismometers
PAM	passive acoustic monitoring
PHF	primary high frequency
MMO	marine mammal observer
SLF	secondary low frequency
SOL	start of line
SRME	surface-related multiple elimination
SVP	sound velocity probe
TWT	two-way travelttime
VVP	Vestbakken Volcanic Province
XSV	expandable sound velocimeter

11 Appendices

11.1 Selected Pictures of Shipboard Operations



Fig. 11.1.1 Winches for seismic streamer (top) and air gun umbilical (bottom).

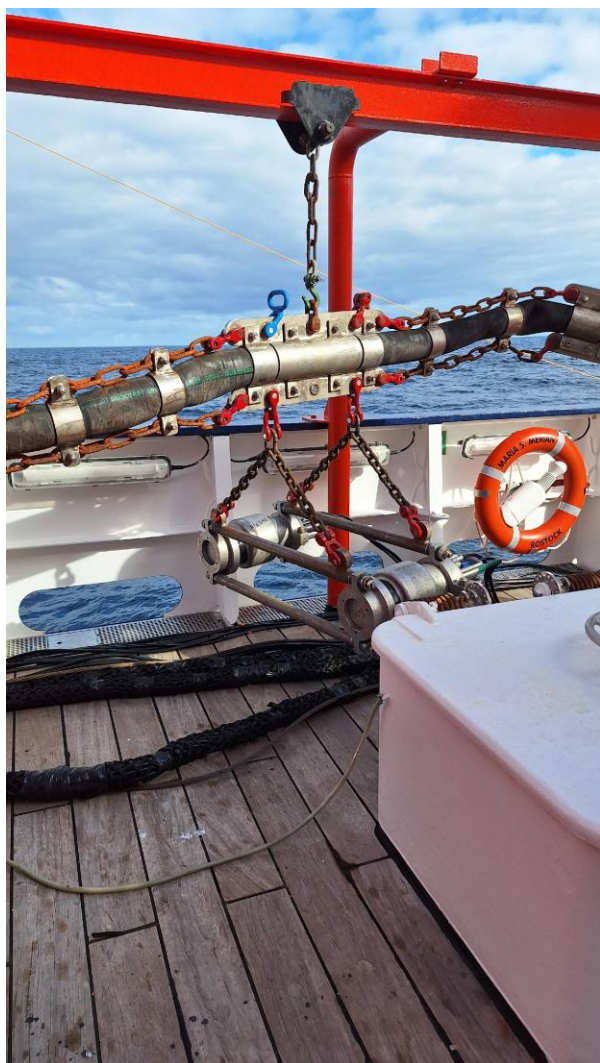


Fig. 11.1.2 Installed air gun cluster and gun rails.

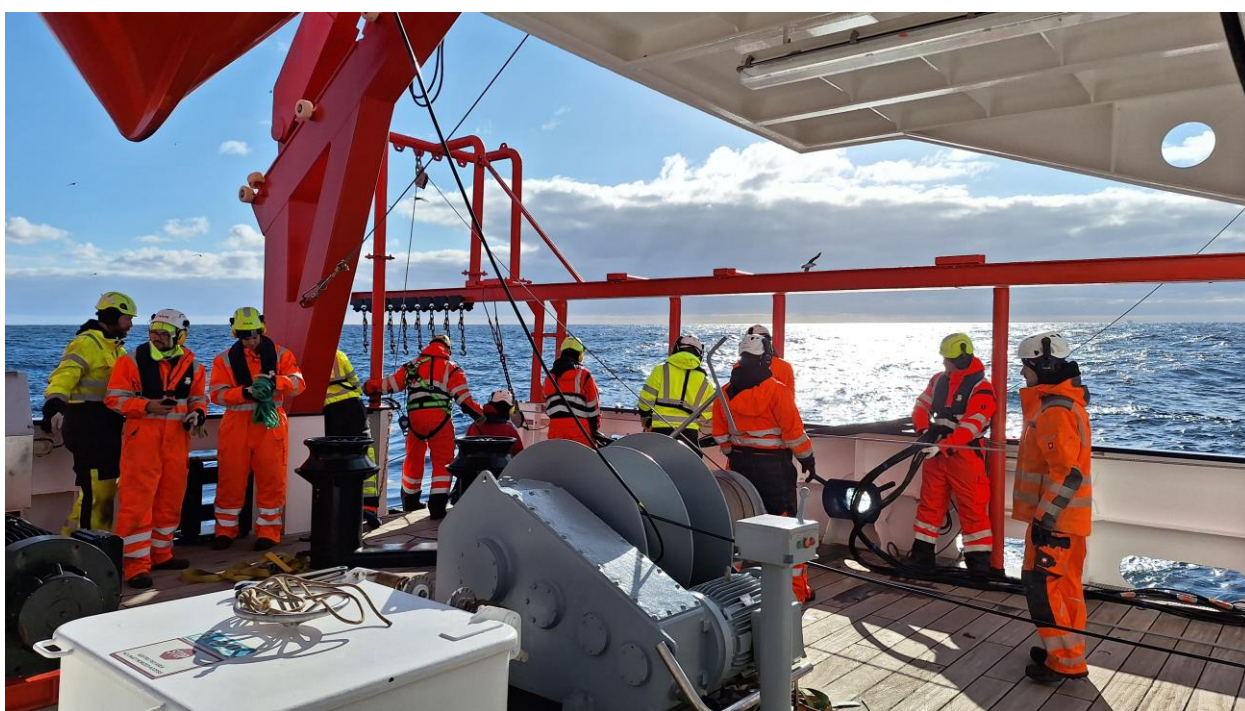


Fig. 11.1.3 Deployment of air guns.

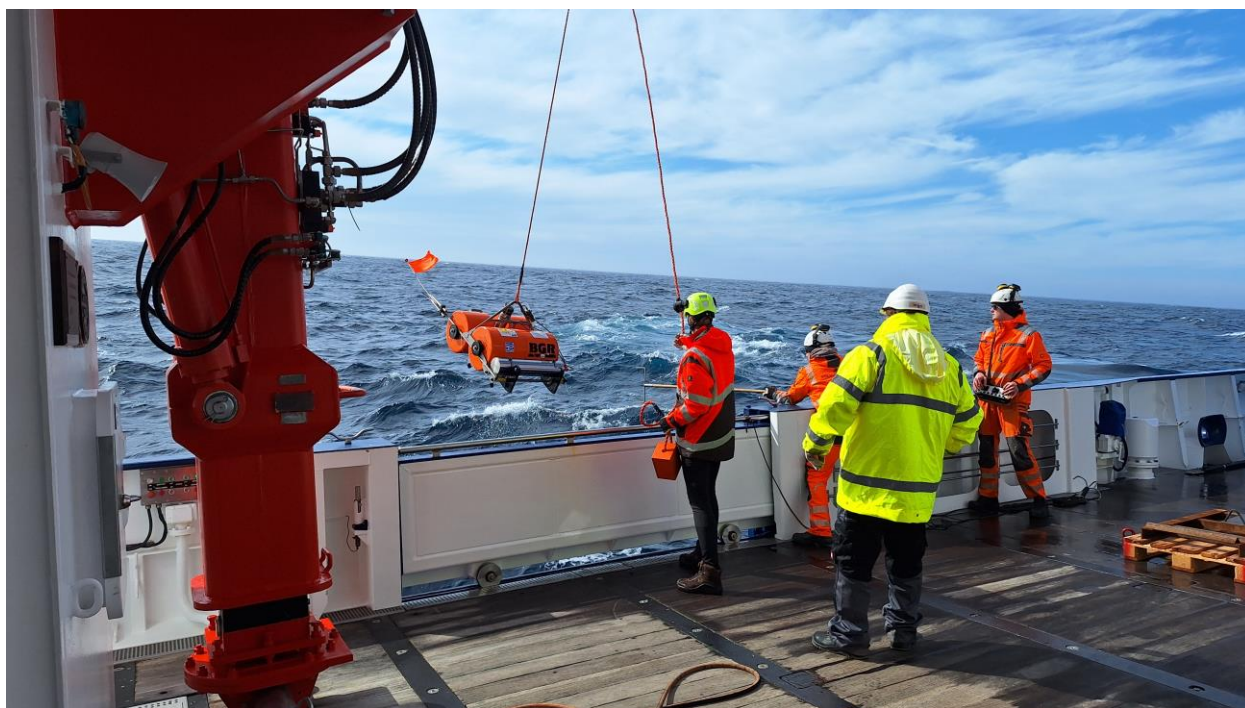
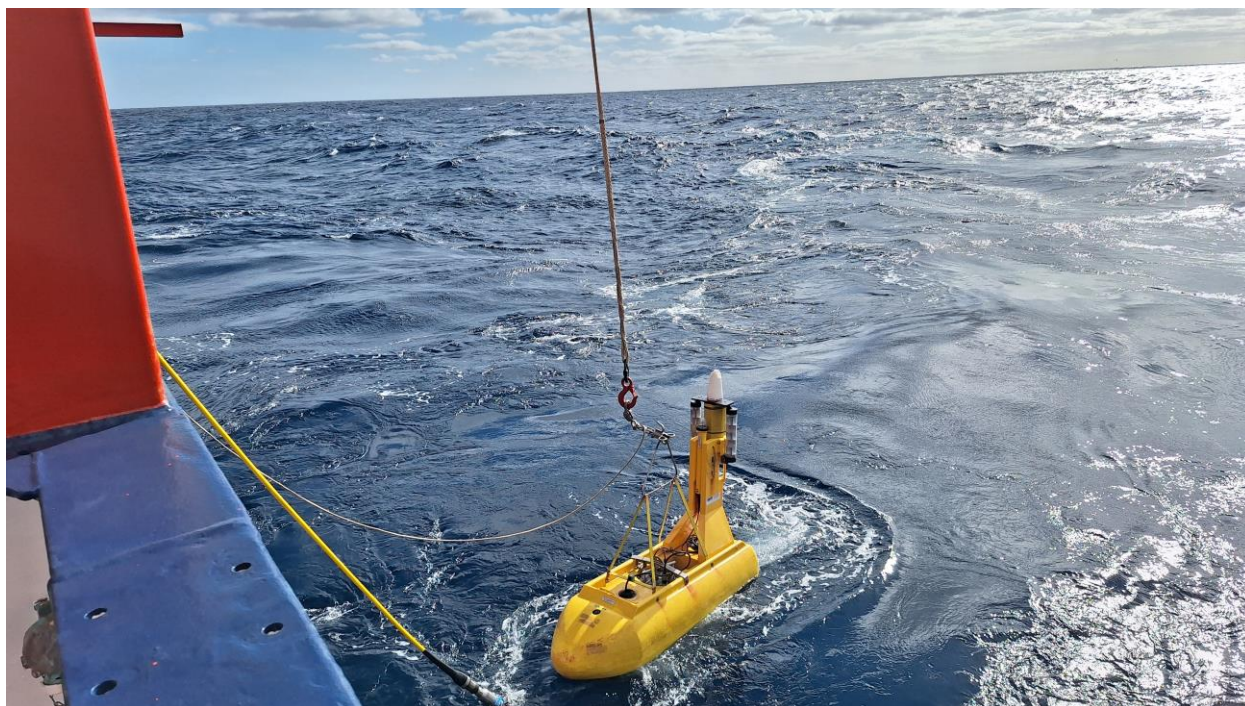


Fig. 11.1.4 Deployment of tail buoy (top) and recovery of an OBS (bottom).

11.2 Ocean-Bottom-Seismometer

Station	Type	Logger	Latitude	Longitude	Depth	Recording/ days	Skew/ms	Skew (ppm)	Comments
BGR25-OBS101	Lobster	6D6	73°24,551	16°17,038	472	12	299.534	0.309	
BGR25-OBS102	Lobster	6D6	73°26,931	16°16,358	475	12			no Sync,
BGR25-OBS103	Nammu	6D7	73°28,789	16°17,668	471	9	5.171	0.006	Recording stopped at 22.05.25 05:03:42
BGR25-OBS104	Lobster	6D6	73°30,986	16°17,974	464	12	424.961	0.457	
BGR25-OBS105	Lobster	6D6	73°32,671	16°18,593	453	11			no Sync
BGR25-OBS106	Nammu	6D6	73°34,584	16°20,141	449	11	16.303	0.018	
BGR25-OBS107	Lobster	6D6	73°32,972	16°25,728	453	13	407.574	0.3999	
BGR25-OBS108	Lobster	6D6	73°33,060	16°31,423	451	13	287.835	0.284	
BGR25-OBS109	Nammu	6D6	73°31,680	16°34,099	452	12	-266.729	-0.275	
BGR25-OBS110	Lobster	6D6	73°30,35	16°39,40	451	13			no Scny, RTC not synchronised
BGR25-OBS111	Lobster	6D6	73°29,056	16°30,662	454	12	475.726	0.496	
BGR25-OBS112	Nammu	6D7	73°30,20	16°26,34	456	11	-5.205	-0.006	
BGR25-OBS113	Lobster	6D6	73°27,96	16°24,31	462	12	340.937	0.366	
BGR25-OBS115	Nammu	6D6	73°27,175	16°33,914	456	11	-76.693	-0.088	
BGR25-OBS116	Lobster	6D6	73°25,542	16°36,101	460	11	450.324	0.502	
BGR25-OBS118	Nammu	6D6	73°23,414	16°22,855	470	11	-92.984	-0.106	
BGR25-OBS119	Nammu	6D6	75°14,147	24°31,3	140	10	-3.767	-0.004	
BGR25-OBS120	Lobster	6D6	75°05,161	24°31,449	177	9	16.994	0.026	
BGR25-OBS121	Lobster	6D6	75°08,558	24°14,608	164	10	310.397	0.417	
BGR25-OBS122	Nammu	6D6	75°04,630	23°50,180	134	9	-76.235	-0.121	
BGR25-OBS123	Lobster	6D6	75°02,214	24°08,752	146	10	246.516	0.335	
BGR25-OBS124	Nammu	6D6	74°57,714	24°05,492	139	0	-63.911	-0.101	Stopped recording after 1 minute
BGR25-OBS125	Lobster	6D6	74°52,020	23°53,953	129	9	160.566	0.222	
BGR25-OBS126	Nammu	6D6	74°54,560	24°25,617	152	8	-203.844	-0.32	
BGR25-OBS127	Lobster	6D6	74°47,857	24°18,592	160	9	327.304	0.46	
BGR25-OBS128	Lobster	6D6	74°46,059	24°42,959	207	8	267.585	0.417	
BGR25-OBS129	Lobster	6D6	74°52,194	24°46,973	181	8	207.727	0.335	
BGR25-OBS130	Lobster	6D6	74°59,396	24°54,374	191	8	177.892	0.281	

11.3 Air Guns, Streamer and Data Acquisition

Seismic Sources

The air gun array includes 16 G-guns subdivided into two gun strings with eight guns each (Fig. 11.3.1). Each gun string consists of four two-gun clusters. The individual gun volumes of the port side array range from 380 in³, 250 in³, 180 in³ to 100 in³ whereas the starboard array volumes vary from 250 in³, 200 in³, 120 in³ to 70 in³. The maximum total volume sums up to 3,100 in³ (50.8 l). The compressed air was provided by three Sauer&Sohn compressors aboard RV MARIA S. MERIAN in order to provide the working pressure of appr. 2,100 psi (145 bar).

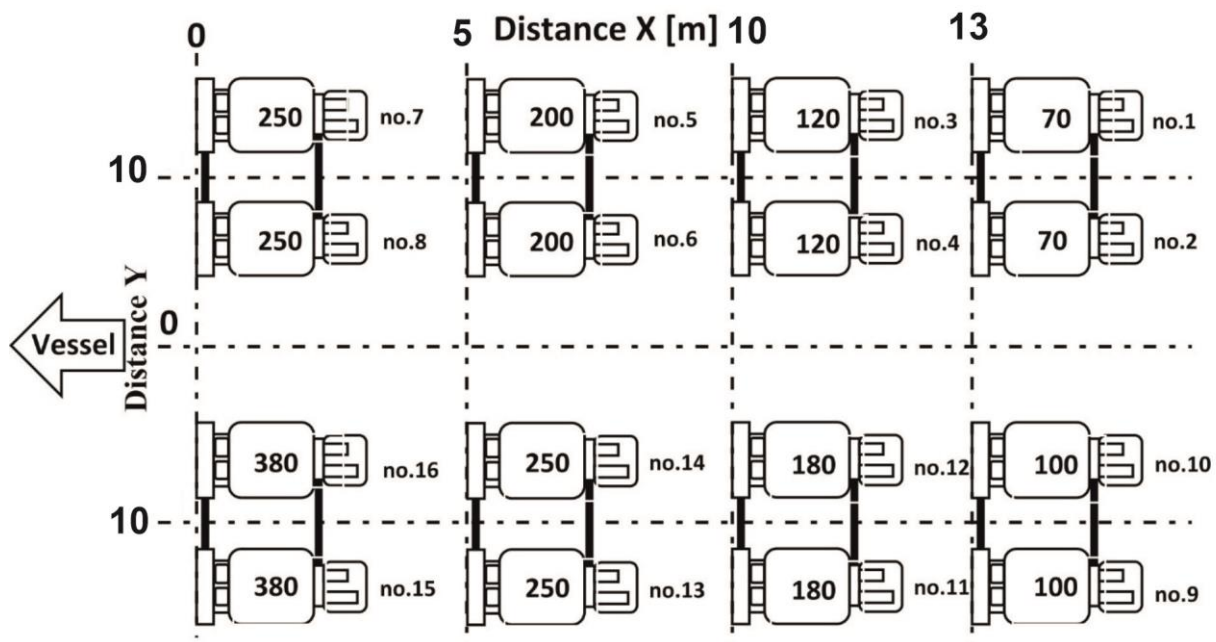


Fig. 11.3.1 BGR's airgun system during cruise MSM137. The individual volumes are given in in³.

The towing depth of the air guns was 5.0 m throughout the survey. The towing distance between the vessel and the center of each gun string is 46.3 m behind the stern of the vessel (Fig. 11.3.2 and Fig. 11.4.4).

Triggering and synchronization are controlled by the BigShot gun-controller from “Real Time Systems/Teledyne”. The input trigger signal comes from the navigation system ORCA controlling the equidistant shot point spacing at 50 m and 25 m, respectively (25 m for the last two profiles only).

Before starting the MCS acquisition we enlarged the air gun power stepwise by a soft-start (ramp-up) procedure. The ramp-up was performed by shooting intervals of 30 s. Starting with the smallest air gun we added every 3 shots one additional gun. The soft start was completed after 22.5 minutes.

Seismic data recording

We used a SEAL 428 seismic recording system and a towed streamer cable with an active length of 6,600 m to record the seismic data. The bird controlling system (DigiCOURSE System3) and the streamer control system were connected to the ORCA navigation system. The

streamer cable sections were deployed from two cable winches that were placed behind the A-frame on the working deck (see Fig. 11.3.3). The detailed configuration of the streamer cable is shown in the Streamerplan (see Fig. 11.3.4). The recording parameters during the survey MSM137 are summarized in table 11.3.1.

The positioning controlling system DigiCOURSE System 3 controlled the vertical streamer position (depth) and measured the heading along the cable by 17 compass birds. DigiCOURSE System 3 is a hardware and software package that controls and collects data from a network of acoustic sensors and streamer positioning devices. The system has online command, diagnostic, and performance-monitoring capability. System 3 employs a modular architecture which provides a variety of configurations and levels of functionality. The minimum system equipment configuration includes two real-time processors: an Operator Interface (OI) and a Data Management Unit (DMU), a Line Interface Unit (LIU), and cable-mounted measuring devices. Further on, a recovery system which has a self-triggering mechanism at a depth of 50 m were attached to the streamer. We operated the cable at a depth of 6 to 8 m.



Fig. 11.3.2 Rear view from the vessel with port side and starboard side airgun arrays (orange buoys) and in the center the lead-in of the streamer cable. During acquisition, the lead-in was fixed with a cable-grip close to the sea surface.

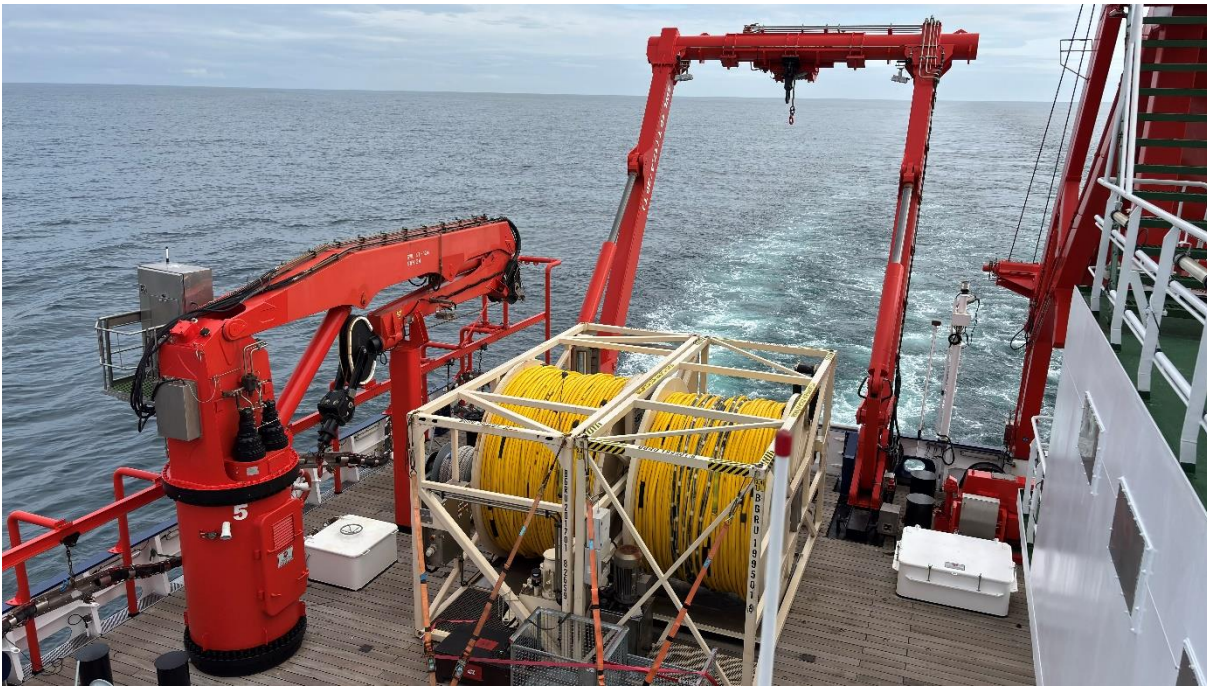



Fig. 11.3.3 Overview on to the working deck with two winches with streamer cable. The streamer was deployed in the center of the vessel, two rails with airguns are on the port side and starboard side of the vessel.

Table 11.3.1 Survey parameters during MSM137. Parameters with (*) belong to lines within working area 3, parameters with (‘) belong to lines BGR25-187A040, BGR25-188A041 and BGR25-189A045, parameters with (“) belong to lines BGR25-196A051 and BGR25-197A052.

Air guns	16 x Sercel G-Guns (from 70 to 380 in ³)
Total volume	3100 in ³ (~51 l)
Working pressure	145 bar (2100 PSI)
Towing depth	5 m
Trigger distance	50 m / 75 m (‘) / 25 m (“)
Near Trace Distance	134 m / 84 m (*)
Streamer Cable	Sercel Sentinel RD (5850 m with 12.5 m group distance and 750 m with 6.25 m)
Sample rate	1 ms
Recording length	14,000 ms

Low-cut	3 Hz
High-cut	200 Hz
Towing depth (Streamer)	6 m (upt to 8 m due to sea conditions)

Fahrt Mibas mit FS Merian												WB		CB1			
Gesamtlänge (Heck - Endboje):6826,87m																	
Aktivlänge: 6600m																	
												Slip Ring					
												8356-0904					
												Lead In		SHS	HAU	HESE	HESA
												110 m		6m		50m	10m
												M338030/ 01		1461	6687739	511300074	404093074

11.4 ORCA Navigation, Vessel Geometry and Data Protocols

Orca Navigation

Orca is an industry standard seismic navigation system for 2D & 3D, aiming to calculate for each shotpoint the exact positions of seismic sources and all receiver hydrophones in the long towed streamer in order to provide the correct geometry for seismic data processing. Orca is processing all geometry and interface data, a dedicated control and planning tool for profile lines (with the option to steer the vessel), enabling QC (quality control) analysis of all sensor data, provides a powerful processing tool (Iris) for all sensor data to significantly improve online solutions (P1 files), generates various reports with figures for each line (e.g. streamer depths and feathering), and stores the complete project in an archive.

At BGR, the Orca software (version 1.16.1) has undergone the sensitive vessel swap procedure from RV SONNE to RV MARIA S. MERIAN and was patched to level 215. A new survey project msm137 with survey parameter, airgun and streamer geometries, and preplots in P1/90 format of planned survey lines have already been set up. On board, vessel geometries have been completed by e.g. antenna positions. Interfaces to the vessel, to the streamer (System 3), to the tailbuoy RGPS, to Seal and gun controller systems were established, as well as modifications of the streamer and survey layout. Mobilizing of the whole Orca system and seismic equipment from Container to first line took four days; all actions during the whole cruise are documented in an Orca Lab-book MSM137.

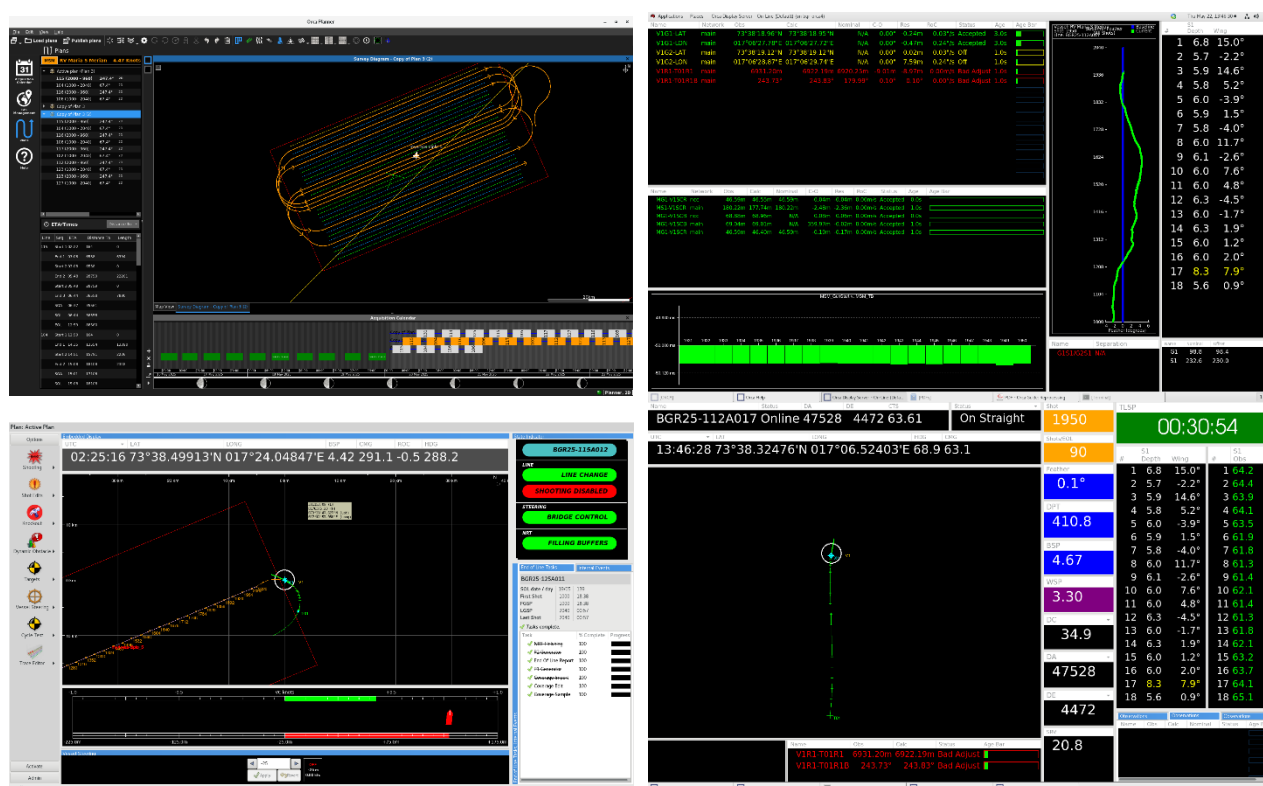


Fig. 11.4.1 Orca1 with Planner (top left) and Control (bottom left), Orca2 with two displays (top & bottom right)

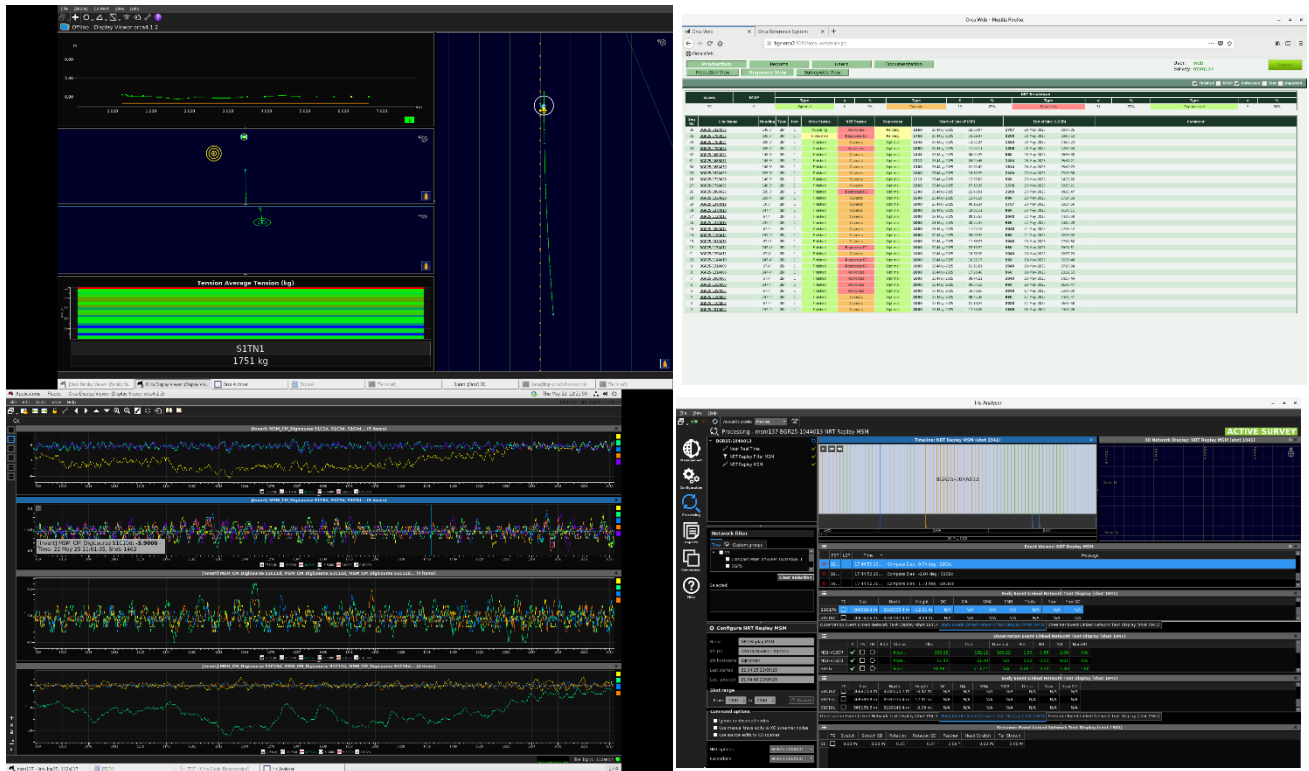


Fig. 11.4.2 Orca4 with Display (top left), QC (bottom left), Iris (bottom right), and Orca5 with Web (top right)

The Orca system is running on five servers plus the power real time navigation unit (PRTNU), the latter is processing all input and output interfaces and triggers and provides the precise timing (heart beat). Each server has a dedicated role: orca1 for control, orca2 for logging, orca3 for processing, orca4 for coverage and orca5 as a hot spare. In addition, a bridge PC for displays exists but was not needed in this 2D case.

MIBAS setup

Seismic profiling has been conducted in three selected target areas: 1, 2 and 3. Each rectangular area consisted of 50 km long parallel straight profile lines extending over ca. 20 km in width, which have been loaded as preplots in Orca Planner with a half kilometer spacing (line numbering increasing from N to S). Additional lines with different azimuths crossing the OBS and parallel lines have been added manually in the Survey Editor. Depending on weather conditions, the turn radius had to be adopted and the next target lines have been selected in the planner accordingly, providing also the timing of upcoming profile lines in a calendar view. The shotpoint (SP) numbering of all 50 km long profile lines started (SOL: start of line) with SP1000 in the W and ended (EOL: end of line) at SP2000 in the E due to the equidistant 50 m shotpoint spacing (Orca Editor). Before a profile, 20 approach shots filled the NRT (near real time) buffer needed for shotpoint predictions, 40 runout shots after the line allowed 2 km streamer to pass the EOL position for better coverage. Approach and runout shots were already part of the ending or beginning turn. Profile shifts (DA and DE) have been set to zero, turn radii varied between 4.7 km (2.5 nm) and 5.7 km (3 nm).

In Orca Control, estimate position 10 minutes before a new line helped to correct the streamer geometry (e.g. tailbuoy offset), which could have been distorted during the 180° turn. During all

turns, a mitigation gun fired once per minute triggered by the Bigshot gun controller. Shortly before the approach, the gun controller switched to external trigger mode and shooting was enabled in Orca Control. Shooting ended automatically at the last shot point of runout and the gun controller switched back to internal mitigation gun triggering. Orca produced 60 more silent shots (blue dots on the map) to enable NRT finding a solution and producing an online P1/90 file, if the NRT quality was sufficient – otherwise reprocessing is obligatory. At the beginning of profiling or after shutdown due to MMO sightings, a soft start was required and triggered internally by the gun controller as well.

During production, the Orca watch keepers continuously checked the quality and state of all incoming data observing various Display Servers and checked processes in Diagnostics. Special attention was given to streamer tension, bird depths, vessel velocity, and the age of incoming observations – all events like MMO shutdowns, soft start, gun failures, variation of streamer depth or any problems are entered in the time-stamped online journal protocol (Orca Web). Two one-page handouts for the watch keeper's tasks and radio communication to bridge and MMOs were created (ORCA-to-do_MSM137.docx & Communication_MSM137.docx).

Orca QC time series workspaces allowed to check online (adding one value per shotpoint) the behaviour of various parameters: E.g. the range to the tailbuoy, streamer tension, speed through water, streamer depths, bird angles, or GPS clock accuracy (shift of DSHIP and Kongsberg GPS against the Orca GPS time stamp). In addition, QC was also very helpful in analysing upcoming problems afterwards (all past profile data could be loaded). Various reports with figures are created at EOL, which also give hints for possible problems and should be checked after each line.

Post-processing with Iris

Orca produces for each line P2 files (P2/94 and P2/11) with all geometry data. In an ideal case, Orca produces P1 files directly after finishing a line based on the NRT solution. However, some profiles indicate bad data quality and require reprocessing. In addition, S-records have been exported to separate files. These contain positions as well as the exact timing (10^{-6} sec) for each shot point and will be used for processing of OBS data.

In general, it is recommended to apply Iris reprocessing for all lines in the same manner, using the advantage of e.g., filtering the whole time series (and not knowing only the past in the online solution). We applied a systematic check of all observations: For GPS data, dynamic SD have been rejected, RGPS data have always been edited and gaps interpolated since data quality was insufficient. A LP (low pass) filter with 120 s cut-off period helped to smooth irregularities and jumping levels. Compass bird data and depths have been checked for gaps or wrong depths (e.g. in the air, which had to be cut out and interpolated). Echosounder data have been filtered with a 60 s LP in order to smooth jumps. Occasionally, bad shots had to be removed in the shotlog table of Sprint (called by Iris edit). This processing scheme solved all caveats indicated by the NRT filter and stated an optimal solution for all profiles. NRT options and exceptions can be modified for single profiles, e.g. for varying streamer depths. Afterwards in Orca Web, the EOL tasks created the final P1 files and all quality reports. The Iris processing scheme has been documented in a separate file (Iris_Processing_MSM137.docx).

Support and Issues

During this survey, several support enquiries could be solved by the 24/7 support team from Sercel Concept Systems Ltd. in Edinburgh & Australia. Problems and solution actions have been documented in separate word-files for future look up. Support questions concerned

- Planner crash (solved by renaming the config file and restarting the process)
- Geometry correction (solved by snapshot procedure in Orca Configuration node)
- An Iris crash turned out to be a major issue, a partition crash on orca3 required a replace of all orca3 tasks to orca4 (role swap procedure) and disk repair of orca3
- Role swap procedure (to move processing role from orca3 to orca4 and vice versa)
- Orca3 crash repair actions (including xfs-repair of partition sdb1)
- Iris line lock removal (as a consequence of the orca3 crash)
- Iris processing of all observations (e.g. echosounder)
- PRTNU heart beat failures (not solved yet)

All major repairs could be conducted during turns without any data loss along lines. The role swap procedure as a consequence of the orca3 crash was critical, needs careful preparation with checklists, and took about one hour. When the Iris database (and NRT) was not available, a complete Iris processing could be performed by importing the P2/11 files instead.

During this survey, several issues approached with the following outcome

- Tailbuoy range data had medium quality, which even decreased during the survey resulting in gaps up to 1 minute. We replaced the omnidirectional antenna on the vessel observation deck to our directional antenna, exchanged antenna cables, and improved the antenna position – however, without success. A replacement of the GPS antenna on the tailbuoy solved the problem.
- We tested timed shooting in turns by Orca. However, Orca treats turns as an extensions of profiles and a switch of timed shooting during turns and distance shooting along the line is not possible. Timed and distance shooting may only be alternated from one line to another.
- Since the streamer depth changed from 6 m to 8 m in bad weather conditions and streamer depth varied sometimes along the profiles, the strict tolerance of 1 m caused a lot of error messages in the journal and crashed sometimes NRT online solutions. An exception file with more tolerance for streamer depths (e.g. 4 to 9 m) solved this issue.
- Some processes were critical (e.g. NRT, Planner, Iris) and stopped sometimes. In diagnostics, these processes can be observed and activation of the verbose debugging mode helps to understand errors.
- Twice, triggering failed along a profile and the reason was a missing heart beat (HB) in the PRTNU. A restart of the PRTNU solved the problem.
- We could not implement acoustics to the streamer and vessel since the vessel moon pool was not accessible. However, manual observations to streamer and guns worked well (with deactivated streamer stretch and rotation).

- Interfaces through DSHIP and the Moxa converter had a time delay between 1.6 to 2.6 s for the vessel's DGPS. This value remained stable throughout the survey and could be accepted. However, a virtual VUDP port for DGPS provided via the vessel's Ethernet is a working alternative. The serial weather data interface (Sagem) did not work this time.
- During EOL tasks, the coverage process stuck completely several times. However, waiting up to one hour solved the problem (process completed by itself).

A 'How-To-Orca-2D' document with more than 20 pages had been written after SO301 and was updated with MSM137 remarks (How-to-Orca-2D-MSM137.docx).

Vessel and seismic equipment geometries

The Geometry of the vessel sensors and seismic equipment in sea is sketched in Figs. 11.4.3 and 11.4.4.

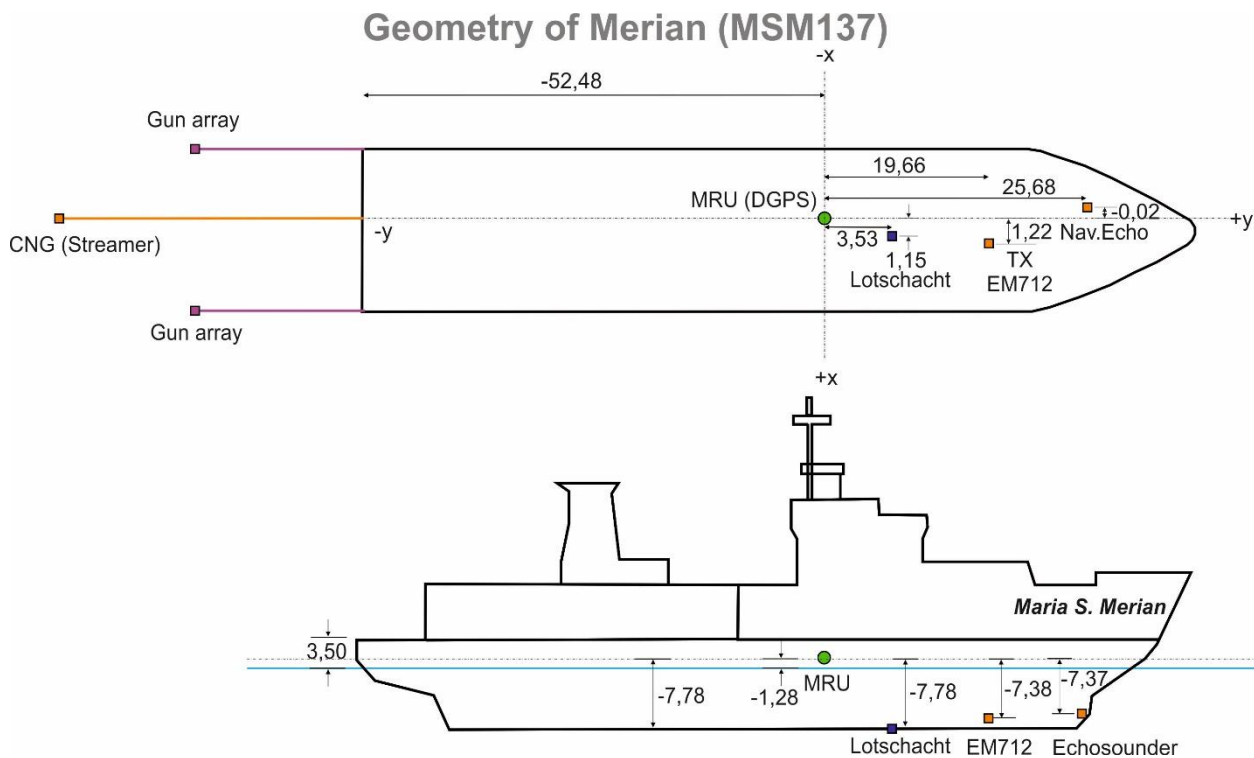


Fig. 11.4.3 Maria S. Merian vessel geometry.

Orca Geometry in water (MSM137)

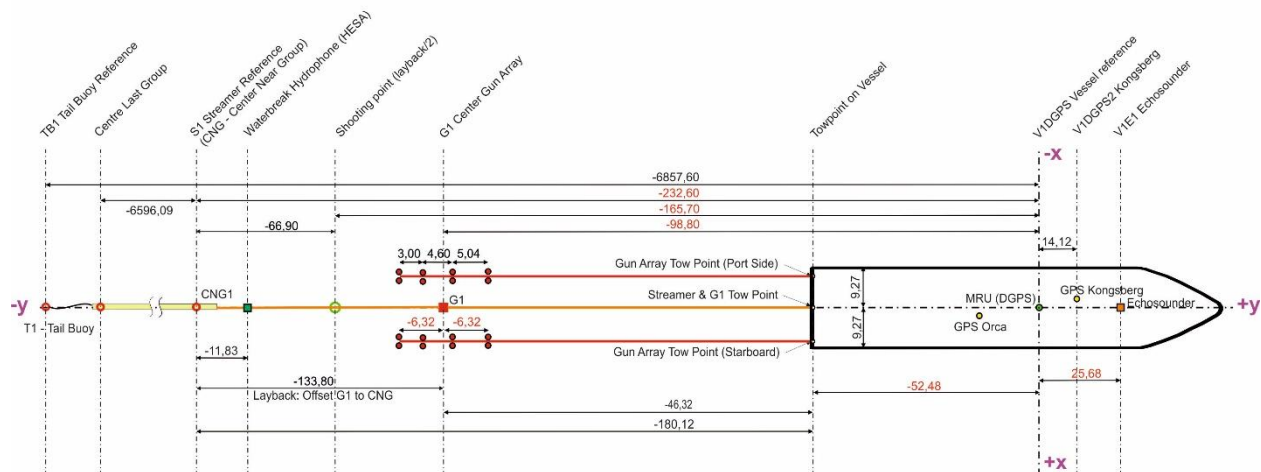


Fig. 11.4.4 Geometry of all seismic equipment in sea for working areas 1 and 2. In working area 3, the Lead In had been shorted by 50 m modifying all streamer reference points accordingly.

PRTNU interfaces and protocols

The PRTNU wiring and interfaces are sketched in Fig 11.4.5. The vessel provided via DSHIP Ethernet network and conversion via a Moxa box the following channels: DGPS (S1), Pitch & Roll (S2), Gyro (S3), Echosounder water depth (S4), Speed through water (S5), and sound velocity (S10). Channel 7 (gun header) and channel 9 (Seal header) were created from Orca. In addition, channels 6 and 8 have been used for input from the Kongsberg RGPS system (sent via Moxa-Ethernet-Moxa from the observation room). Protocol examples are listed below:

S1	DG_NMEADGPS DGPS Vessel	38400 8N1	\$GPGGA
\$GPGGA,005120.00,7459.193,N,02331.918,E,2,34,0.4,21.2,M,26.00,M,5.00,123*43			
S2	PH_NMEA Pitch Roll	38400 8N1	\$PRDID
\$PRDID,-0.500,-1.70,328.420,-0.020*58			
S3	GY_NMEA Heading	38400 8N1	\$GPHDT
\$GPHDT,327.96,T*0C			
S4	EC_NMEA Echosounder (waterdepth)	4800 8N1	\$EMDPT
\$EMDPT,150.940*43			
S5	XX_NMEA_ANY Speed Through Water (m/s)	38400 8N1	\$WATSP
\$WATSP,2.47,-0.15*69			
S6	DG_NMEAGPS2 GPS Kongsberg	9600 8N1	\$GPGGA
\$GPGGA,020448.01,7509.3419,N,02447.2426,E,1,08,01.0,+47.6,M,+00.0,M,00.0,0000*76			
S7	GN_GCS90 Gun Controller (Bigshot)	9600 8N1	
*GCS900452-186A026000000176603E25/05/26:19:05:1612161600000000203100 ...			
S8	RG_MULTIFIX Kongsberg Range & Bearing	9600 8N1	
122723.00S1 6925.4147.390-23.2 7 1.1S2 .0 .000 .0 0 .0S3 .0 .000 .0 0 .0S4 .0 .000 .0 0 .0			
S9	HDR_SEAL Seal 19200 8N1		
\$10627001103020540.30387920250527UTC001767 BGR25-186A026 75.156674 24.785509 152.2 75.155924 24.787354328.2332.3 4.6 26001000608180.6008344543.500058.0-0080.1328.314 ...			
S10	XX_NMEA2 Sound velocity	4800 8N1	\$SVKEEL
\$SVKEEL,1448.80*01			
S11	SP_SAGEM Weather	4800 8N1	\$WIMDA
failed (but worked 2023 on Merian)			

PowerRTNU - Verkabelung MSM137 (2025)

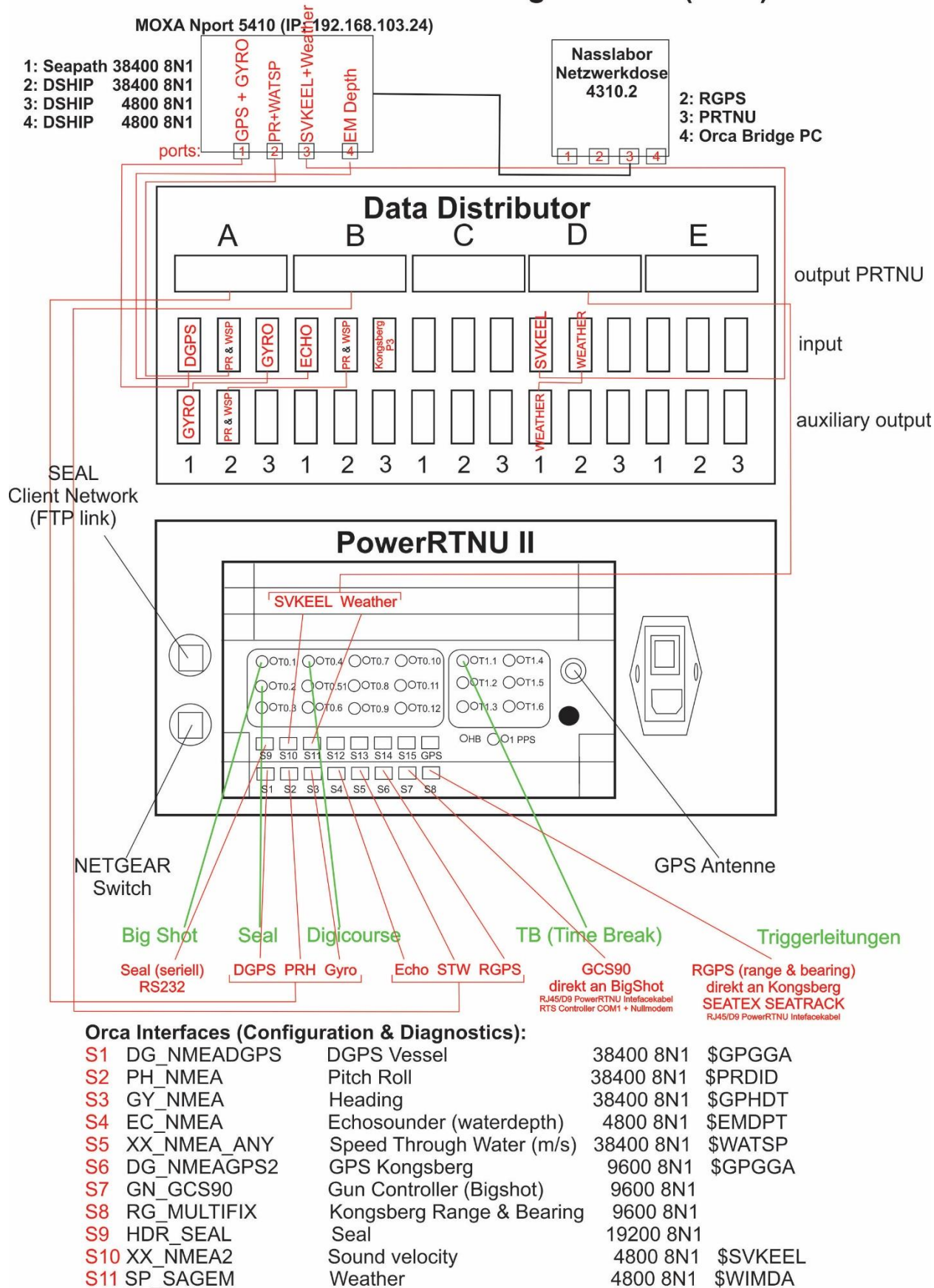


Fig. 11.4.5 Power RTNU wiring during MSM137 and list of interfaces (channels S1 to S11).

Navigation plan protocols of all profiles

MSM137 MIBAS - NAVIGATION PLAN Nb. 1 in Area A								
Preplot	PASS	SEQ	FSP (approach)	SOL date	SOL time	EOL time	LSP (runout)	REMARKS
101	A	02	17:47:11	16.05.2025	17:53:26	23:39:26	23:46:26	timed shooting 60s during whole profile (different SP numbering), at 20:24:26 change of CTB signal from high to low (before 10 ms too late), around SP1790 streamer front low
110	A	03	01:11:44	17.05.2025	01:18:24	06:41:36	06:54:21	
119	A	04	08:39:11	17.05.2025	08:45:38	14:32:33	14:45:47	Since Run 4: runout elongated from 20 to 40 SPs (either SP960 or SP2040), shots 1574-1576 without BB gun 1&2
129	A	05	16:41:57	17.05.2025	16:46:34	22:27:44	22:41:08	sailing right & left swing along profile between SP1470 - SP165
118	A	06	00:47:19	18.05.2025	00:54:18	06:34:42	06:48:47	
108	A	07	08:37:13	18.05.2025	08:44:21	14:44:18	14:57:44	one compressor down: SP1228-SP1657, pressure between 120-143 bar Q BSP 4.2 kn
121	A	08	17:21:28	18.05.2025	17:28:46	22:59:35	23:12:53	
131	A	09	01:04:12	19.05.2025	01:11:01	06:46:43	07:00:04	
114	A	10	10:15:28	19.05.2025	10:22:17	15:59:10	16:13:48	
125	A	11	18:31:16	19.05.2025	18:38:28	00:42:56	00:57:29	streamer off due to leakage errors, data gap between SP1923-SP1958
115	A	12	03:06:14	20.05.2025	03:13:22	09:00:51	09:14:51	
104	A	13	11:31:25	20.05.2025	11:38:27	17:31:06	17:44:50	bird 17 knocked out (erroneous depth values)
116	A	14	20:02:36	20.05.2025	20:09:32	01:58:39	02:13:02	bird 17 knocked out (erroneous depth values), streamer depth 8 m since several profiles
106	A	15	11:34:50	21.05.2025	11:42:19	17:33:41	17:47:12	bird 17 knocked out, streamer depth 6 m
123	A	16	20:44:04	21.05.2025	20:51:37	02:48:20	03:02:29	

MSM137 MIBAS - NAVIGATION PLAN Nb. 2 in Area A								
Preplot	PASS	SEQ	FSP (approach)	SOL date	SOL time	EOL time	LSP (runout)	REMARKS
112	A	17	08:09:24	22.05.2025	08:09:24	14:04:40	14:18:59	gun 7 port side (380 cuin) failed since SP1690
127	A	18	18:54:09	22.05.2025	19:02:11	01:29:03	01:43:11	gun 5 port side (250 cuin) failed since SP2008 & gun 6 port side (250 cuin) failed since SP1991
134	A	19	06:10:31	23.05.2025	06:16:24	10:27:50	10:34:56	gun 5 port side (250 cuin) & gun 6 port side (250 cuin) not working
133	A	20	13:39:44	23.05.2025	13:46:18	17:09:45	17:17:16	gun 5 port side (250 cuin) & gun 6 port side (250 cuin) not working

Fig. 11.4.6 Navigation plan in working area 1.

MSM137 MIBAS - NAVIGATION PLAN Nb. 3 in Area B								
Preplot	PASS	SEQ	FSP (approach)	SOL date	SOL time	EOL time	LSP (runout)	REMARKS
186	A	26	22:43:01	27.05.2025	22:43:01	04:31:30	04:45:47	FSP already on line at SP1200, streamerdepth very variable, partly at surface
172	A	27	07:03:13	27.05.2025	07:10:26	10:55:21	-	EOL due to MMO shutdown (SP1530), starboard gun 6 down since SP2021
172	B	28	-	27.05.2025	12:53:02	14:08:18	14:22:26	SOL with soft start on line (SP1211 12:53 - SP1151 13:14)
182	A	29	16:05:29	27.05.2025	16:12:29	22:56:35	23:10:38	port side gun 3 down since SP1520, streamerdepth 8 m
168	A	30	01:45:54	28.05.2025	01:52:42	03:49:23	-	EOL due to MMO shutdown (SP1814), streamerdepth 6 m
168	B	31	-	28.05.2025	04:24:46	05:41:21	-	SOL with soft start (SP1712 4:24 - SP1652 4:45). Gun 7 (250 cuin) starboard down 04:55. EOL due to MMO shutdown .
168	C	32	-	28.05.2025	06:01:25	08:44:07	08:58:35	SOL with soft start (SP1441 06:01 - SP1381 06:24).
178	A	33	11:02:44	28.05.2025	11:07:11	12:54:35	-	Soft start 10:39 - 11:01. EOL due to MMO shutdown (SP1494), streamerdepth 6 m
178	B	34	-	28.05.2025	13:07:24	14:07:23	-	SOL with soft start 13:07-13:28. Gun 8 (250 cuin) starboard down since 13:58. EOL due to MMO shutdown
178	C	35	-	28.05.2025	15:29:47	17:50:03	18:03:53	SOL with soft start 15:29-15:51. Gun 8 starboard still down.
142	A	36	22:22:49	28.05.2025	22:30:07	05:52:02	06:07:42	Gun 8 starboard still down. Gun 6 (200 cuin) starboard down since 0:10.
164	A	37	09:50:06	29.05.2025	09:57:25	11:28:11	-	EOL due to MMO shutdown
164	B	38	-	29.05.2025	11:57:32	16:57:28	17:12:24	SOL with soft start (11:57-12:21)
150	A	39	19:29:18	29.05.2025	19:36:35	02:37:51	-	
187	A	40	04:15:10	30.05.2025	04:23:52	09:20:29	09:28:10	(no mitigation gun after EOL)

MSM137 MIBAS - NAVIGATION PLAN Nb. 4 in Area B								
Preplot	PASS	SEQ	FSP (approach)	SOL date	SOL time	EOL time	LSP (runout)	REMARKS
188	A	41	13:07:15	30.05.2025	13:18:39	21:24:50	21:47:56	SOL with soft start (13:07 - 13:28), 75 m SP spacing
162	A	42	00:35:56	31.05.2025	00:42:49	07:03:49	-	EOL due to trigger failure since SP2062 (Orca: NRT down, HB down, digicourse), no shooting, gun 6 starboard with sensor problems
146	A	43	01:15:38	31.05.2025	10:23:10	17:12:16	17:26:15	Soft start from 9:44 - 10:06 before approach
156	A	44	19:17:04	31.05.2025	19:24:13	02:06:52	02:21:27	streamer at 6 m depth since SP1020
189	A	45	05:34:17	01.06.2025	05:43:23	13:06:33	-	streamer at 6 m depth since SP1737, 75 m SP spacing

Fig. 11.4.7 Navigation plan in working area 2.

MSM137 MIBAS - NAVIGATION PLAN Nb. 5 in Area D								
Preplot	PASS	SEQ	FSP (approach)	SOL date	SOL time	EOL time	LSP (runout)	REMARKS
190	A	46	-	04.06.2025	14:57:20	20:46:10	21:00:04	Soft start 14:29-14:52 before approach, no HB during approach - reboot PRTNU, FSP at SP2000
191	A	47	23:20:09	04.06.2025	23:27:03	03:58:23	-	
192	A	48	05:12:55	05.06.2025	05:16:18	09:27:29	09:41:01	Gun tests during runout
193	A	49	12:03:04	05.06.2025	12:09:59	15:55:12	-	LSP 1650 already in turn (profile shortened)
194	A	50	-	05.06.2025	17:16:55	20:59:42	20:59:34	SOL at SP1620 (profile shortened)
196	A	51	-	05.06.2025	22:39:11	01:36:48	-	SOL at SP1003, 25 m SP spacing, only starboard array firing (1280 cuin), approaching line slowly in S-shape starting with DC 4500 m over more than 1 hour
197	A	52	-	06.06.2025	02:54:53	05:29:04	-	SOL at SP1924, 25 m SP spacing, only starboard array firing (1280 cuin), EOL SP994

Fig. 11.4.8 Navigation plan in working area 3.

11.5 Hydroacoustics

Multibeam Echosounder – Technical Description

RV MARIA S. MERIAN is equipped with two Kongsberg Maritime multibeam echosounders. During the cruise MSM137, mapping of the seafloor morphology was carried out with the hull mounted Kongsberg EM712 and EM124 multibeam echosounders (MBES), respectively. For both echosounders, two linear transducer arrays, with separate units for the transmission and receipt of signals, are aligned in a Mills cross configuration, where the transmit array is mounted along the length of the ship and the receive array is mounted across the vessel. The EM124 system operates at 12 kHz and covers water depths from 20 m below the transducers up to full ocean depth but was only used briefly on the transit to the working area. The EM712 system offers a broader frequency ranges between 40 and 100 kHz and is designed for water depth ranging between 3 m and a maximum of 3,600 m but preferred on this vessel to appr. 1,000 m. Within our dedicated study areas, we exclusively used the EM712. Two different transmit pulses can be selected: a CW (Continuous Wave) or FM (Frequency Modulated) chirp. The sounding mode can be either equidistant or equiangular, depending on operation preferences and requirements. Both systems can be operated in single-ping or dual-ping mode, where one beam is slightly tilted forward and the second ping slightly tilted towards the aft of the vessel. The whole beam can also be inclined towards the front, or the back and the pitch of the vessel can be compensated dynamically. The EM712 system generates 512 beams for a maximum spreading angle of 148° and offers a high beam density mode and up to 800 soundings per swath. However, we operated the device usually with a swath angle of 148°. The EM712 system installed on RV MARIA S. MERIAN is of a 1° x 0.5° design.

The echo signals detected from the seafloor go through a transceiver unit (Kongsberg Seapath) into the data acquisition computer or operator station. The data were stored in the KONGSBERG acquisition software SIS. The ship's position was provided by the onboard Seapath system, that also provided motion and heading data. Positioning is implemented onboard RV MARIA S. MERIAN with conventional GPS/GLONASS/GALILEO plus Real Time Kinematic positioning (RTK). By means of combining GPS satellite signals with signals from a local base station, which in turn receives correction signals from a local land station, a correction of the signal is made. A dm vertical accuracy can be achieved using this setup. Therewith the tidal variation ranging 0.15 m were corrected in postprocessing using the EGM-2008 geoid. Beamforming also requires sound speed data at the transducer head, which is available from an inbuilt keel sound velocity probe. This signal goes directly into the SIS operator station. In addition to bathymetric information, the EM712 system registers the average amplitude and sidescan time series (Snippet) of each beam. The system also allows recording of the entire water column. The amplitude signals correspond to the intensity of the echo received at each beam. It is registered as the logarithm of the ratio between the intensity of the received signal and the intensity of the output signal, which results in negative decibel values. For each ping, the EM712 records 800 backscatter values.

PARASOUND – Technical Description

The PARASOUND System DS3 (PS70) is a hull-mounted parametric echosounder developed by TELEDYNE ATLAS HYDROGRAPHIC GmbH. The transducer transmits signals with a

maximum transmission voltage 160 V, enabling a maximum penetration depth of up to 150 m in soft sediments. The system makes use of the parametric effect that occurs when very high (finite) amplitude sound waves are generated. If two waves of similar frequencies are generated simultaneously, the sum and the difference of the two primary frequencies is also emitted through the parametric effect. The primary high frequency (PHF) of the PARASOUND system onboard RV MARIA S. MERIAN is emitted within a 4.5° wide beam and the low parametric frequencies inherit this beam characteristic - much narrower than, for example, the 30° wide beam of a 4 kHz signal when emitted directly from the same transducer. This results in a high lateral resolution and superior imaging of small-scale structures on the seafloor in comparison with conventional systems. The primary high frequency (PHF) and secondary low frequency (SLF) can be varied between 18 and 24 kHz, and 0.5 and 7.0 kHz respectively. The PARASOUND system supports three different pinging modes – quasi-equidistant, pulse train, and single pulse mode.

Overall, we used one set of acquisition parameters for the PARASOUND during MSM137, which was adapted with only minor adjustments. The PHF was set to 18 kHz and the SLF was set to 4 kHz, which resulted in pulse resolution of 0.188 m at water velocity for both PHF and SLF spectrums. The output sample rate was set to 12.207 kHz. We used the single pulse ping mode with a continuous wave with a rectangular shape. While operating simultaneously with the EM712, the PARASOUND was triggered externally by the Kongsbergs K-sync trigger box in a 1:2 (PS:EM712) ping ratio. The transmission source level was set to 150 V and later to 160 V after maintenance work on May 26. Data was acquired during transits with a speed of 10 kn, during seismic surveys with a speed of 4.5 kn, during bathymetric survey with a speed of 6 kn, and during flare imaging survey with a speed of 2 to 3 kn. The recording window length was set to 200 m. The time variable gain was set to automatic with a gain shift of 25 dB after some testing.

11.6 Magnetics

Marine Magnetics SeaSpyII Gradiometer

The SeaSpyII Marine Gradiometer System manufactured by Marine Magnetics Corp. normally consists of two proton precession magnetometers, enhanced with the Overhauser effect. In its standard configuration two exactly equivalent magnetometers are towed 150 meters apart as a longitudinal array 750 meters astern of the ship. Both sensors measure the total intensity of the magnetic field simultaneously. The difference between the two measurements is an approximation for the longitudinal gradient of the field in the direction of the profile line. Provided that the time variations are spatially constant over the sensor spacing, the differences are free from temporal variations and their integration restores the variation-free total intensity or magnetic anomaly (apart from a constant value).

A standard proton precession magnetometer uses a strong DC magnetic field to polarize itself before a reading can be taken. Overhauser sensors work similar to proton magnetometers with the exception that the excitement of the proton spin (polarization) is done by radio waves which excite the spin of the electrons in an organic fluid within the sensors. The electrons then transfer their spin to the protons in the fluid via a quantum mechanical process called Overhauser effect. Similar to every other proton magnetometer the relaxation frequency of the protons is a measure for the magnitude of the ambient magnetic field. The polarization power required is much smaller than that needed by normal proton magnetometer systems and the AC field may be left active while the sensor is producing a valid output signal. This allows the sensor to cycle much faster and to produce more precise results than a standard proton magnetometer. The signal is digitized by the electronics assembly within the tow fishes which then transmit digital data strings via a two conductor tow cable to the vessel. The tow cable is connected to a deck leader which is in turn connected to the power supply and the logging computer. As configured for this survey, the Overhauser sensors had a cycle time of one second. The sensors are specified with a noise level of $0.01 \text{ nT}/\sqrt{\text{Hz}}$, a resolution of 0.001 nT , and an absolute accuracy of 0.2 nT .

SeaSpy Vector Magnetometer

As an additional option, Marine Magnetics offers a Vector Magnetometer consisting of a towfish equipped with a fluxgate magnetometer from Magson company in Berlin. The system consists of i) a digital 3-axis fluxgate magnetometer yielding excellent precision, ii) a two-axis tilt-meter, iii) a high-precision IMU device, capable of measuring 3-axis acceleration and gyro angle, and iv) sensors for temperature, pressure, and humidity. Fluxgate and inclinometers are mounted on a common platform. The data from the Vector sensor are transmitted via the same communication protocol to the ship over the tow cable.

The Magson fluxgate uses the principle of vector-compensating all three ring-core-sensors by means of three independent Helmholtz-coils. The internal feedback circuit, using digitally controlled DC-currents fed into the Helmholtz-coils maintains precise nulling of the field inside the ring-core. Thus, the amplitude of this current can be used as a signal to measure the vector components of the magnetic field. A factory calibration is required to provide offset, scale factor and non-orthogonality angle for each axis. All electronic components are integrated on the board of the data acquisition microprocessor. The Magson fluxgate sensor is specified with a noise level of $0.02 \text{ nT}/\sqrt{\text{Hz}}$, a resolution of 0.008 nT and a long term stability $< 10 \text{ nT/year}$.

A high precision of angle measurement is necessary to rotate the field components measured in the sensors coordinate system of the moving fluxgate towfish into the horizontal geomagnetic coordinate system. By Euler rotation it is possible to separate the vertical from the horizontal field vector components. The accuracy of the vector data is limited by the accuracy of the rotation angles. For example, a 0.01° tilt deviation may result in up to 10 nT component error in the survey area. Without any yaw angle estimation, the orientation of the horizontal field vector (i.e. the north and east component) remains unknown. A crude approximation might be ship's course. Utilising magnetic heading from the fluxgates themselves removes seafloor anomalies by default, however, a numerical yaw approximation has been introduced by Engels et al. (2008), demonstrating the advantages of vector component data analysis.

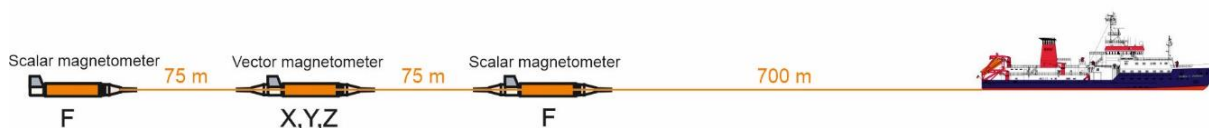


Fig. 11.6.1 Sketch of BGR's towed magnetometer system. During the cruise MSM137, mostly two towed sensors separated by a 150 m interfish cable were deployed.

Table 11.6.1 Magnetometer configurations used during cruise MSM137.

Profile	Main towcable	Sensor 1 serial No.	Interfish cable 1	Sensor 2 serial No.	Interfish cable 2	Sensor 3 serial No.
Test	700-N1	14095	75-N4	24001	75-N2	14097
BGR25-101 110 119 129 118 108 121 131 114	700-N1	14095	150-N1	14139		
BGR25-125 115 104 116 106 123 112 127 134 133	700-N1	24001	150-N1	14139		
BGR25-186 172 182 168 178 142 164 150 187 188	700-N1	24002	150-N1	14139		

162						
146						
156						
189						
Test	700-N1	14140	75-N4	14141		
BGR25-193	700-N1	14139				
194						
196						
197						

Data Processing

The magnetic raw data recorded by the Overhauser and fluxgate magnetometers were processed in time domain in order to obtain high quality magnetic data which are essential for further data analyses. Processing of total magnetic field gradients results in reconstructed variation free total field values. Single sensor fluxgate data provide anomalies in vector components which may still contain a variation contribution. Further processing of the vector component data with time and spectral domain methods will be part of the post-cruise work.

We use two standard processing sequences for total field magnetic data. The first one contains of a simple algorithm for cleaning erroneous data of one Overhauser sensor before the magnetic reference field (IGRF 2020) (Alken et al., 2021) is removed. The resulting magnetic anomalies are stored using a 1 second sampling rate.

The second processing sequence is more sophisticated and uses the records of one Overhauser and one towed Magson sensor. The philosophy is to pre-process raw data in the time domain in a comprehensive straight-forward and transparent way before gradiometer anomaly reconstruction and further component analysis. This processing will be applied to selected profiles during post-cruise data analysis and interpretation.

Fluxgate sensors require calibrations which are typically performed as loops (circles sailed by the ship for this purpose). However, sailing full circles while towing a seismic streamer is difficult and very time consuming. One almost complete loop with two towed magnetometer sensors and the streamer deployed was carried out on May 23rd, 2025, between 10:27 and 13:46 while changing from line 134 to line 133.

For the purpose of a quick on-board processing, the IGRF-corrected data were filtered with high-pass and low-pass filters in the local domain, which at a constant ship's survey speed is effectively equal to filtering in the time-domain. The cut-offs were set at 10 km and 120 km, resp., which equals roughly 1 hour and 12 hours, resp., at a constant survey speed around 5 kn. The crossover error analysis (see below) shows that with this filtering much of the external variations of the Earth's magnetic field could be removed from the data while preserving the contributions of magnetized rocks in the shallow sub-seafloor of the surveyed regions.

Data Quality

The magnetic data observed during the cruise are in general of good quality. The instruments performed well during most of the cruise. The combination of three towed sensors did not work correctly during a short test on the transit to the working area. Because of the failed test and because of relatively shallow water depths in the working areas, during the seismic work only two towed sensors were deployed in work areas 1 and 2 and only one sensor in work area 3 with water depths of less than 100 m. At the ship's typical speed during a seismic survey of 4.5 kn, the rear sensor in a combination of two sensors and a total cable length of 800 m operates at a

depth of around 70 m below the water surface and sinks even deeper when the ship has to slow down for operational reasons. With the additional weight of a third sensor, this operation depth would be some 10 to 20 m deeper and thus getting close to the safety limit of 100 m which during this cruise should not be exceeded due to the water depth. The sensors themselves have a depth rating of 300 m.

The Earth magnetic activity was moderate during much the cruise while magnetic measurements have been carried out with the towed magnetometer system. However, a magnetic storm occurred towards the end of the work in Area 2 on June 1. Figure 11.6.2 shows the Earth magnetic activity represented by Kp values after Bartels (1957) for the time between February and June 2025. The red line shows the times when the towed magnetometer system was in use parallel to the acquisition of seismic data.

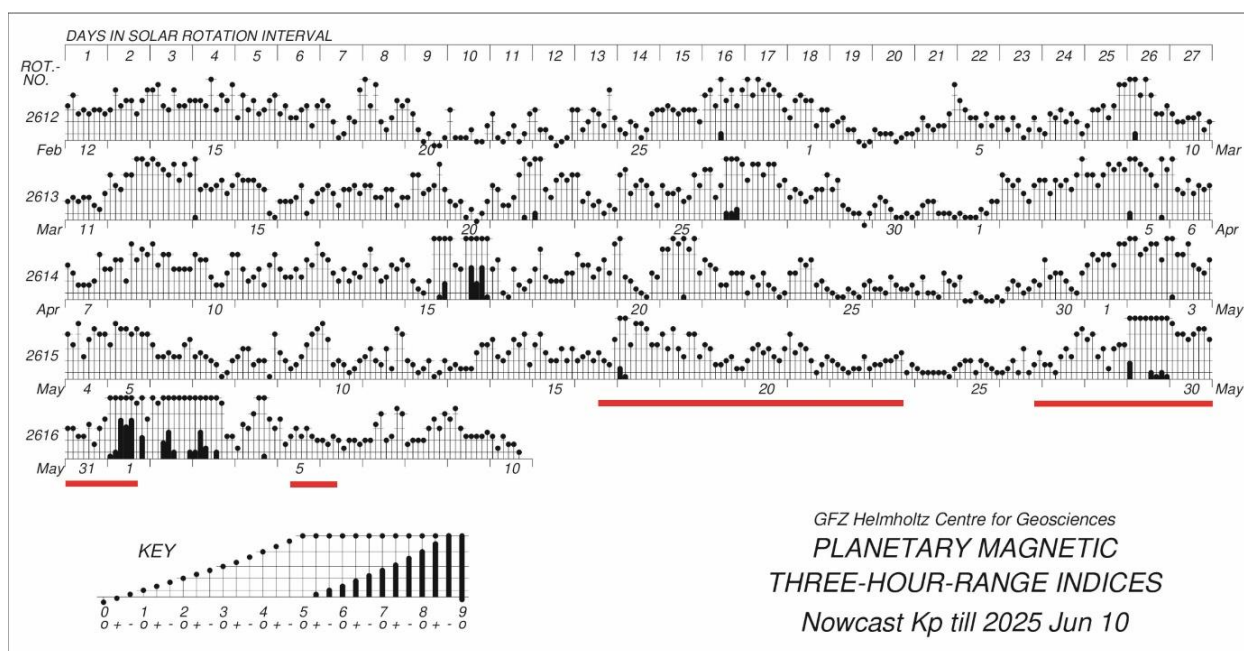


Fig. 11.6.2 Planetary magnetic three-hour-range indices for winter and spring of 2025. Low indices indicate low Earth magnetic activity and thus only moderate disturbance of magnetic measurements. The time period of magnetic measurements with the towed magnetometer array during cruise MSM137 is shown by the red bar.

At high latitudes, the time depending variations of the Earth's magnetic field reach amplitudes of several hundred nT in 24 hours even at low Earth magnetic activity and thus have higher amplitudes than the expected magnetic anomalies originating from shallow crustal sources in the working area. Therefore, in the post-cruise data processing the data from two nearby observatories will be used for correcting the external variations. Fig 11.6.3 shows the magnetic variations recorded at station Hornsund (Svalbard) at 77° N and 15.55°E, close to the survey area of cruise MSM137. The upper panel shows data from a magnetically relatively quiet day, May 31, with a maximum Kp of 4. The lower panel shows the magnetically massively disturbed June 1 with a maximum Kp of 8. The quiet day sees a variation amplitude of 800 nT in 24 hours, in the case of the disturbed day the amplitude is 1800 nT. In contrast, the typical amplitude of the observed magnetic anomalies in the survey area with crustal sources is only 200 nT.

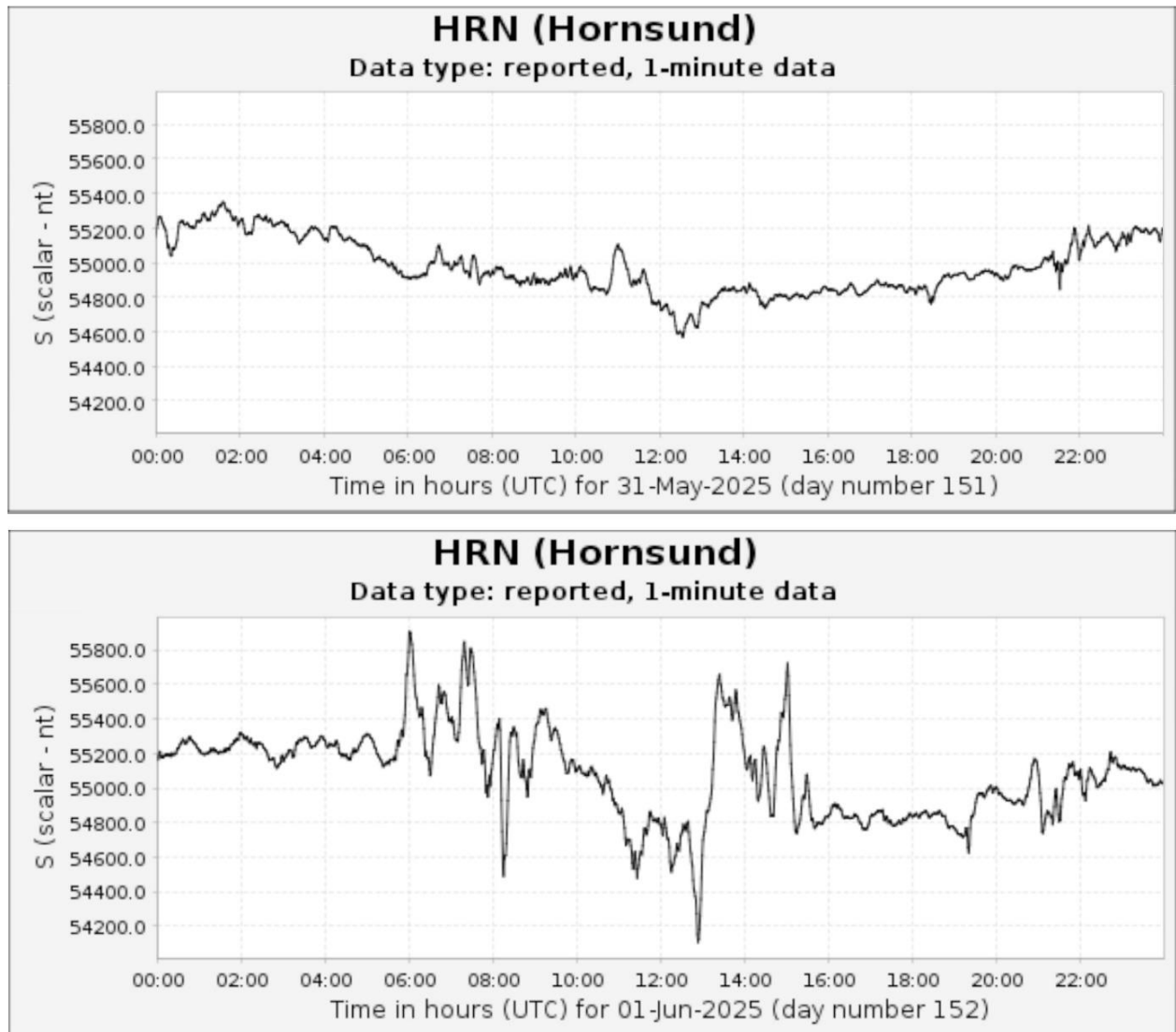


Fig. 11.6.3 Earth magnetic observatory data from station Hornsund (Svalbard) at 77° N and 15.55°E, close to the survey area of cruise MSM137. The upper panel shows data from a magnetically relatively quiet day, May 31, with a maximum Kp of 4. The lower panel shows the magnetically massively disturbed June 1 with a maximum Kp of 8.

Since the magnetic profiles of cruise MSM137 have a good number of crossovers, it was possible to determine the crossover errors for each survey area as a measure for the data quality after processing (Table 11.6.2). The crossover errors are remarkably low in Area 1 given the challenging circumstances for magnetic measurements at high latitudes described above. For Area 2, the crossover errors are also very low after excluding the last profile BGR25-189 from the dataset which was massively affected by the magnetic storm on June 1 (see Fig. 11.6.3). The small number of crossovers in Area 3 is possibly not representative for the whole dataset, but the very small crossover error hints at a good data quality after processing in this case too.

The map magnetic anomaly maps compiled from the datasets for survey areas 1, 2, and 3 after all corrections is shown in chapter 5.5, Figs. 5.12 through 5.14.

Table 11.6.2 Result of crossover analysis of magnetic data.

	Number of profiles	Number of crossovers	RMS error [nT]
Area 1	19	33	4.5 / max. 16
Area 2	13	11	6.2 / max. 17
Area 3	3	2	0.87

References

- Alken, P. Thébaud, E., Beggan, C.D. et al. (2021), International Geomagnetic Reference Field: the 13th generation, *Earth, Planets and Space* 73:49. doi: 10.1186/s40623-020-01288-x.
- Bartels, J., 1957. The geomagnetic measures for the time-variations of solar corpuscular radiation, described for use in correlation studies in other geophysical fields. *Ann. Intern. Geophys.* 4, 227-236.
- Engels, M., Barckhausen, U. and Gee, J.S., 2008. A new towed vector magnetometer: methods and results from a Central Pacific cruise. *Geophys. J. Int.*, 172, 115-129. doi: 10.1111/j.1365-246X.2007.03601.x.

11.7 Gravity

Method and Description

During cruise MSM137 MIBAS a sea gravimeter system KSS32-M was installed in the gravimeter room one level below the main deck (Fig. 11.7.1 and 11.7.2). The sea gravimeter sensor was located approximately 1 m above the vessel's nominal water line, 0.6 m to portside from the centerline, and 53.7 m forward of the stern. The KSS32-M (S/N 21) is owned by BGR and was installed on May 8 when RV MARIA S. MERIAN moored in Reykjavik harbor. The system was installed as early as possible to maximize the heating and running in time before leaving for the cruise.

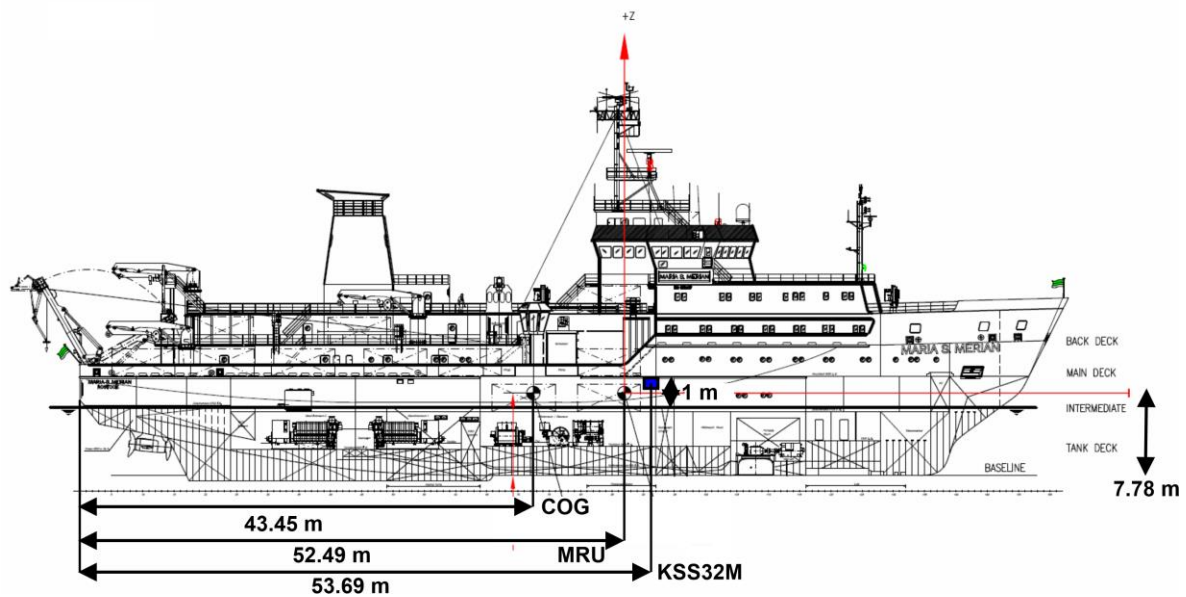


Fig. 11.7.1 Sketch of RV MARIA S. MERIAN with the location of the sea gravimeter (blue).



Fig. 11.7.2 KSS32-M gravimeter system mounted in the Gravimeter Lab on RV MARIA S. MERIAN.

The gravimeter system KSS32-M is a high performance instrument for marine gravity measurements, manufactured by the Bodenseewerk Geosystem GmbH. While the sensor is based on the Askania type GSS3 sea gravimeter designed by Prof. Graf in the 1960ties, the development of the horizontal platform and the corresponding electronic devices took place at Bodenseewerk Geosystem in the beginning of the 1980ties. The system was completely modernized and modified in 2011 by the successor company BGGs (Bodensee Gravimeter Geosystem GmbH, Meersburg). Before, the system consists of two main assemblies: the gyro-stabilized platform with the gravity sensor and a rack containing the control electronics, the data handling subsystem and the power supply. After the modernization the system electronics and the power supply are integrated in the platform. The system is controlled by a notebook (HP ProBook 6550B). The main software to operate the KSS32-M is DACQS developed by BGGs. It allows to change a number of settings (for example: parameters of the Bessel Filter applied to the measured data) and provides detailed information about the status of the system. The data acquisition is also managed by DACQS, whereby a wide range of values not only the gravity but also, for example, the attitude and horizontal accelerations of the platform could be recorded. A second notebook (Lenovo T510i) running the updated DACQS2 software was set up simultaneously to test and evaluate the new software. It turned out that DACQS2 delivers the serial gravity data much more reliably and was used therefore for the data acquisition.

The gravity sensor GSS30 consists of a tube-shaped mass that is suspended on a metal spring and guided frictionless by 5 threads. It is non-astatized and particularly designed to be insensitive to horizontal accelerations. This is achieved by limiting the motion of the mass to the vertical direction. Thus, it is a straight-line gravity meter avoiding cross coupling effects of beam-type gravity meters. The main part of the total gravity acceleration is compensated by the mechanical spring, but gravity changes are compensated and detected by an electromagnetic system. The displacement of the spring-mass assembly with respect to the outer casing of the instrument is measured using a capacitance transducer.

The levelling subsystem consists of a platform stabilized in two axes by a vertical, electrically erected gyro. The stabilization during course changes is improved by providing the system with online navigation data. The stabilized platform will keep the sensor in an upright position with an accuracy of levelling in the order of 0.5 arc-minutes. This is particularly important as the sensor is very sensitive to tilting and the corresponding effects of horizontal accelerations. Vertical accelerations, however, cannot be eliminated. Luckily on a ship the vertical acceleration oscillates symmetrically with the ship's motion. The period of the oscillation is in the order of several seconds. This signal can be eliminated easily by means of low-pass filtering.

The data are transmitted via the notebook to the BGR data acquisition and processing system in the Processing Lab on the main deck and online navigation data from this system are sent with a rate of 1 Hz to support the stabilizing platform.

Gravity Ties to Land Stations

To compare the results of different gravity surveys, the measured data have to be tied in a world-wide accepted reference system. This system is represented by the International Gravity Standardization Net IGSN71. Furthermore, the instrumental drift of the KSS32-M can be derived by tie measurements at the beginning and the end of each cruise. The marine geophysical group of BGR uses a LaCoste&Romberg gravity meter, model G, no. 666 (LCR G666) for the gravity

connections. Descriptions and absolute gravity values for reference stations were taken from the database of the Bureau Gravimétrique International (BGI) in Toulouse. As these descriptions are mainly from the 1970s, we contacted colleagues from the University of Iceland (E. Piispa and M. T. Gudmundsson) to get access to the most reliable station, the national base, in the basement of the old Science Institute (RVIK AA). Additionally, we measured at the free accessible station near Hallgrímskirkja (RVIK B). A third station near the Catholic Church could not be used, as the described triangulation pillar does not exist anymore and obviously the ground was flattened there as well.

RV MARIA S. MERIAN moored at the Grandabryggja pier of Reykjavik Harbor (Fig. 11.7.3, A). On May 9, 2025, measurements at point A on the pier opposite the gravimeter room on RV. MARIA S. MERIAN have been made (Fig. 11.7.4). Point A is located in the middle between bollards 21 and 22. The connection measurements resulted in an average absolute gravity value of 982266.479 mGal (with water level –2.6 m, IGSN71) for point A, whereby the more reliable difference to RVIK AA was considered. That results in an absolute gravity value of 982266.906 mGal for the location of the gravity sensor. The reading of the KSSM32-M at the leaving time (May 10, 2025, 08:10 UTC) from the pier was 2391.694 mGal. The draught of RV MARIA S. MERIAN was 6.40 m.

Gravity stations:

A: Reykjavik Harbor, Grandabryggja pier, halfway between bollards 21 and 22

B: Reykjavik Harbor, Nordurgardur pier, bollard 5

Reference Stations:

01: National base, basement of old Science Institute, Dunhagi 3, Station RVIK AA, OS5450, National Energy Authority (NEA) 982264.785 mGal (IGSN71)

02: Base of Monolith near Hallgrímskirkja, Station RVIK B, OS5451, NEA 982258.785 mGal (IGSN71)

Differences between gravity and reference stations:

A – 01 = +1.694 mGal

A – 02 = +7.989 mGal

01 – 02 = +6.296 mGal (expected +6 mGal)

Absolute gravity for A from difference to 01 982266.479 mGal (IGSN71 system)

Absolute gravity at gravity sensor 982266.906 mGal

(1 m above water level, water level at –2.6 m) used for the gravity tie on 10.05.2025 (8:10 UTC)

Reading of sea gravimeter KSS32-M at that time: 2391.694 mGal

B – 02 = +7.997 mGal

Absolute gravity for B from difference to 02 982266.782 mGal (IGSN71 system)

Absolute gravity for B from difference to 01 982266.489 mGal (IGSN71 system)

(considering difference 01 – 02, see above)

Absolute gravity at gravity sensor 982267.073 mGal

(1.3 m above water level, water level at –3.5 m) used for the gravity tie on 13.06.2025 (11:55 UTC)

Reading of sea gravimeter KSS32-M at that time: 2389.23 mGal

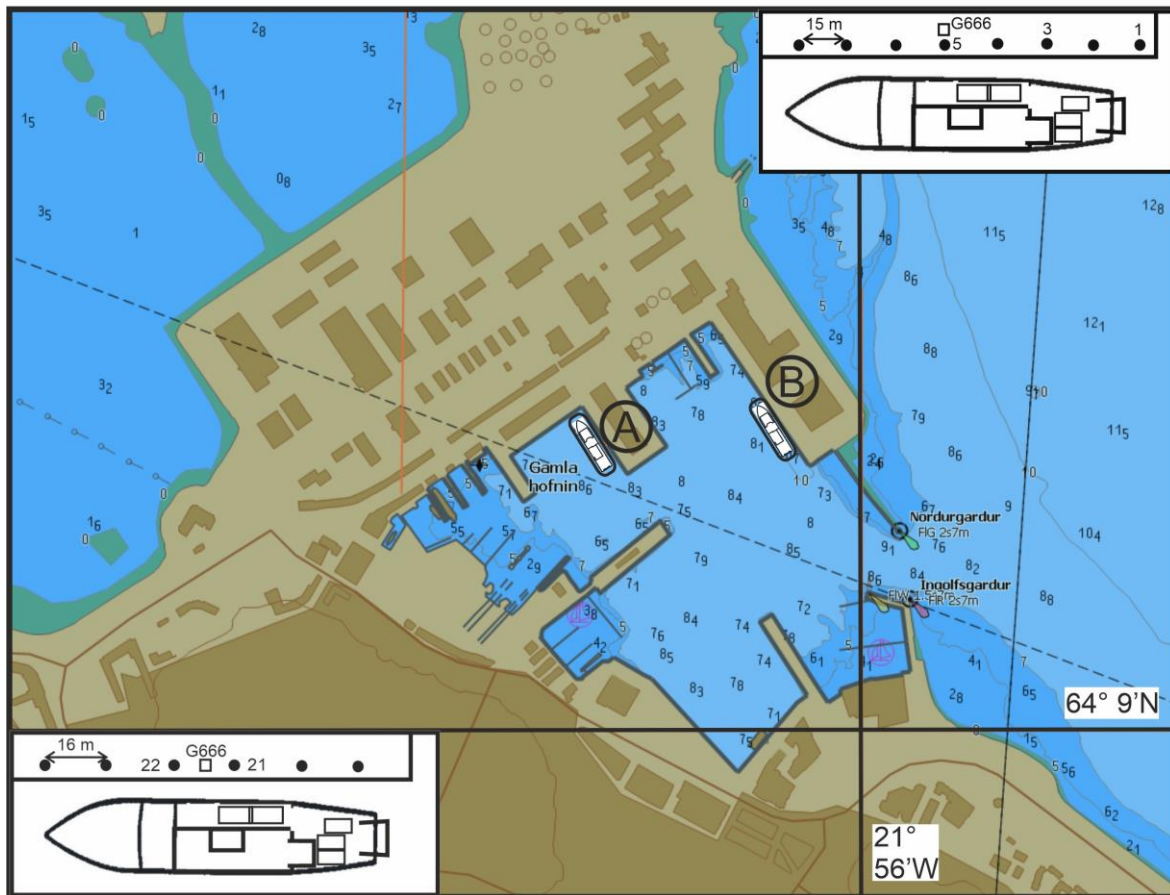


Fig. 11.7.3 Location of the mooring site of RV MARIA S. MERIAN at Grandabryggja pier (A) before leaving and at the Nordurgardur pier (B) after return). The insets show the details of the mooring sites including the numbered bollards and the locations of the tie measurements.

At the end of the cruise RV MARIA S. MERIAN moored at the Nordurgardur pier of Reykjavik Harbor (Fig. 11.7.3, B). June 13, 2025, measurements at point B on the pier opposite the gravimeter room on RV MARIA S. MERIAN have been made. Point B is located near bollards 5. Connection measurements could be done only to 02 (RVIK B), but the difference to 01 (RVIK AA) was measured on May 9 (see above). The connection measurements resulted in an average absolute gravity value of 982266.479 mGal (with water level -3.5 m, IGSN71) for point B. That results in an absolute gravity value of 982267.073 mGal for the location of the gravity sensor, taking into account that the draught of RV MARIA S. MERIAN was 6.10 m and thus 0.3 m less than before departure. The reading of the KSSM32-M at the nearly the same time (11:55 UTC) was 2389.23 mGal.

The instrumental drift derived from the readings and the connection measurements above amounts to -2.631 mGal/34.16 days or -0.077 mGal/day. This drift rate is within the expected range and a proof for the excellent quality of the sensor. It was applied to the measured data.



Fig. 11.7.4 Gravity measurement at the vessel before leaving (left) and at the reference station RVIK B near Hallgrímskirkja (right) in Reykjavik.

Table 11.7.1 Observation report of the gravity tie measurements in Reykjavik.

Station	Observer	Date	Time UTC	Reading Units	Gravity value [mGal]
A	H	09.05.25	12:56	5783.20	5849.137
A	H	09.05.25	12:58	5783.20	5849.137
01	H	09.05.25	13:25	5781.58	5847.499
02	H	09.05.25	14:10	5775.35	5841.198
02	H	09.05.25	14:12	5775.36	5841.209
A	H	09.05.25	14:50	5783.30	5849.238
A	H	09.05.25	14:52	5783.32	5849.258
B	H	13.06.25	12:00	5782.38	5849.319
B	H	13.06.25	12:02	5782.37	5849.309
02	H	13.06.25	12:36	5774.45	5841.299
02	H	13.06.25	12:38	5774.43	5841.279
B	H	13.06.25	13:25	5782.32	5849.258

Observer: H = Heyde, Gravity in mGal using LCR G 666 scaling table.

Gravity Data Processing

Processing of the gravity data consists essentially of the following steps:

- a time shift of 76 seconds due to the overcritical damping of the sensor,
- conversion of the output from measured voltage to mGal by applying a conversion factor of 4.7271 mGal/mV. This was done directly during data acquisition in the DACQS software from BGS.
- connection of the harbor gravity value to the world gravity net IGSN 71,
- correction for the Eötvös effect using the navigation data,
- subtraction of the normal gravity (GRS80),
- correction for the instrumental drift.

As a result, we get the so-called free-air gravity anomaly (FAA) which is in case of marine gravity simply the Eötvös-corrected, observed absolute gravity minus the normal gravity. Gravity values were recorded with a data rate of 1 Hz. This data rate is kept during data processing. The KSS32-M anomalies show short-wavelength oscillations in the order of 1-2 mGal especially during higher ship velocities. Therefore, a median filter with a length of 300 s was applied to the data. Infrequent outliers were removed manually in advance. Additionally, data recorded during sharp turns and rapid speed changes of the vessel show disturbed values and were removed manually. So, for example, the gravity data collected during shorter transits and the deployment and recovery of OBS were usually disregarded and removed.

Gravity Database and Gravity Anomaly Maps

Gravity measurements were carried out continuously during the complete cruise. However, the data acquisition started only after leaving the EEZ of Norway (13.05.2025, 12:50 UTC), respectively was stopped leaving the working area (08.06.2025, 01:52 UTC). Additionally data on the transit back were acquired in international waters on the 09.06.2025 (02:27 – 13:40 UTC). Therefore gravity data along all survey profiles and transit profiles to and between the three survey areas with a total length of about 4,650 km were measured. The details of the seismic and magnetic survey profiles including the numeration and location are listed in Chapter 6.2. Fig. 11.7.5 shows the overview map of the free-air gravity anomalies acquired during the cruise.

Figs. 11.7.6 to 11.7.8 show the maps of the free-air gravity anomalies in survey areas 1, 2 and 3. Gravity data along the marked survey lines and marked additional ship tracks were used for the compilation of the underlying gravity grids for the maps presented in chapter 5.6.

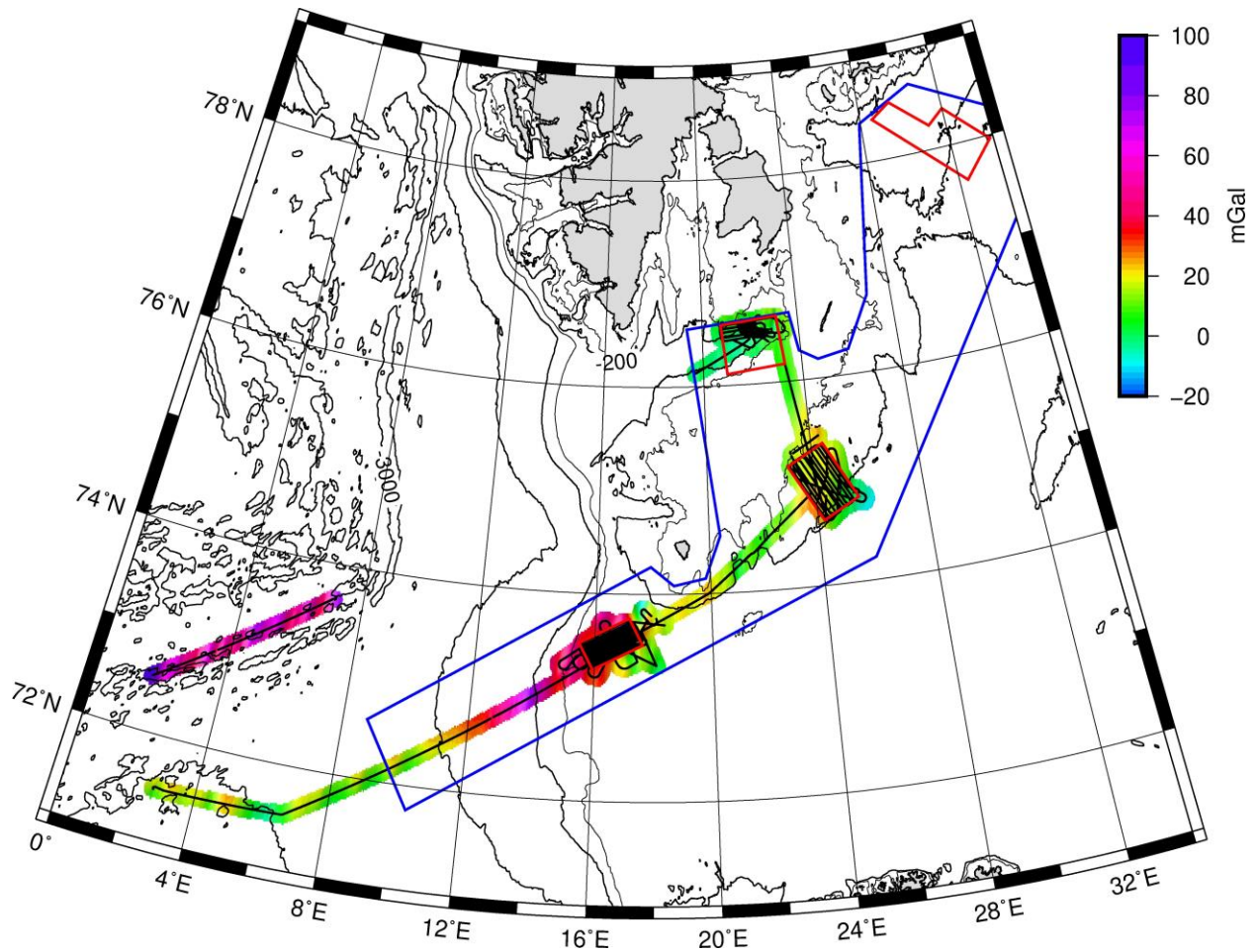


Fig. 11.7.5 Map of the free-air gravity anomalies acquired during cruise MSM137 with the ship track in black. The four survey areas and the extended working area are marked. in survey area C. The map is drawn up to a distance of 10 kilometers from all tracks with useable data. The map is based on a 1 x 1 (arc)-minutes grid and is underlain by the GEBCO_2024 bathymetry.

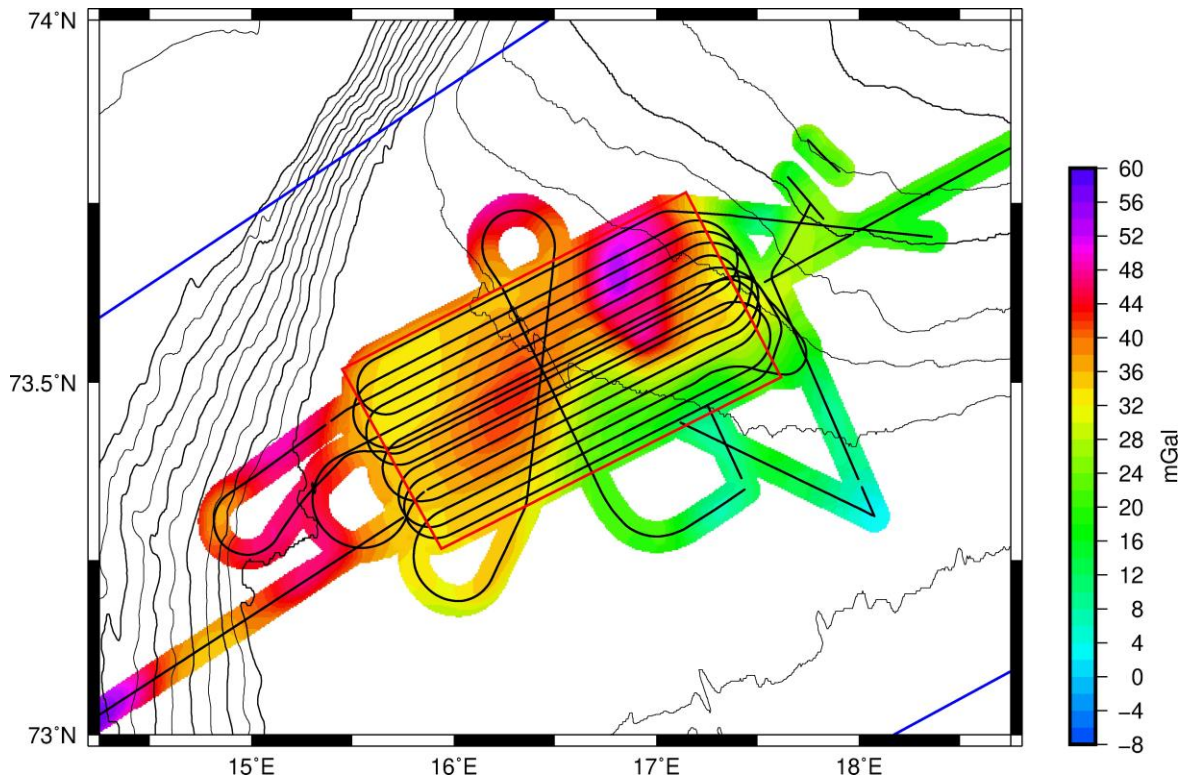


Fig. 11.7.6 Map of the free-air gravity anomalies acquired during cruise MSM137 in survey area 1. The survey lines and additional tracks with considered data are shown. The map is drawn up to a distance of 2.5 kilometers from the tracks. The map is based on a 0.25 x 0.25 km grid and is underlain by the GEBCO_2024 bathymetry.

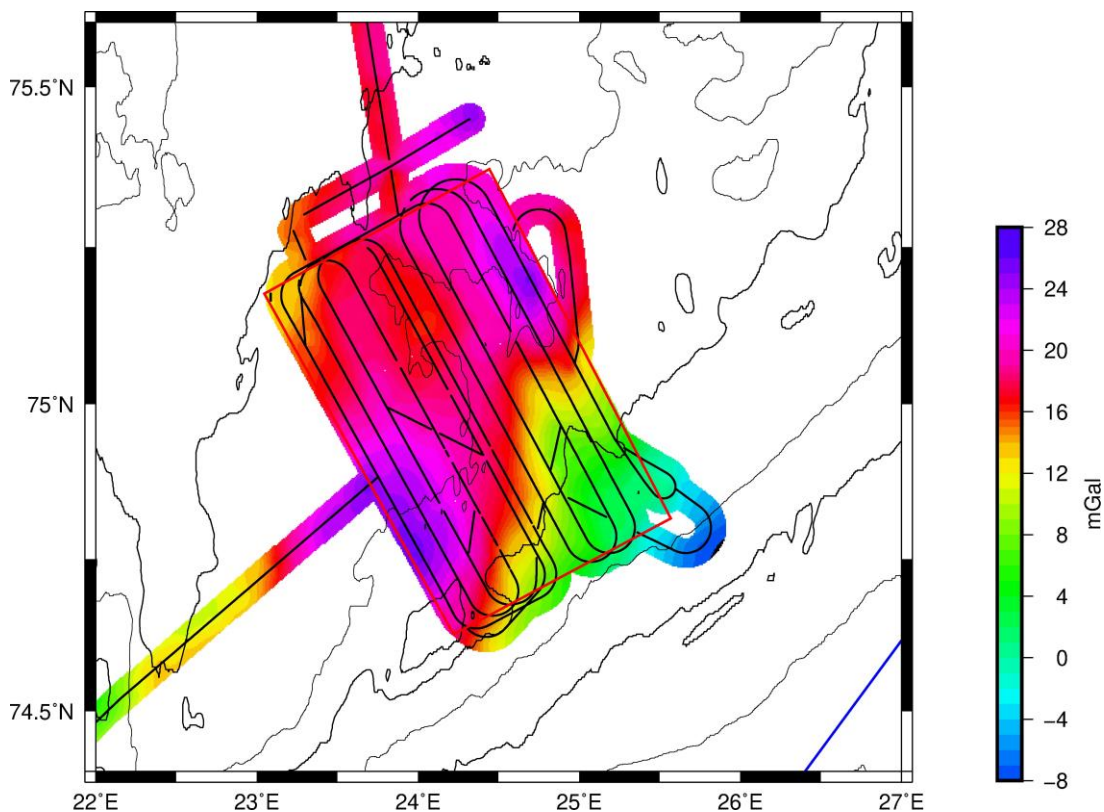


Fig. 11.7.7 Map of the free-air gravity anomalies acquired during cruise MSM137 in survey area 2. The survey lines and additional tracks with considered data are shown. The map is drawn up to a distance of 2.5 kilometers from the tracks. The map is based on a 0.25 x 0.25 km grid and is underlain by the GEBCO_2024 bathymetry.

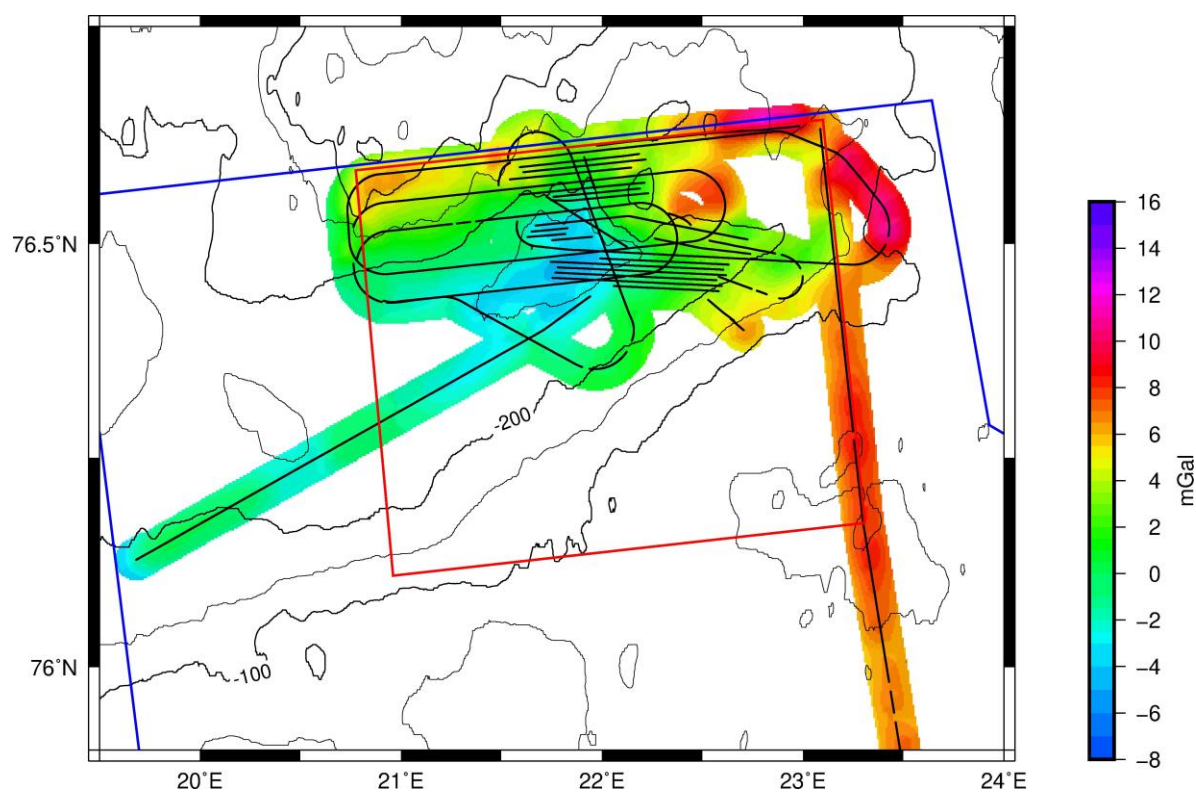


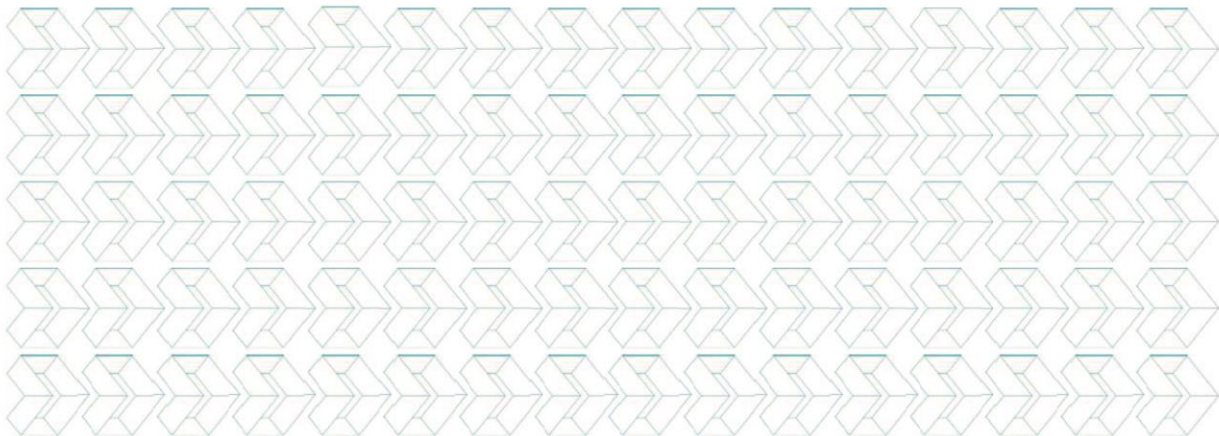
Fig. 11.7.8 Map of the free-air gravity anomalies acquired during cruise MSM137 in survey area 2. The survey lines and additional tracks with considered data are shown. The map is drawn up to a distance of 2.5 kilometers from the tracks. The map is based on a 0.25 x 0.25 km grid and is underlain by the GEBCO_2024 bathymetry.

11.8 MMO Report



PSO – PAM Final Report Marine Seismic Survey MIBAS MSM137

Prepared for Geowissenschaften und Rohstoffe (BGR)



Client:	Geowissenschaften und Rohstoffe (BGR)
Surveyor:	N/A
Area:	Svalbard, Barents Sea (Norwegian waters)
Survey:	Research Cruise MSM137 MIBAS
Dates:	10 May 2025 through 13 June 2025
Vessel:	R/V <i>Maria S. Merian</i>



1 Introduction

1.1 Executive Summary

Between the 10 May to 13 June 2025, Geowissenschaften Bundesanstalt und Rohstoffe (BGR) conducted the research cruise MSM137 – MIBAS with the research vessel (R/V) *Maria S. Merian*. This research expedition consisted of various geophysical operations and was conducted in Norwegian waters, south of the Svalbard archipelago in the Barents Sea.

In an effort to minimize the potential impacts of seismic survey operations on marine mammals, BGR adhered to the Joint Nature Conservation Committee (JNCC) Guidelines for Minimising the Risk of Injury and Disturbance to Marine Mammals for Seismic Surveys (JNCC, 2017) and in addition, followed the outlined German-based best-practice monitoring and mitigation procedure set up by a committee from the Portal Deutsche Forschungsschiffe, the Federal Ministry of Education and Research, and the German Science Foundation: Mitigation measures for the Operation of Seismic and Hydroacoustic Sources with Pulsed Sound Emissions (PTJ, 2023). This protocol was submitted and approved under BGR's Norwegian Survey Permit n°908/2025.

Two dual role trained marine mammal observers (MMOs) and passive acoustic monitoring (PAM) operators supplied by EPI Group were onboard to undertake the visual and acoustic watches, implement mitigation actions, and conduct data collection to uphold the regulatory guidelines and reporting requirements. Bridge and scientific crew helped with observations whenever the designated MMO/PAMO required a break to reduce observer fatigue.

There were seven mitigation actions and zero non-compliance issues for the duration of the project. All communication between the MMO/PAMO and seismic crew was effective in ensuring all source operations were conducted in compliance with the guidelines set forth for this project. Table 1 provides a report overview.

Table 1. Report data overview.

Report Overview
Number of reporting days (including transit, source testing, and data acquisition): 36 days
Visual monitoring totalled 224:24
Acoustic monitoring totalled 139:56
The total number of source sequences (attempts at or full lines) from 16 May 2025 to 06 June 2025 was zero test line and 46 data acquisition lines.
Sound source was active for a total of 326:04 for the duration of this reporting period.
There were 20 visual observations during the reporting period.
There was one acoustic detections during the reporting period.
There were seven source mitigation actions required for this survey period.
There were zero non-compliance issues.

1.2 Project Information

BGR is the Federal Institute for Geosciences and Natural Resources of Germany and the central geoscientific authority providing advice to the German Federal Government in all geo-relevant questions. It is subordinate to the Federal Ministry for Economic Affairs and Energy (Bundesministerium für Wirtschaft und Energie).

The research cruise MSM137 had for objectives the acquisition of geophysical data to characterize shallow magmatic systems and study their impact on sedimentary basins in the Barents Sea.

The survey took place in Norwegian waters, south of Svalbard islands in the Barents Sea. There were three areas of interest labelled from A, B, and D.

Table 2. Survey Area.

Area	Barents Sea
Survey Design	Parallel inlines and crosslines
Number of sail lines	46
Heading (deg) / Reciprocal heading (deg)	Various

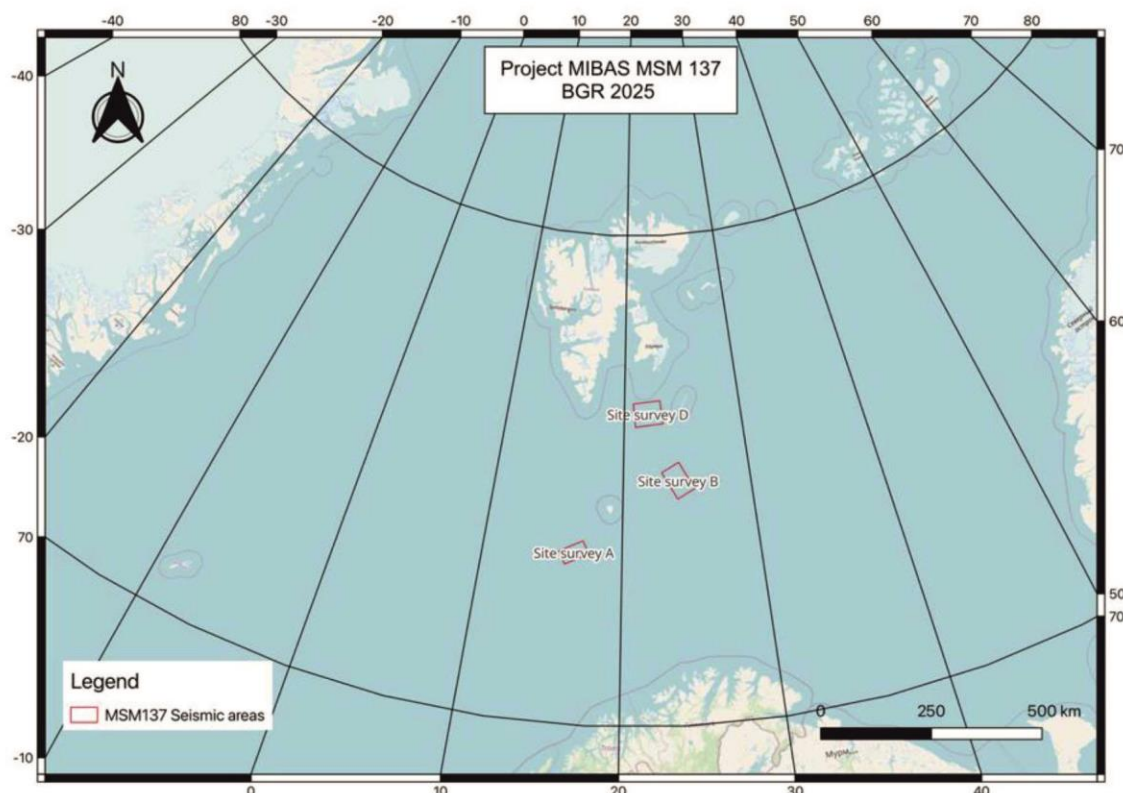


Figure 1. Project location.



2 Seismic Operations

The use of the seismic source for the acquisition of seismic reflection and refraction profiles required the following mitigation protocols.

2.1 Pre-Clearance Search Periods

A 60-minute search period was conducted prior to turning on the source either with visual or acoustic monitoring

The visibility of the Exclusion Zone (EZ) was adequate (twice the applicable EZ) during the pre-clearance search otherwise; the search was conducted with the PAM system.

2.2 Delays to Initiating Seismic Source

If a marine mammal was detected inside the EZ during the 60-minute search period, initiation of the seismic source was delayed until:

- All marine mammals have been confirmed to have exited the relevant EZ
- OR**
- 20 minutes from the last detection of marine mammal if not observed leaving the EZ

2.3 Soft-start

Soft-start of the survey equipment was carried out over the course of a minimum of 20 minutes.

2.4 Testing

Testing of the full seismic source required a full soft-start (minimum 20 minutes) prior to conducting the source test.

Testing of a single source element was conducted without a soft-start.

2.5 Shutdown

In this project, continuous monitoring of the EZ and shutdowns for marine mammals were applicable as the sources were greater than 150 in³.

If any marine mammal was detected visually or acoustically within its EZ, an immediate shutdown of the seismic source was required.

The restart of the seismic source following a marine mammal shutdown began with a soft-start:

- When all marine mammals were confirmed to have been exited the relevant EZ

OR

- 20 minutes from the last detection of marine mammal if not observed leaving the EZ

2.6 Silent Periods

- **Less than 10 minutes:** Measurements continued if no marine mammals were observed within the EZ. If a marine mammal was observed within the radius, operations were resumed via a soft start once the animal has left the EZ.
- **Greater than 10 minutes:** Measurements began with a soft start assuming that no marine mammals were observed in the EZ.

Table 6. Pre-watch events.

Pre-watch Event	Number of events
Visual pre-watch	8
Acoustic pre-watch	5
Visual and acoustic pre-watch	1
Total	14

Table 7. Soft-start events.

Soft-start	Number of events
Soft-start events	13
Total	13

Table 8. Source operations.

Source Operations	Time (HH:MM)
Full volume (on-line acquisition)	233:06
Soft-start	05:12
Reduced volume (line turns for OBS + testing)	92:57
Total	331:15



3 Visual and Acoustic Monitoring Effort

3.1 Observer Methods

Visual and acoustic monitoring were consistent, diligent, and free of distractions for the duration of the watch.

The MMO/PAM Operator was on watch during:

- Seismic source activities including testing
- During search periods prior to activating the seismic source

The following guidelines applied to these watch periods:

- No additional duties were assigned to the MMO or PAM Operator during visual/acoustic monitoring watch
- No person on watch as an MMO or PAM Operator was assigned a combined watch schedule of more than 12 hours in a 24-hour period
- Bridge crew and scientific crew supported the MMO and PAM Operator during times when the observer required a break

3.1.1 Visual Observer Survey Methods

The MMOs maintained visual watch from the bridge, bridge wings, and upper deck, where a 360-degree view of the exclusion zones was best achieved. As there was 24 hours of daylight in the survey area at this period of the year, visual monitoring was the main type of monitoring used. Acoustic monitoring was carried out when the sea state conditions were not favourable and the ability of detecting marine mammals was compromised (fog, Beaufort 6 or above, rough sea state).



Figure 7 : View from the bridge



Figure 8 : View from the upper deck

Areas of interest on the water (e.g., waves going against the prevailing direction, white water during calm periods, dark shapes, splashes, and bird activity) were used as visual clues. When positive sightings occurred, the distance to the animal(s) was estimated using binocular reticules Braun 7x50mm and Steiner navigator pro 7x30mm and photos were taken using a Canon EOS 400D+Canon zoom lens EF f1/4- f1/5.6 70-300mm and a Nikon D500+AFS Nikkor f1/4 300mm.



Figure 9: Reticule Binoculars and Cameras

Whenever a marine mammal was observed, the MMO took care of any necessary mitigation actions, or if no mitigation actions were required, noted and monitored the position (including latitude/longitude of the vessel and relative bearing and estimated range to the animal) until the animal dove or moved out of visual range of the observer.

The species identification was based on observer experience, and with the use of an identification field guide (Shirihai and Jarrett, 2006). All communication between the MMOs and the seismic lab occurred via VHF radio (channel 3).



3.1.2 Acoustic Operator Survey Methods

As there was daylight 24 hours a day at this latitude, the main monitoring type used was the visual monitoring. However, acoustic monitoring was used whenever the conditions of visibility were degraded (fog, choppy/rough sea state, Beaufort above 6).

The PAM station was located in the data lab office, behind the hangar on the main deck of the vessel (Figure 10).



Figure 10 : PAM station

PAM System:

The PAM system is designed to provide a flexible approach to monitoring for marine mammals using a towed hydrophone system. The system uses PAMGuard software modules such that the optimum system can be configured for the application, vessel, and deployment method. The source vessel had two acoustic monitoring systems, a primary system and a secondary system, available as a back-up in case of any issues encountered with the primary system.

The PAM system has been designed to monitor for marine mammal species found in offshore waters, covering a broad range of frequencies up to 200 kHz. Mid (MF) and high frequency (HF) marine mammal vocalizations are processed by an internal sound card. MF vocalizations include sperm whale click trains and codas and delphinid whistles in the frequency range of approximately 200 Hz to 24 kHz. *Kogia* species, beaked whales, and delphinid echolocation clicks are emitted

at very high frequencies in excess of 80 kHz which are processed by a specialized sound card in the buffer unit, an external National Instruments sound card, capable of sampling audio at 500 kHz.

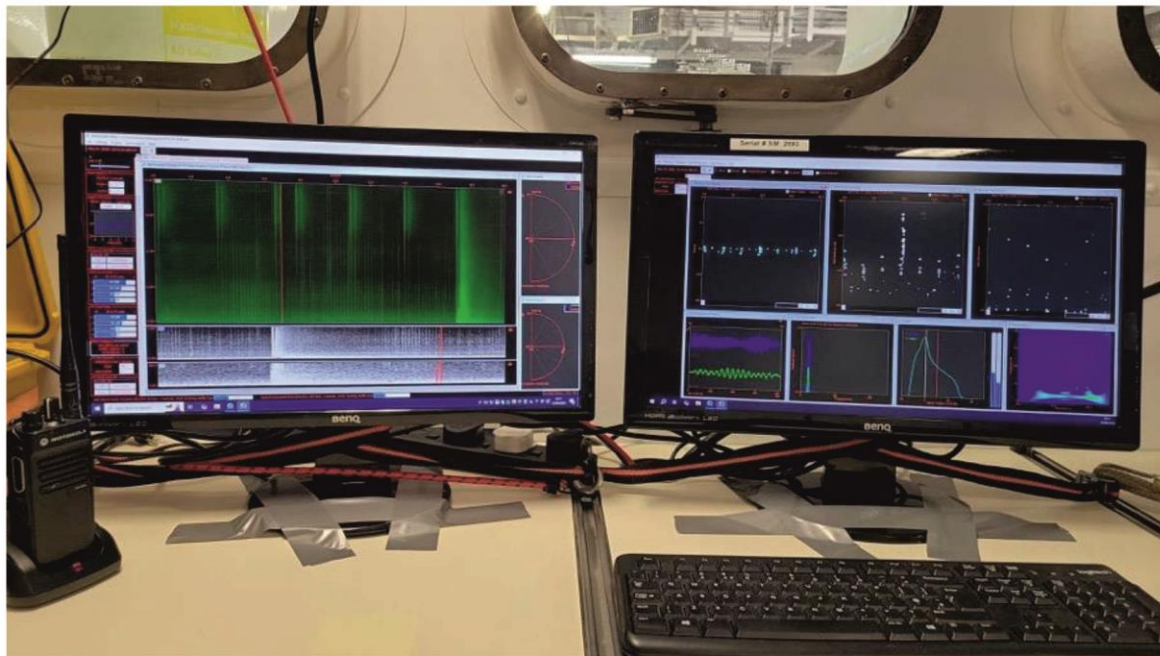


Figure 11: PAMGuard

The Seiche PAM equipment was comprised of the following items:

- 250-metre hydrophone array cable containing two low frequency hydrophones (10 Hz to 24 kHz), two ultra-broadband hydrophones (200 Hz to 200 kHz), and two broadband hydrophones (2 kHz to 200 kHz)
- 100-metre deck cable
- Electronic data capture and processing unit including:
 - Headphones RF transmitter
 - Fireface audio interface
 - Rackmount PC
 - Buffer interface unit
 - Integral screen and keyboard
- Backup System (100% Redundancy)

PAM Deployment/Recovery Procedure:

The MMO/PAM Operator developed, in cooperation with the vessel crew, a vessel-specific deployment and retrieval procedure that considered both the minimization of entanglement risks with other towed equipment while maximizing the acoustic range of the system.

The PAM hydrophone cable deployment commenced on 14 May 2025. The preferred method of deployment for the PAM array on the R/V *Maria S. Merian* was to stream the cable from the



overhead auxiliary winch on the streamer deck on the port side of the vessel. Prior to deployment a tap test was carried out at each hydrophone to ensure they all operated correctly.

Before the deployment, the hydrophone cable was measured and marked every 20 metres. The final deployment length was 120 metres. The array cable was connected to a PAM base station via a 100 m deck cable.

The method of deployment for the PAM cable is shown in the photos below (Figure 12).



Figure 12 : PAM deployment

Distance Estimation Procedure:

There are a variety of methods that can be used to estimate the distance to vocalizing marine mammals using the acoustic detection software, PAMGuard. When the distance to a vocalizing animal cannot be determined by PAMGuard, the PAM Operator can make a distance estimation assisted by the noise or detection score system developed by Gannier et al. (2002). Gannier et al. monitored sperm whales in the Mediterranean both visually and acoustically. A scale was developed based upon the strength or intensity of the sperm whale clicks at various distances that were then measured when the sperm whales surfaced and were visually observed. Although the scale is subjective, and sounds produced in marine environments will vary according to local conditions, the scale provides a measure for approximating distances when using a single, linear hydrophone array.

3.2 Observer Effort

Table 9 and Table 10 outline the monitoring effort conducted during this project by observation type and source operation.



Table 9. Monitoring effort by observation type overview.

Monitoring Type	Active Source Monitoring (HH:MM)	Inactive Source Monitoring (HH:MM)	Total Monitoring Effort (HH:MM)
Visual Monitoring	197:13	27:11	224:24
Acoustic Monitoring	124:44	15:12	139:56
Total	321:57	42:23	364:20

Table 10. Monitoring effort by source operation overview.

Source Operation	Visual Monitoring Effort (HH:MM)	Acoustic Monitoring Effort (HH:MM)
Full volume (on-line acquisition)	139:18	87:45
Soft-start	03:18	01:54
Reduced volume (line turns, test)	54:37	35:05
Total Active Source	197:13	124:44



4 Detections and Mitigation Actions

4.1 Protected Species Detection Overview

4.1.1 Visual Sightings

The MMOs recorded a total of 20 marine mammal sightings, including one killer whale (*Orcinus orca*), three unidentified dolphins (*Delphinidae*), five white-beaked dolphins (*Lagenorhynchus albirostris*), one humpback whale (*Megaptera novaeangliae*), and 10 unidentified baleen whales (*Balaenopteridae*) sightings. The source was active during 15 of the 20 visual sightings. There were seven shutdowns implemented, resulting in 05:08 mitigation action time and 06:03 production lost. Table 15 provides a list of the visual protected species sightings recorded during the reporting period.

4.1.2 Acoustic Detections

The PAM Operator recorded one acoustic detection of unidentified dolphin (*Delphinidae*). Due to the weak vocalization signal, the dolphin was considered outside the EZ. The source was active during the acoustic detection. There was no mitigation action requested, and no production lost. Table 16 provides a list of the acoustic marine mammal detections recorded during the reporting period.

Table 11. Visual protected species sightings by source activity

Source activity at sighting	Number of whale observations	Number of dolphin observations
Silent	2	3
Soft-start/Reduced/Testing	0	1
Full volume	9	5
Total	11	9

Table 12. Acoustic protected species detections by source activity

Source activity at detection	Number of whale detections	Number of dolphin detections
Silent	0	0
Soft-start/Reduced/Testing	0	0
Full volume	0	1
Total	0	1

Table 13. Visual sightings by species

Species	Number of observations	Number of individuals
White-beaked dolphin	5	40
Killer whale	1	8



Species	Number of observations	Number of individuals
Unidentified dolphin	3	11
Humpback whale	1	1
Unidentified baleen whale	10	14
Total	20	74

Table 14. Acoustic detections by species

Species	Number of observations	Number of individuals
Unidentified dolphin	1	1
Total	1	1



Table 15. Visual protected species sightings overview.

Date	Time (UTC)	Sighting Number	Common Name	Number of Individuals	Source Activity Initial Detection	Closest Approach Source (m) ¹	Closest Approach Vessel (m)	Mitigation Action	Duration Mitigation (HH:MM) ²	of Action	Duration Production Loss (HH:MM) ³	of Loss
10/05/2025	15:00	01	Killer whale	8	Inactive	Unknown	Unknown	None	00:00		00:00	
16/05/2025	05:29	02	White-beaked dolphin	8	Inactive	1000	1000	None	00:00		00:00	
16/05/2025	13:57	03	Unidentified baleen whale	1	Inactive	300	300	None	00:00		00:00	
17/05/2025	04:15	04	Unidentified baleen whale	1	Active	1000	1000	None	00:00		00:00	
26/05/2025	15:48	05	Unidentified dolphin	2	Inactive	200	200	None	00:00		00:00	
27/05/2025	09:17	06	Unidentified baleen whale	3	Active	1150	1000	None	00:00		00:00	
27/05/2025	10:36	07	Unidentified baleen whale	1	Active	250	100	Shutdown	01:21		01:58	
27/05/2025	11:56	08	Unidentified baleen whale	1	Inactive	550	500	None	00:00		00:00	
27/05/2025	22:11	09	Unidentified baleen whale	1	Active	1650	1500	None	00:00		00:00	
28/05/2025	03:49	10	Unidentified baleen whale	1	Active	550	400	Shutdown	00:28		00:35	
28/05/2025	05:40	11	White-beaked dolphin	8	Active	155	5	Shutdown	00:13		00:20	
28/05/2025	08:44	12	Unidentified baleen whale	1	Active	950	800	None	00:00		00:00	
28/05/2025	09:55	13	White-beaked dolphin	3	Active	200	100	Shutdown	00:06		00:06	
28/05/2025	11:11	14	White-beaked dolphin	6	Active	850	700	None	00:00		00:00	
28/05/2025	11:43	15	Unidentified dolphin	5	Active	850	700	None	00:00		00:00	
28/05/2025	12:45	16	White-beaked dolphin	15	Active	600	450	Shutdown	00:09		00:13	
28/05/2025	14:07	17	Unidentified baleen whale	3	Active	170	20	Shutdown	02:22		02:22	
29/05/2025	10:51	18	Humpback whale	1	Active	450	300	Shutdown	00:29		00:29	
31/05/2025	10:30	19	Unidentified baleen whale	1	Active	1500	1500	None	00:00		00:00	
01/06/2025	11:17	20	Unidentified dolphin	4	Active	850	1000	None	00:00		00:00	

¹ Includes estimates when the source was not deployed.² Duration of mitigation measures calculated as follows: ramp-up delay is the difference between the time the vessel would have begun ramp-up had the mitigation zones been clear and the time the MMOs gave clearance to begin ramp-up; shut-down is the entire period from when the source was turned off plus through the required waiting period following the last observation within the exclusion zone.³ Duration of production loss calculated as follows: ramp-up delay is the difference between the time the vessel would have begun ramp-up had the mitigation zones been clear and the time the MMOs gave clearance to begin ramp-up; shut-down is the entire period from when the source was turned off until the source is activated again.

Table 16. Acoustic marine mammal detection overview.

Date	Time (UTC)	Detection Number	Common Name	Number of Individuals	Source Activity Initial Detection	Closest Approach Source (m) ¹	Mitigation Action	Duration Mitigation (HH:MM) ²	of Action	Duration Production Loss (HH:MM) ³	of Loss
27/05/2025	16:56	501	Unidentified dolphin	1	Active	1000	None	00:00		00:00	

¹ Includes estimates when the source was not deployed. NL = not localized² Duration of mitigation measures calculated as follows: ramp-up delay is the difference between the time the vessel would have begun ramp-up had the mitigation zones been clear and the time the PAMs gave clearance to begin ramp-up; shut-down is the entire period from when the source was turned off plus through the required waiting period following the last observation within the exclusion zone.³ Duration of production loss calculated as follows: ramp-up delay is the difference between the time the vessel would have begun ramp-up had the mitigation zones been clear and the time the PAMs gave clearance to begin ramp-up; shut-down is the entire period from when the source was turned off until the source is activated again.

4.2 Observation Distance and Closest Point of Approach

The average sighting distance for visual observation overall was 1140 meters. Average detection distance for source active and inactive was 1320 metres and 3000 metres respectively. The single acoustic detection was localised at a range of 1000 metres, with an active source.

The average of closest point of approach between active and inactive source given by group and species are described in Table 17 and Table 18:

Table 17. Average closest point of approach by species type.

Species Type	CPA to Inactive source (m)	CPA to Active Source (m)	Overall CPA (m)
Dolphins*	733	584	634
Whales	400	852	770
Total	600	745	709

*Dolphins are inclusive of all delphinid species, including blackfish

Table 18. Average closest point of approach by species.

Species	CPA to Inactive source (m)	CPA to Active Source (m)	Overall CPA (m)
Killer whale	1000	N/A	1000
White-beaked dolphin	1000	451	561
Unidentified dolphin	200	850	633
Humpback whale	ND	450	450
Unidentified whale	400	902	802
Total	600	745	709

4.3 Observation Rates

The observation rates for source activity and monitoring type are described in Table 19, Table 20, and Table 21.

Table 19. Visual and acoustic observation rates by source activity.

Observation Rate (Observations per hour of Monitoring Effort)			
	Source Active	Source Inactive	All Monitoring
Visual monitoring	0.07606	0.18394	0.08913
Acoustic monitoring	0.00802	0.00000	0.00715



Table 20. Visual observation rates by species.

Species	Number of observations	Observation rate per number of observations	Total number of individuals	Observation rate per number of individuals
White-beaked dolphin	5	0.02228	40	0.17825
Killer whale	1	0.00446	8	0.03565
Unidentified dolphin	3	0.01337	11	0.04902
Humpback whale	1	0.00446	1	0.00446
Unidentified baleen whale	10	0.04456	14	0.06239
Total	20	0.08913	74	0.32977

Table 21. Acoustic observation rates by species.

Species	Number of observations	Observation rate per number of observations	Total number of individuals	Observation rate per number of individuals
Unidentified dolphin	1	0.00715	1	0.00715
Total	1	0.00715	1	0.00715

4.4 Source Mitigation Actions

The mitigation procedures in place for this project were either a delay to start of operations or a shutdown if the operation was started, whenever a marine mammal was observed inside the EZ.

In total, seven source mitigation actions were implemented during the survey program on 27, 28, and 29 May 2025. There were zero delays and seven shutdowns that resulted in 05:08 of mitigation time and 06:03 of production loss. Table 22 summarizes the number of source mitigation actions by species group and Table 23 provides a detailed summary of each mitigation action. Mitigation narratives are provided in **Appendix A and F**.

Table 22. Mitigation Actions by Species Group.

Species Group	Number of Delays	Number of Shutdowns	Total Duration of Mitigation (HH:MM)	Total Duration of Production Loss (HH:MM)
Whales	0	4	04:40	05:24
Dolphins	0	3	00:28	00:39
Total	0	7	05:08	06:03



Table 23. Source mitigation action details.

Detection Number	Date	Detection type	Common Name	Number of Individuals	Source Activity Initial Detection	Closest Approach to Source (m) ¹	Closest Approach to Vessel (m)	Mitigation Action	Duration of Mitigation Action (HH:MM) ²	Duration of Production Loss (HH:MM) ³
07	27/05/2025	Visual	Unidentified baleen whale	1	Full volume	250	100	Shutdown	01:21	01:58
10	28/05/2025	Visual	Unidentified baleen whale	1	Full volume	550	400	Shutdown	00:28	00:35
11	28/05/2025	Visual	White-beaked dolphin	8	Full volume	155	5	Shutdown	00:13	00:20
13	28/05/2025	Visual	White-beaked dolphin	3	Reduced power	200	100	Shutdown	00:06	00:06
16	28/05/2025	Visual	White-beaked dolphin	15	Full volume	600	450	Shutdown	00:09	00:13
17	28/05/2025	Visual	Unidentified baleen whale	3	Full volume	170	20	Shutdown	02:22	02:22
18	29/05/2025	Visual	Humpback whale	1	Full volume	450	300	Shutdown	00:29	00:29



6 Conclusions and Recommendations

6.1 Compliance with Guidelines

There were no records of non-compliance throughout the duration of the survey MIBAS MSM137.

BGR demonstrated a proactive and conservative approach to marine mammal mitigation monitoring by fully complying with all operational requirements of seismic activities underlined by the JNCC Guidelines (JNCC, 2017) and by the Mitigation Guidelines set up by the Portal deutsche Forschungsschiffe, Federal Ministry of Education and Research, and German Science Foundation (PTJ, 2023).

The communication between the MMO/PAM Operators, the survey team, and the maritime crew was excellent. The survey team provided help and support on the set-up, deployment, and recovery of the PAM equipment whenever it was needed and were keen to take over watches whenever the observer needed to take a break. Both departments worked diligently and cohesively together to ensure all safety regulations and requirements set forth by the JNCC and the PTJ guidelines were both adhered and followed.

6.2 Conclusions

The scientific crew of the R/V *Maria S. Merian* successfully completed a multichannel seismic reflection and OBS seismic refraction acquisitions as part of the MIBAS project lead by BGR offshore Svalbard in the Barents Sea during the cruise MSM137 from 10 May to 13 June 2025.

Both visual and acoustic monitoring were performed on a continuous watch during the seismic acquisitions' profiles. Active source included full power, soft-start, reduced power, and test occurred during a total period of 331:15 hours. Overall, a total of 364:20 of monitoring effort was carried out during the project, including a total visual monitoring effort of 224:24 hours and a total acoustic monitoring effort of 139:56 hours.

As there was daylight at any time at this latitude, visual watches were conducted preferentially whenever the weather conditions were favourable (i.e. Beaufort ≤ 5 , no mist or fog). However, the good weather windows were limited during this project (only 57% of the time), due to the presence of heavy fog or rough weather: poor ($< 1\text{km}$) to moderate (1-5km) visibility, Beaufort > 6 , medium (2-4m) swell height. The PAM system was used whenever the conditions were not favourable to visual monitoring. Environmental conditions could impact the probability of detecting marine mammals.

Throughout this project there was one acoustic detection of an unidentified dolphin and 20 visual sightings including:

- One killer whale (*Orcinus orca*) while the vessel was transiting offshore Icelandic waters with recognizable large, dark rounded-bodies, tall dorsal fin, mainly black with contrasting white throat to abdomen and rear flanks, grey saddle behind dorsal fin.



- Five white-beaked dolphins (*Lagenorhynchus albirostris*) on survey areas, with robust body, short-beaked, large and falcate dorsal fin, black to dark grey cape with pale grey-whitish patches in upper flanks and tailstock. This species is known to be a resident at this latitude (Kinze, 2009).
- Three unidentified dolphins (*Delphinidae*) that could have belonged to the white-beaked dolphins which were the only species of *Delphinidae* observed during this project.
- One humpback whale (*Megaptera novaeangliae*), recognizable with the hump on the dorsal fin, the bushy blow and the visible fluke while diving. This species is known to migrate in the feeding grounds located at this latitude during summertime (Clapham, 2009).
- 10 unidentified baleen whales (*Balaenopteridae*), which among them, seven sightings of small size whales, with distinctive sickle-shaped dorsal fin and no visible blow that could have belonged to the common minke whale species (*Balaenoptera acutorostrata*) as this species is known to be observed in the Barents Sea (Perrin, Robert, Brownell, 2009). The three remaining unidentified baleen whales were larger in size and were showing bushy blows and visible flukes. Hence, these whales could have belonged to the humpback whale species (*Megaptera novaeangliae*).

Several species of birds were also reported such as Ruddy Turnstone (*Arenaria interpres*), Arctic Skua (*Stercorarius parasiticus*), Lesser Black-backed Gull - scandinavian race (*Larus fuscus fuscus*), Peregrine Falcon (*Falco peregrinus*), Northern Fulmar (*Fumarus glacialis*), Black-legged Kittiwake (*Rissa tridactyla*), Common Guillemot (*Uria aalge*), and Glaucous Gull (*Larus hyperboreus*).

In total, seven source mitigation actions were implemented during the survey program on 27, 28, and 29 of May 2025. There were zero delays and seven shutdowns that resulted in 05:08 of mitigation time and 06:03 of production loss.

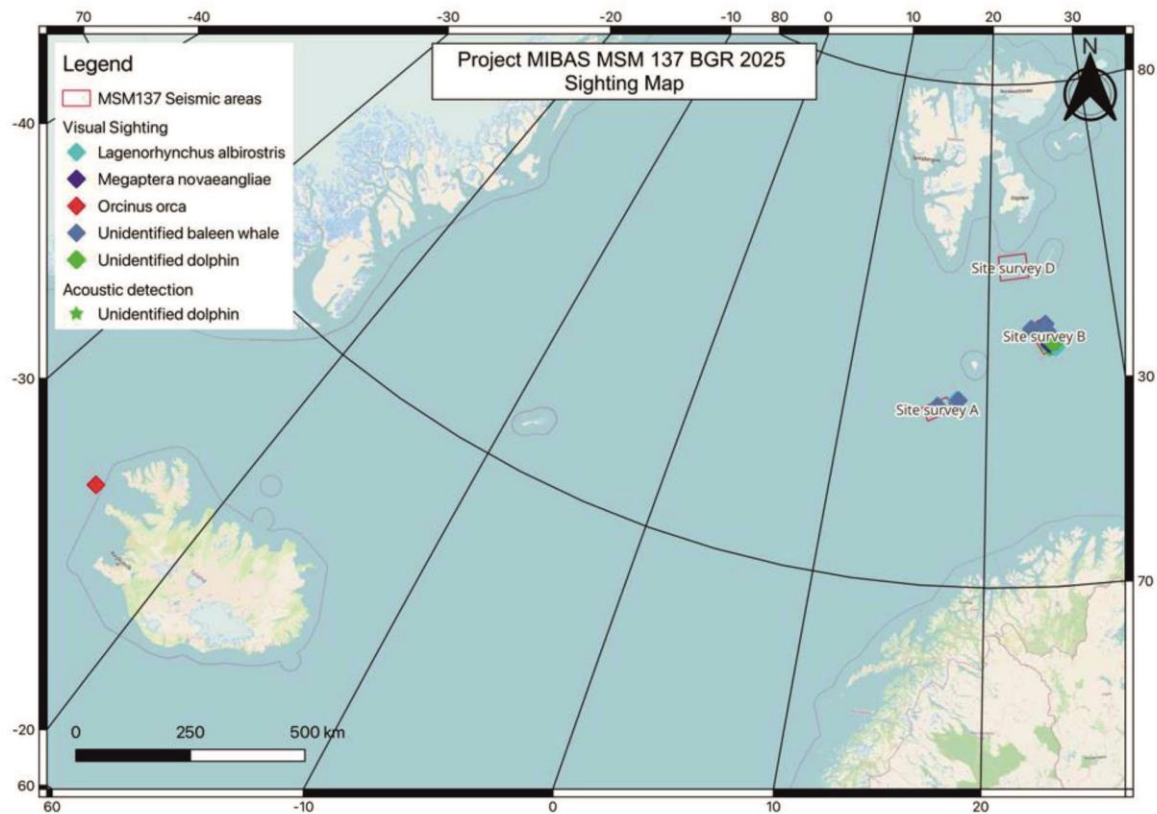
The results presented in this report can represent useful indicators of wildlife occurrence in the Svalbard, Barents Sea at this time of year. These findings could be helpful for future survey planning and for future environmental research on this area.

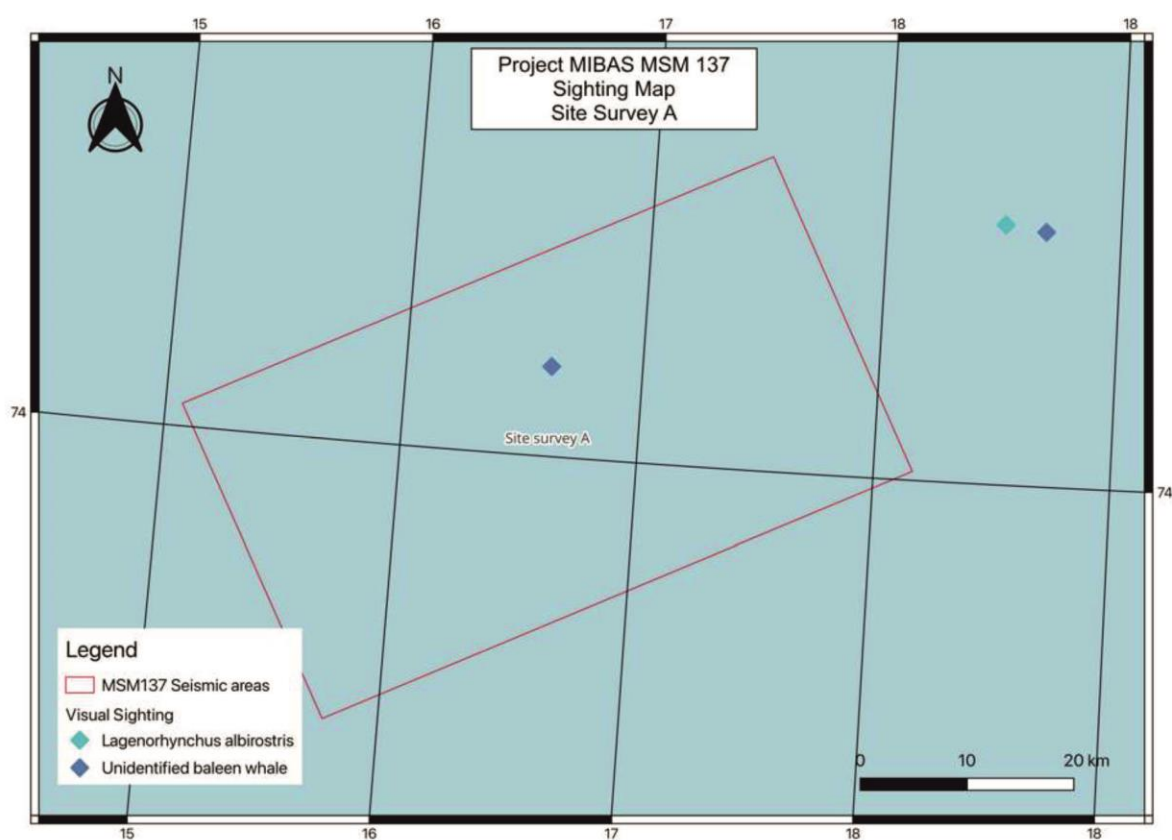


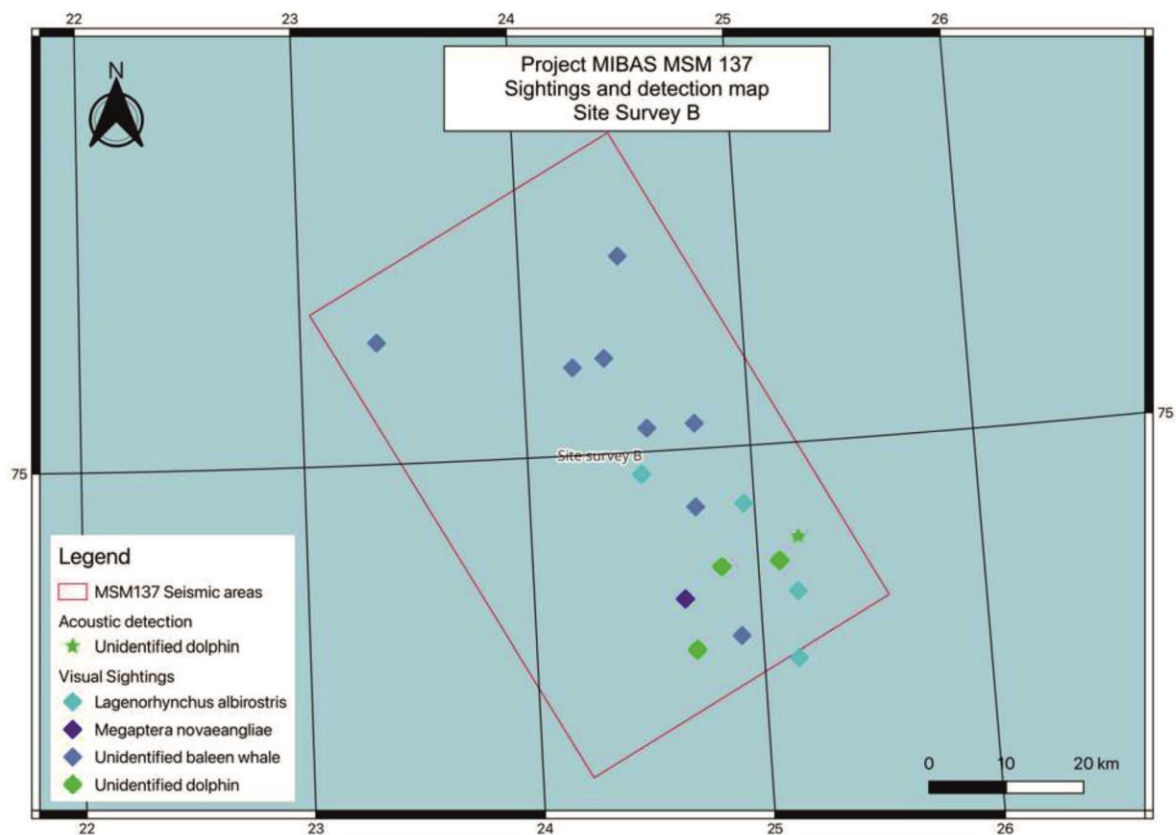
References Cited

- Bannister J.L. (2009), Baleen whales (Mysticetes). In: Perrin W. F., Würsig B., Thewissen J.G.M. (Eds.), *Encyclopedia of Marine Mammals* (second ed.), Academic Press, New York, pp. 582-585
- Clapham P.J. (2009), Humpback whale (*Megaptera novaeangliae*). In: Perrin W. F., Würsig B., Thewissen J.G.M. (Eds.), *Encyclopedia of Marine Mammals* (second ed.), Academic Press, New York, pp. 80-89
- Gannier et al. (2002). Distribution and relative abundance of sperm whales in the Mediterranean Sea. *Marine Ecology Progress. Series.* 243, pp. 281-293
- Kinze C.C. (2009), White-beaked dolphin: *Lagenorhynchus albirostris*. In: Perrin W. F., Würsig B., Thewissen J.G.M. (Eds.), *Encyclopedia of Marine Mammals* (second ed.), Academic Press, New York, pp. 1255-1258
- JNCC (2017). Guidelines for minimising the risk of injury to marine mammals from geophysical surveys. - Joint Nature Conservation Committee, Aberdeen, UK, Aug. 2017, 1-28 pp.
- Perrin W.F., Robert L., Brownell, Jr. (2009), Minke whales (*Balaenoptera acutorostrata* and *B. bonaerensis*). In: Perrin W. F., Würsig B., Thewissen J.G.M. (Eds.), *Encyclopedia of Marine Mammals* (second ed.), Academic Press, New York, pp. 733-735
- PTJ (2023). Mitigation measures for the operation of seismic and hydroacoustic sources with pulsed sound emissions. Appendix 3 of the Cruise Proposal Preparation Instructions, edited by Portal Deutsche Forschungsschiffe (PTJ), Federal Ministry of Education and Research, and by German Science Foundation (DFG).
- Shirihai, H. & Jarret, B. (2006). Whales, dolphins and seals: A field guide to the marine mammals of the World. A&C Black Publishers.

Appendix E. Marine Mammals Observation Maps









Appendix F.Mitigation Action Summary

27 May 2025

Sighting #7 – Unidentified baleen whale, *Balaenopteridae*

At 10:36 UTC an unidentified whale was sighted 800 meters off the port side bow of the boat, bearing of 110 degrees. At 10:55 UTC, the whale was spotted 100 meters off the starboard side of the vessel, at a bearing of 180 degrees. The source was active, and a shutdown required and implemented. whale dived and surfaced at 11:10 UTC, 500 meters off the starboard beam, at a bearing of 230 degrees. At 11:30 UTC the whale was sighted again 400 meters off the bow, a bearing of 154 degrees and was not seen again after that time. The vessel was turning, and soft start was at 12:53 UTC. The duration of the mitigation action was 01:21. The loss of production was 01:58.

28 May 2025

Sighting #10 – Unidentified baleen whale, *Balaenopteridae*

At 03:49 UTC, an unidentified whale was observed at approximately 400 meters of the portside of the vessel and 550 meters from the active source. A shutdown was immediately requested. The whale was observed surfacing slowly every 5 minutes, with no blow visible, crossing ahead of the vessel and heading in the SW direction. The whale was last observed outside of the exclusion area at 1000 meters from the vessel at 04:17 UTC. Operation resumed with a soft start at 04:24 UTC. The duration of the mitigation action was 00:28. The loss of production was 00:35.

28 May 2025

Sighting #11– White-beaked dolphin, *Lagorhynchus albirostris*

At 05:40 UTC, a pod of approximately eight white-beaked dolphins was spotted at 1000 meters away the portside of the vessel. As the pod was progressing toward the vessel, a shutdown was requested at 05:41 UTC. The pod entered in the exclusion area from 05:42 to 05:50 UTC when the source was inactive. They were last seen at 05:58 UTC at approximately 1500 meters away the vessel heading SW. Operation resumed with a soft start at 06:01 UTC. The duration of the mitigation action was 00:13. The loss of production was 00:20.

28 May 2025

Sighting #13 – White-beaked dolphin, *Lagorhynchus albirostris*

At 09:55 UTC, a pod of white-beaked dolphins was seen about 1200 meters off the bow of the boat, jumping and moving in an easterly direction. At 09:58 UTC three white-beaked dolphins crossed the bow of the vessel at a distance of 100 meters. The source was active and immediately shutdown. The dolphins were moving away from the boat rapidly in a SE direction and at 10:02 UTC were seen outside the exclusion zone. The source returned to the mitigation gun and a soft start was implemented at 10:37 UTC. The duration of the mitigation action and loss of production was 00:06.

**28 May 2025****Sighting #16 – White-beaked dolphin, *Lagorhynchus albirostris***

At 12:45 UTC, a pod of approximately 15 white-beaked dolphins was spotted 3000 meters away from the portside of the vessel, heading in the SE direction, in the opposite direction as the vessel and outside the exclusion zone. At 12:54 UTC, two individuals were observed heading on the vessel and a shutdown was requested. The pod continued its progression to the SE and were last seen at 13:03 UTC at 1600 meters away from the stern of the vessel. The duration of the mitigation action was 00:09. The loss of production was 00:13.

28 May 2025**Sighting #17 – Unidentified baleen whale, *Balaenopteridae***

At 14:07 UTC, an unidentified whale was observed surfacing with no blow visible at 200 meters off the starboard side of the vessel, heading in the same direction than the vessel (NW) while the source was active. A shutdown was immediately requested. At least three individuals were observed in the area. The last sighting was at 15:09 UTC when one of the individuals was observed surfacing at 700 meters away from the portside of the vessel, heading W. The operation resumed with a soft start at 15:29 UTC. The duration of the mitigation action and loss of production was 00:22.

29 May 2025**Sighting #18 – Humpback whale, *Megaptera novaeangliae***

At 10:51 UTC, a humpback whale was observed blowing at more than 4000 meters away, off the portside, heading in the same direction as the vessel. At 11:28 UTC, a shutdown was requested as the whale was approaching the exclusion zone at a fast pace. The animal entered the mitigation area at 11:29 UTC, and dove with the fluke visible in front of the vessel. The whale was last observed blowing at 11:37 UTC at an unknown distance from the vessel, heading SE. A delay of 20 minutes was applied, and soft start was able to resume at 11:57 UTC. The duration of the mitigation action and loss of production was 00:29.